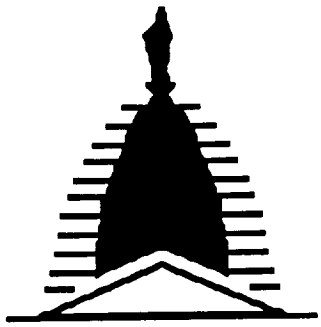

UNIVERSITY of
NOTRE DAME

NASA/USRA UNIVERSITY ADVANCED DESIGN PROGRAM 1991-1992

UNIVERSITY SPONSOR
BOEING COMMERCIAL AIRPLANE COMPANY

FINAL DESIGN PROPOSAL

Hermes CX-7

Air Transport System Design Simulation

May 1992

Department of Aerospace and Mechanical Engineering
University of Notre Dame
Notre Dame, IN 46556

Hermes CX-7

Submitted by:
Brian Amer
John Barter
Jay Colucci
Caryn Foley
James Kockler
David Rapp
Matthew Zeiger

Table of Contents

1. Executive Summary

The Hermes CX-7 has been designed to service the overnight parcel package delivery needs of the cities of Aeroworld as determined in the G-Dome Enterprises market survey. The design optimization centers on the prime goal of servicing the needs of these cities as efficiently and profitably as possible. The greatest factors which affect the design of an aircraft for the mission outlined in the Request for Proposal are cost, construction feasibility and effectiveness of the design. Other influencing factors are given by the constraints of the market, including a maximum takeoff and landing distance of 60 feet, storage capability in a container of size 5 ft. x 3 ft. x 2 ft., cargo packages of 2 inch and 4 inch cubes, and ability to turn with a radius no larger than 60 feet. Safety considerations such as flying at or below Mach one (30 ft/s) and controllability and maintainability of the aircraft must also be designed into the aircraft. Another influential factor is the efficiency of the aircraft which involves optimizations and tradeoffs of such factors as weight, lifting surface sizing, structural redundancy, and material costs.

The design market will consist of all Aeroworld cities except C,D, E and O due to these cities low demand and excessive distances from the northern cities. A routing system was designed to service the needs of these cities overnight using a fleet of 22 planes. The routing system is based on two main hubs at cities F and K. Each aircraft will make 2 round trips on one leg of the route. To minimize cost, the route structure is designed such that it uses as few aircraft as possible and these aircraft cover the shortest distance possible each night.

The constraint which sized the engine and propeller was takeoff performance. The Hermes CX-7 employs the Astro 15 engine and the TopFlight 12x6 propeller. This engine/ propeller combination provides the necessary power needed for takeoff in less than 60 feet while minimizing the fuel burned during cruise. The Astro 15 was the engine that weighed the least of the engines which provided sufficient power for takeoff. The TopFlight 12x6 was the smallest diameter propeller which fulfilled the necessary takeoff distance requirement. The TopFlight version of this propeller was chosen because it exhibits the best efficiency of the brands available. The aircraft will be powered by 12 Panasonic 600 milli-amp hour batteries having voltage capacity of 1.2 volts each. These provide sufficient power for both takeoff and cruise conditions to meet the restrictions on takeoff distance and on range needed.

The wing section will be constructed from the NACA 6412 airfoil. This airfoil section was chosen because it provides the desired lift capability while also

minimizing the difficulty in construction because of its simple structure. The wing has an area of 8 square feet and an aspect ratio of 12. There is no sweep or taper on the wings because this will greatly simplify construction. The wings will be mounted as two plug in sections low on the fuselage and at a dihedral of 6 degrees and at an angle of incidence of 1 degree. The wing will have three spars and will be built primarily from spruce, bass, balsa, and monokote.

The fuselage will have a rectangular cross section of area 4.625 in. x 6.875 in. and a length of 54 in. It is constructed of spruce and balsa wood and includes a cargo space 4 in. x 4 in. x 40 in. The aircraft was laid out such that the center of gravity is located 24 in. from the front of the fuselage regardless of whether the aircraft is empty or full of cargo.

The Hermes CX-7 is designed to be controlled with rudder and elevator deflections. There are no ailerons. This minimizes the number of servos needed to control the aircraft. Turning is achieved through the use of the rudder and dihedral effects. The horizontal and vertical surfaces of the tail both consist of flat plates for simplicity. The elevator area is 30% of the horizontal tail and the rudder area is 50% of the vertical tail. The c.g. travel is constrained by static and dynamic stability considerations and is limited to 10% forward and 5% aft of the design c.g. position (24 inches from the front of the fuselage).

The Hermes CX-7 will meet and surpass the performance requirement of the mission and market. The take off distance is 32 feet and the landing distance is 47 feet, well below the constraint of 60 feet. The design range is 10,655 feet and endurance is 355 seconds. The maximum range is also 10,655 feet and the maximum endurance is 356 seconds. The aircraft can execute a 48 foot radius turn, which is less than the 60 foot restriction, at a 30 degree bank angle.

The Hermes CX-7 will cost an estimated $390,000 (in Aeroworld dollars). The recommended charge is $10.50 per cubic inch for an average delivery distance. This will enable G-Dome Enterprises to break even in less than half of the life of the aircraft.

1.1 Summary of Specifications

Basic configuration	
Total weight(empty)	72.5 oz.
Payload(max)	19.2 oz.
Payload volume	640 $in.^3$
Fuselage length	54 in.
Fuselage width	4.625 in.
Fuselage height	6.875 in.

Performance	
Cruise Velocity	30 ft./s
Takeoff Vel.	27.6 ft/s
Takeoff distance	37 ft.
Landing distance	47 ft.
Range at cruise	10,655 ft.
Endurance at cruise	355 sec.
Max Range	10,655 ft.
Max Endurance	356 sec.
Turn radius	48 ft.
Max rate of climb	10 ft/s
Min. glide angle	3.8 deg.

Aerodynamics	
Wing area	8 ft^2
Aspect ratio	12
airfoil(wing)	NACA 6412
span	10 ft.
Dihedral	6 deg.
Wing Incidence Angle	1°
CL max	1.15
Cdo	.0239
L/D max	17.78

Empennage	
Airfoil section	flat plate
Area(horizontal)	1.2 ft^2
Area(vertical)	0.67 ft^2
Elevator area	0.36 ft^2
Rudder area	0.33 ft^2
Max deflection rudder	+/- 15°
Max deflection elevator	+/- 15°
Horz. Tail Incidence	-1.1°

Propulsion	
Engine	Astro 15
Propeller	TopFlight 12-6
Number of batteries	12
Battery capacity	600 mAhr.
	1.2 volts
Gear ratio	2.385

Economics	
Total Production cost	$390,000
Production hours	150
Flight- break even	76 days

The Hermes CX-7

(note: all dimensions are in inches)

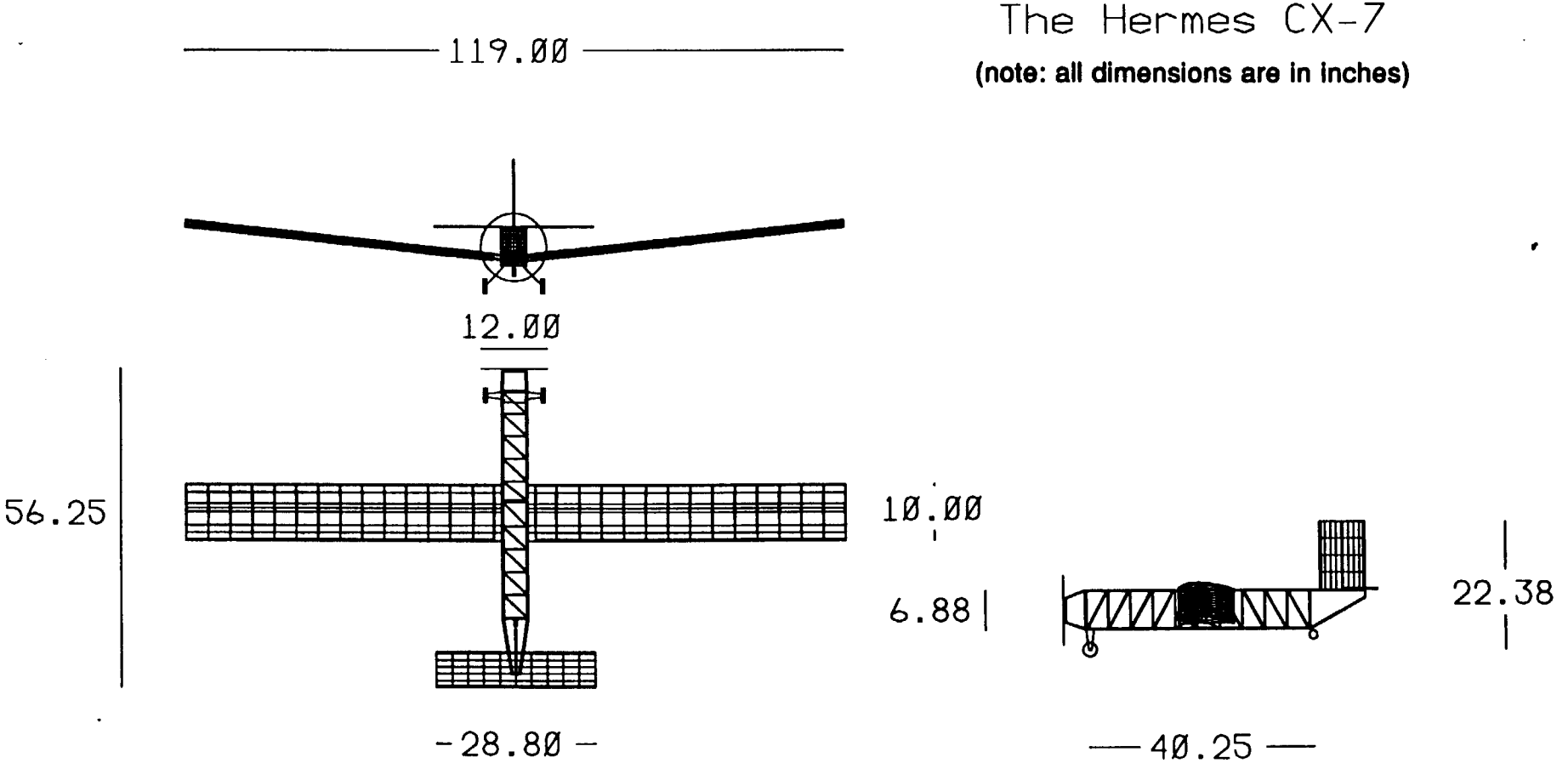

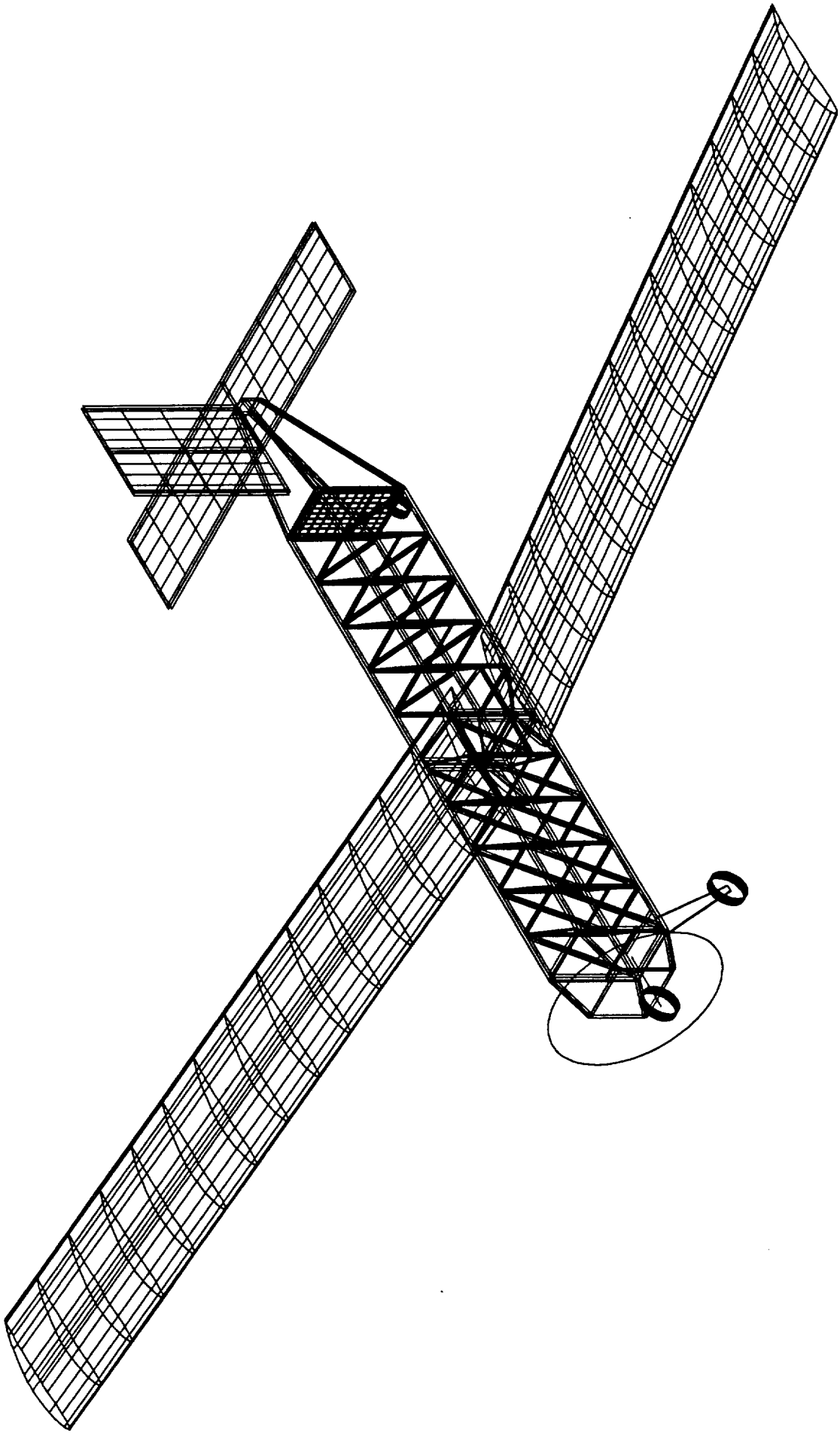

1.2 Critical Data Summary

Parameter	Estimated	Final
<u>Design Goals:</u>		
Cruise Velocity	30 ft/s	30 ft/s
Cruise Altitude	20 ft.	20 ft.
Turn Radius	48 ft.	48 ft.
Endurance	355 s	355 s
Maximum Payload Volume	640 in^3	640 in^3
Range-Maximum Payload	6500 ft.	10,655 ft
Payload at Maximum Range	0 lbf.	0 lbf.
Range-Minimum Payload	10928 ft.	10,928
Maximum Takeoff Weight	6.1 lbf	6.2 lbf
Design Life Cycles	650	650
Aircraft Sales Price	$390,000	$379,000
Target Cost per Cubic Inch Payload	$6.70	$6.70
Target Cost per Ounce Payload	$200	$200
<u>Basic Configuration</u>		
Wing Area	8 ft^2	8 ft^2
Empty Weight	4.5 lbf	4.4 lbf
Maximum Weight	6.1 lbf	6.1 lbf
Wing Loading (max. weight)	12.2 oz/ft^2	12.2 oz/ft^2
Length	54 in.	54 in.
Span	10 ft.	10 ft.
Height	18.875 in.	18.875 in.
Fuselage Width	4.625 in	4.625 in.
Location of Reference Axis Origin	at nose 3.375 in. below prop hub	at nose 3.375 in. below prop hub
<u>Wing</u>		
Aspect Ratio	12	12
Span	10 ft.	10 ft
Area	8 ft^2	8 ft^2
Root Chord	10 in.	10 in.

Tip Chord	10 in.	10 in.
Taper Ratio	1	1
Cmac	-0.156	-0.156
Leading Edge Sweep	0°	0°
1/4 Chord Sweep	0°	0°
Dihedral	6°	6°
Twist	none	none
Airfoil Section	NACA 6412	NACA 6412
Design Reynolds Number	135000	135000
t/c	12%	12%
Incidence Angle	1°	1°
Horizontal Position of 1/4 MAC	23.1 in.	23.1 in.
Vertical Position of 1/4 MAC	6.86 in.	6.86 in.
Oswald Efficiency Factor	.9	.9
Cdo-wing	.0152	.0152
Clo-wing	0.62	.62
Clalpha-wing	0.071/deg.	0.071/deg.
<u>Fuselage</u>		
Length	54 in.	54 in.
Maximum Width	4.625 in.	4.625 in.
Minimum Width	1 in.	1 in.
Average Width	4.17 in.	4.17 in.
Fineness Ratio	8.49	8.49
Payload Volume	640 in^3	640 in^3
Total Volume	1255 in^3	1255 in^3
Planform Area	1.55 ft^2	1.55 ft^2
Frontal area	31.8 in^2	31.8 in^2
Cdo-fuselage	0.00278	0.00278
Clalpha-fuselage	0.0	0.0
<u>Empennage</u>		
Horizontal Tail		
Area	1.2 ft^2	1.25 ft^2
Span	2.4 ft.	2.5 ft.
Aspect Ratio	5	5

Root Chord	5.9 in.	5.9 in.
Tip Chord	5.9 in.	5.9 in.
Taper Ratio	1	1
Leading Edge Sweep	0°	0°
1/4 Chord Sweep	0°	0°
Horizontal Position 1/4 MAC	53 in.	53.5 in.
Vertical Position 1/4 MAC	6.875 in.	6.875 in.
Airfoil Section	flat plate	flat plate
Oswald Efficiency Factor	0.9	0.9
Cdo-horizontal	0.00066	0.00066
Clo-horizontal	0.0	0.0
CLalpha-horizontal	0.078 / deg.	0.078/deg.
Clde-horizontal	0.039 / deg.	0.039/deg.
Cmac-horizontal	0.0	0.0
Vertical Tail		
Area	0.667 ft^2	0.667 ft^2
Aspect Ratio	1.5	1.5
Root Chord	8 in.	8 in.
Tip Chord	8 in.	8 in.
Taper Ratio	1	1
Leading Edge Sweep	0°	0°
1/4 Chord Sweep	0°	0°
Horizontal Position of 1/4 MAC	50 in.	50 in.
Vertical Position of 1/4 MAC	12.875 in.	12.875 in.
Airfoil Section	flat plate	flat plate
<u>Summary Aerodynamics</u>		
Airfoil Clmax	1.39	1.39
Aircraft Clmax	1.15	1.15
Aircraft Lift Curve Slope	0.071 / deg.	0.071/deg.
Aircraft Cdo	0.0239	0.0239
Aircraft efficiency Factor	0.9	0.9
Aircraft Alpha Stall	10 °	10°
Aircraft Alpha Zero Lift	-6 °	-6°
Aircraft Maximum L/D	17.5	17.5

Aircraft Alpha L/D Maximum	2 °	2°
<u>Weights</u>		
Total Empty Weight	4.3 lbf	4.5 lbf
C.G.- most forward x & z	x = 24.01 in.	x = 23.5 in.
no cargo	z = 2.87 in.	z = 2.87 in.
C.G.- most aft x & z	x = 24.01 in.	x = 23.7 in.
max. cargo	z = 3.32 in.	z = 3.32 in.
Avionics	6.05 oz.	6.05 oz.
Maximum Payload	1.6 lbf	1.6 lbf
Engine and Engine Controls	12.3 oz.	10.9 oz.
Propeller	1.0 oz.	0.7 oz.
Battery	12.24 oz.	13.2 oz.
Structure	38.16 oz.	40.35 oz.
Wing	12.4 oz.	14.1 oz.
Fuselage/Empennage	19.96 oz.	20.55 oz.
Landing Gear	5.8 oz.	5.7 oz.
Icg - Maximum Weight	I_{xx} = 31.34 slg in^2	not possible to
	I_{yy} = 41.51 slg in^2	measure
	I_{zz} = 70.51 slg in^2	
	I_{xy} = 0.0 slg in^2	
	I_{xz} = 0.316 slg in^2	
	I_{yz} = 0.0 slg in^2	
Icg - Empty	I_{xx} = 31.14 slg in^2	not possible to
	I_{yy} = 34.74 slg in^2	measure
	I_{zz} = 63.81 slg in^2	
	I_{xy} = 0.0 slg in^2	
	I_{xz} = 0.405 slg in^2	
	I_{yz} = 0.0 slg in^2	
<u>Propulsion</u>		
Type	Astro 15	Astro 15
Number	1	1
Placement	front	front
Maximum Power Available	210 W	210 W
Required Power for Cruise	40 W	40 W

Maximum Current Draw	12.4 A	12.4 A
Cruise Current Draw	5.5 A	5.5 A
Propeller Diameter	12 in	12 in
Propeller Pitch	6 in.	6 in.
Number of Blades	2	2
Maximum Propeller RPM	12000 rpm	12000 rpm
Cruise Propeller RPM	4120 rpm	4120 rpm
Maximum Thrust	2.1 lbf	2.1 lbf
Cruise Thrust	0.34 lbf	0.34 lbf
Battery Type	Sanyo 600 mAhr.	Sanyo 600 mAhr.
Number	12	12
Individual Capacity	600 mAhr.	600 mAhr.
Individual Voltage	1.2 V	1.2 V
Pack Capacity	600 mAhr.	600 mAhr.
Pack Voltage	14.4 V	14.4 V
Stability and Control		
Neutral Point	25.4 in.	25.4 in.
Static Margin	15%	15%
Horizontal Tail Volume Ratio	0.43	0.43
Vertical Tail Volume Ratio	0.017	0.017
Elevator Area	0.36 ft^2	0.36 ft^2
Elevator Maximum Deflection	+/-15°	+/-15°
Rudder Area	0.33 ft^2	0.33 ft^2
Rudder Maximum Deflection	+/- 15°	+/- 15°
Aileron Area	0	0
Aileron Maximum Deflection	0	0
Cm alpha	-0.0143 / deg.	-0.0143 / deg.
Cn beta		
Cl alpha tail	0.078 / deg.	0.078 / deg.
Clde tail	0.039 / deg.	0.039 / deg.
Performance		
Minimum Velocity	23 ft/s	23 ft/s
Maximum Velocity	80 ft/s	80 ft/s
Stall Velocity	23 ft/s	23 ft/s

Maximum Range	10655 ft.	10655 ft.
Endurance at Maximum Range	355 s	355 s
Maximum Endurance	356 s	356 s
Range at Maximum Endurance	10252 ft.	10252 ft.
Maximum Rate of Climb	10 ft/s	10 ft/s
Takeoff Distance	35 ft.	35 ft.
Takeoff Rotation Angle	0.0°	0.0°
Landing Distance	47 ft	47 ft
Catapult Range	970 ft.	not tested
Systems		
Landing Gear Type	tail dragger	tail dragger
Main Gear Position	5.0 in.	5.0 in.
Main Gear Length	4.0 in to ground	4.0 in to ground
Main Gear Tire Size	2.25 in.	2.25 in.
Tail Gear Position	40.5 in.	40.5 in.
Tail Gear Length	1.2 in.	1.2 in.
Tail Gear Size	1.0 in.	1.0 in.
Engine Speed Control		
Control Surfaces	2	2
Technology Demonstrator		
Payload Volume		640 in^3
Payload Weight		1.2 lbf
Gross Takeoff Weight		5.7 lbf
Operating Empty Weight		4.5 lbf
Zero Fuel Weight		4.8 lbf (with max. cargo)
Wing Area		8.0 ft^2
Horizontal Tail Area		1.25 ft^2
Vertical Tail Area		0.667 ft^2
C.G. Position		23.5 in.
1/4 MAC Position		23.6 in.
Static Margin %MAC		20 %
Takeoff Velocity		27.0 ft/s
Maximum Range		10655 ft.

Maximum Endurance		356 s
Cruise Velocity	30 ft/s	30 ft/s
Turn Radius	48 ft	48 ft
Airframe Structural Weight	32.36 oz.	34.65 oz.
Propulsion System Weight	25.54 oz.	24.8 oz.
Avionics Weight	6.05 oz.	6.05 oz.
Landing Gear Weight	5.8 oz.	5.7 oz
Estimated Catapult Range	970 ft.	970 ft.
<u>Economics</u>		
Unit Materials Cost	$125	$127.50
Unit Propulsion System Cost	$250	$232.50
Unit Control System Cost	$225	$212.50
Unit Total Cost	$600	$572.50
Scaled Unit Total Cost	$240,000	$229,000
Unit Production Manhours	150	150
Scaled Production Costs	$150,000	150,000
Total Unit Cost	$390,000	$379,000
Cargo Cost ($/in^3)	$6.70	$6.70
Single Flight Gross Income	$3507	$3507
Single Flight Operating Cost	$2228	$2228
Single Flight Profit	$1279	$1279
Number of Flight to Break Even	76	74

2. Mission Analysis and Design Requirements and Objectives

Before designing the aircraft it was necessary to establish the mission it would be required to fulfill. This mission requirement would serve to define the important parameters which the aircraft must be designed to meet.

2.1 Market Analysis

Group C conducted a trade study to determine how best to satisfy the commercial cargo transportation market. A number of different concepts were explored to determine the most profitable system and several hub arrangements based on different cities were examined.

In order to minimize the cost of operating the fleet, Group C aimed at a hub system that would reduce the number of flights per night and the number of feet flown per night. Reducing the number of flights per night lowered the number of aircraft that were needed to service the system. This reduction cut down the initial cost required to begin operations. Since fuel costs are directly proportional to the distance flown by the aircraft, reducing the number of feet flown per night to deliver a given amount of cargo will reduce the fuel costs.

With these two methods of minimizing cost, Group C settled on a modified two hub arrangement built around cities F and K as shown in figure 2.1-1 below. Because F and K are two of the highest density cities, fewer flights were needed than if lower density cities such as city H had been used as a hub. By using two hubs, fewer flights were required for this system than for a system with more hubs, and the feet flown per night was less than for a system with fewer hubs.

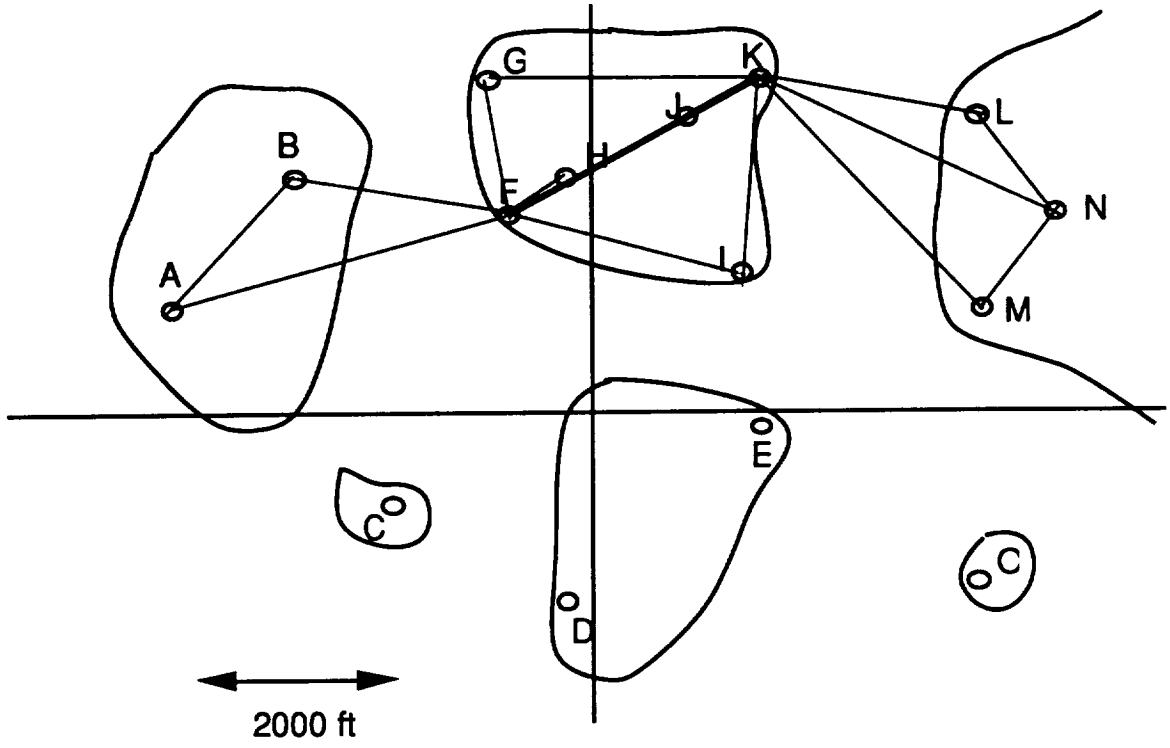

Figure 2.1-1: Proposed Route Structure

The network is described as having a modified hub arrangement because not all of the minor cities feed through one hub or the other. An aircraft will make one of its round trip missions between cities A and B, instead of both missions between cities A and F. A second, similar shuttle run will be set up between cities L, M, and N. In addition to the two shuttle runs, cities I and G will divide their planes between both hubs rather than sending them all to just one. These modifications resulted in a 25% decrease in the number of flights flown per night and the number of feet flown per night when compared to a strict two hub system based on F and K. This system allows for delivery of all packages overnight while minimizing the distance flown per night.

Group C has not included cities C, D, E, or O in the network. The demand for service to and from these cities did not justify the expense of additional aircraft and flight time. Furthermore, the shorter runways at cities C and O would have required special consideration in designing the Hermes CX-7 to decrease its take-off and landing distance. G-Dome Enterprises has the option of servicing cities D and E if they desire to do so. However, adding these cities will increase the average cost of delivering a package by 10 to 15 cents per cubic inch. If G-Dome chooses to begin service to cities C and O, Group C can initiate design of a smaller derivative aircraft with a shorter take-off and landing distance and better economics. The smaller size,

and hence cargo capacity, of the aircraft will not pose a problem in delivering all of the packages in these cities. The demand to cities C and O is low enough to be handled by the derivative aircraft.

Group C can provide G-Dome Enterprises with the capability of servicing the entire northern hemisphere with commercial cargo transportation. The 22 aircraft required for this fleet can be purchased at a unit production cost of $390,000. Larger derivative aircraft will also become available to service high density cities in Aeroworld, thereby reducing the daily costs of operating the fleet. The Hermes CX-7 family of cargo carriers will enable G-Dome Enterprises to capture the large Aeroworld commercial cargo market.

2.2 Mission Requirements

In order for the Hermes CX-7 to be a viable candidate to meet the needs of Aeroworld, it must meet certain requirements based on the route structure outlined above. This section will discuss those requirements which were imposed on the design by the route structure which was selected. An original and complete set of the design requirements and objectives is found in Appendix A.

The most important requirement for the aircraft is for it to be able to fly 6500 ft. at 30 ft/s with a full load of cargo and then loiter for one minute. The longest flight in the route system is 4500 ft between cities A and F. In order for the airplane to be able to legally fly this route, it must be able to divert to the nearest airport and loiter for one minute. In order for the airplane to be able to divert, it must be able to fly an additional 2000 ft. and loiter; hence the need to be able to fly 6500 ft. and loiter for one minute. The airplane must be able to cruise at 30 ft/s in order for all flights to be completed overnight.

The full load of cargo was defined as 640 cubic inches with an average cargo density of 0.03 ounces per cubic inch. This average cargo density is based on the range of 0.01 to 0.04 ounces per cubic inch given in the RFP. It was determined that it was unnecessary to be able to carry full cargo volume at the maximum cargo density since it was decided that this situation is highly improbably. Thus 0.03 ounces per cubic inch was decided as a suitable average cargo density for which to design because it was greater than the mathematical average of the two extremes but less than the maximum.

The route structure outlined above also placed requirements on the takeoff and landing performance. The shortest runway among the cities chosen for service is 60 ft. Thus it will be necessary for this airplane to takeoff and land within this distance.

To minimize the number of aircraft required to service the route structure, the aircraft will have to be designed so that it can be turned around quickly. In line with this it was decided that the batteries must be able to be changed in one-half of a man-minute. This is also advantageous because it will reduce maintenance costs.

3. **Concept selection**

In evaluating the concept for the design of an aircraft to meet the mission requirements three concepts were discussed. The bases of comparison were the available data base of information and thus the reliability of the concept, the ease in which the concept could be built and the effects on performance characteristics such as lift and drag.

3.1 The Joined Wing Concept

The first concept discussed was the joined wing concept in which two lifting surfaces join the main wing structure as pictured in figure 3.1-1.

Figure 3.1-1: The Joined Wing Concept

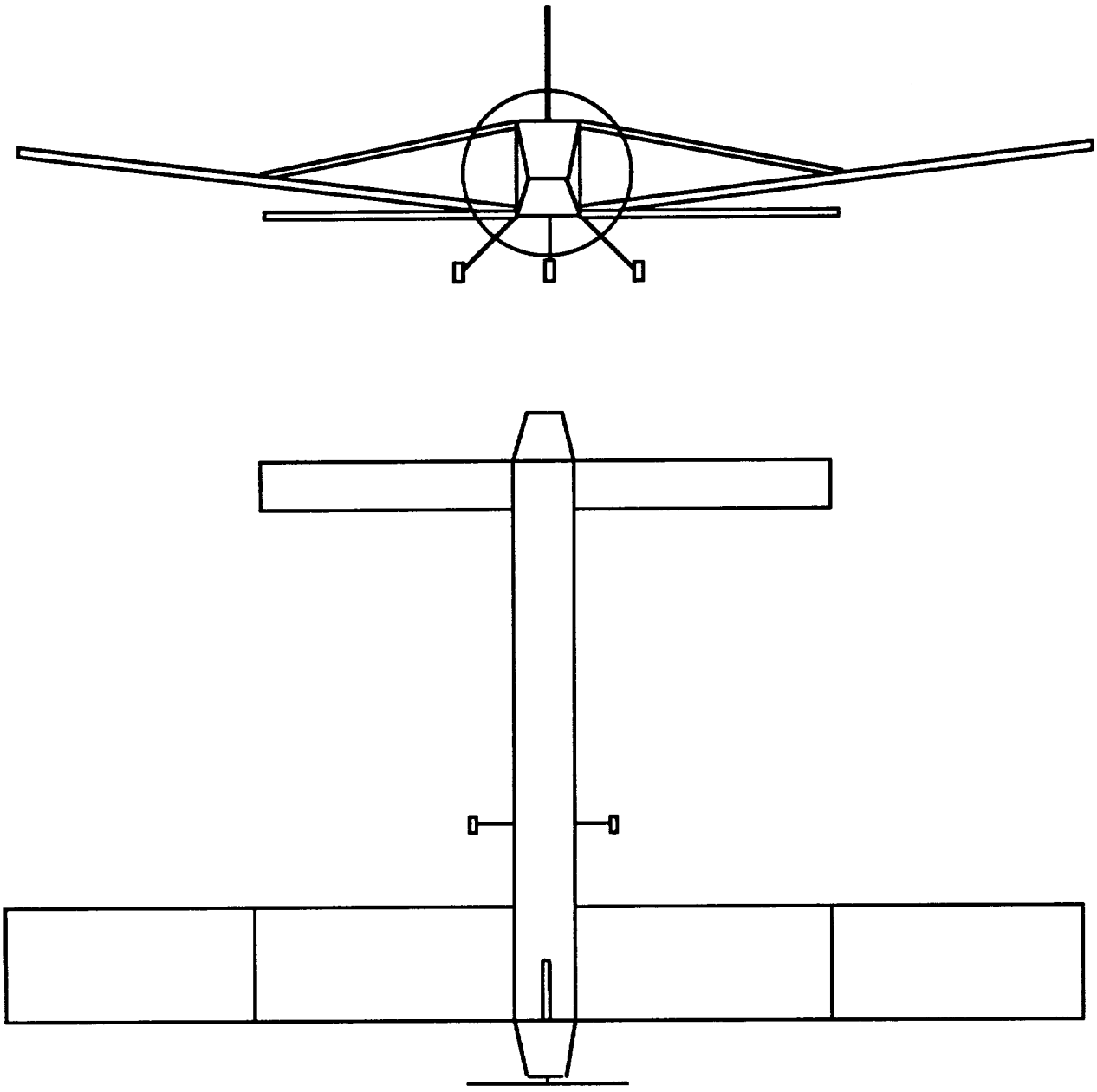

This concept involves advanced technologies with relatively little experimental data available. The benefits of the design relative to a conventional layout partially stem from the surfaces attached to the wing. These surfaces are positioned such that they provided lift and in addition help offset the large wing bending moments. Thus it was expected that a a lighter wing structure could be designed. Through the addition of a canard, it was expected that drag could be reduced and takeoff performance improved because of the additional positive lift provided by the canard.

There are some very significant disadvantages to this design. The first of these is center of gravity travel. In order to achieve adequate stability, it was necessary to position the c.g. of the airframe well aft of the c.g. of the cargo. Consequently, when the cargo was removed from the airplane the c.g. of the airplane shifted dramatically and the airplane became unstable. Another disadvantage was to do with construction difficulty. One of the requirements for this airplane is that it must be able to be disassembled and packed into a 2 ft. x 2 ft. x 5 ft. container. It was impossible to design the airplane such that it would be both easy to construct and easy to disassemble and package. The third disadvantage was that this concept is an unproven technology with no significant historical database from which to draw information. Consequently, this concept was considered very high risk and was not pursued.

3.2 The Canard Concept

The next concept considered was for a canard wing configuration as pictured in figure 3.2-1.

Figure 3.2-1: The Canard Concept

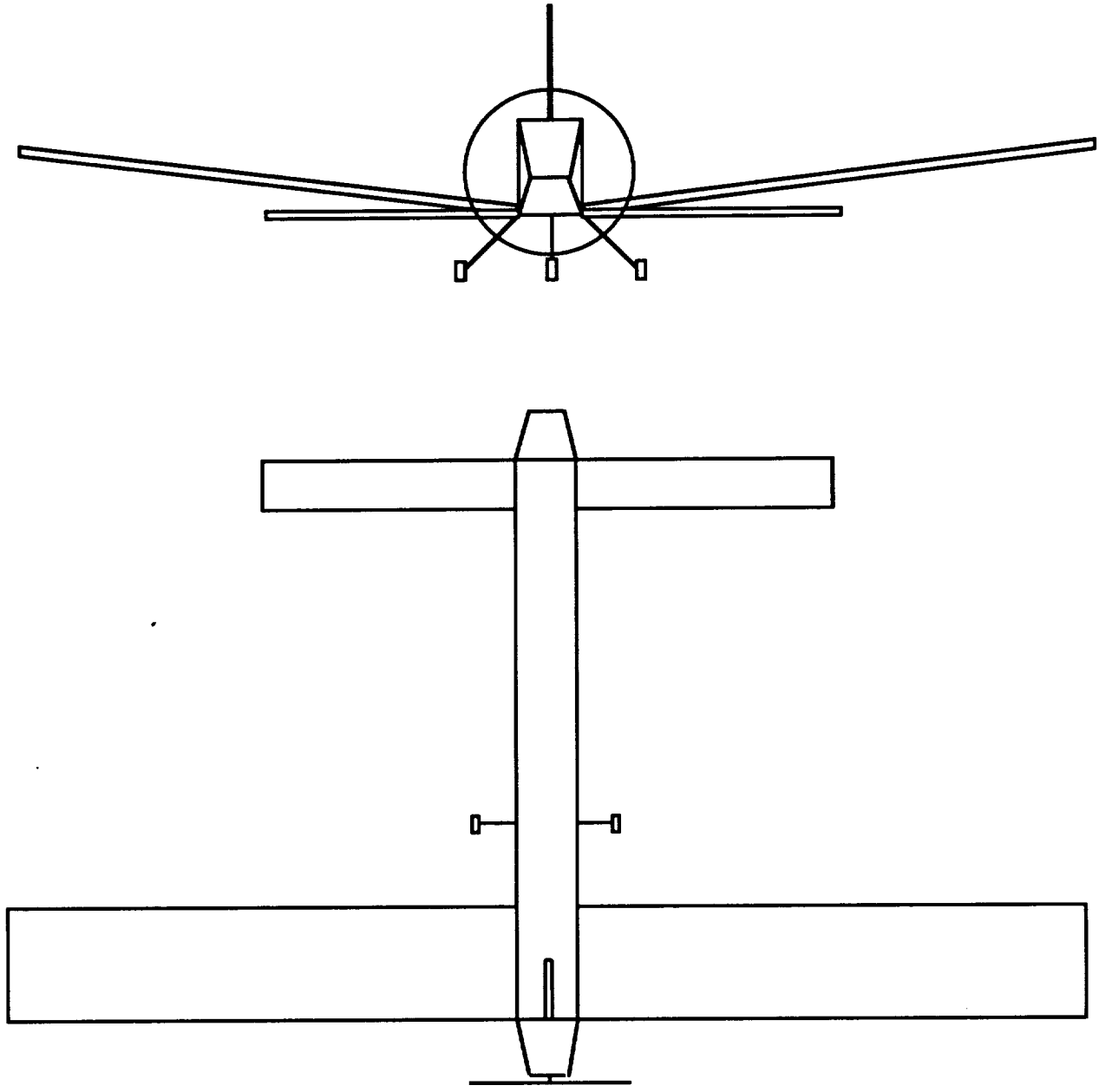

The advantage of this concept over a conventional design is that all lifting surfaces generate positive lift and therefore it was expected that this concept could have improved cruise and takeoff performance. The concept involved control through the use of a rudder and an all-movable canard and no elevators.

As further analysis was performed to determine the needed sizings for the wing and canard to carry an aircraft weighing 5.8 pounds and with fuselage length of 55 inches, it was determined that the canard surface sizing was so large it became more of a second wing. The first disadvantage of this concept arose as result of expected interaction effects of the canard on the air flow over the wing. The second disadvantage of this concept was that it had the same problem with c.g. travel that the joined wing had. Given these two disadvantages, it was decided to pursue a different concept.

3.3 The Conventional Concept

The last concept considered and ultimately chosen for the design of Hermes CX-7 was a conventional low wing aircraft as pictured in figure 3.3-1. This concept includes a conventional tail surface with rudders and elevators. There are no ailerons on the wing surface. The low wing was selected so that the carry-through structure did not interfere with the positioning of the cargo and it does not have taper or sweep to make it easier to construct. This concept is advantageous in that there is a large data base available to provide estimates, predictions, and goals for the design. A conventional aircraft with no taper or sweep and only two control surfaces provides simplicity in construction and in analysis. The center of gravity of the aircraft empty and full are approximately equal thus allowing the plane to be easily flown, trimmed, at any cargo capacity. The disadvantage of this concept is that its cruise and takeoff performance are not expected to be as good as is possible with either of the two concepts outlined above.

Figure 3.3-1: The Conventional Concept

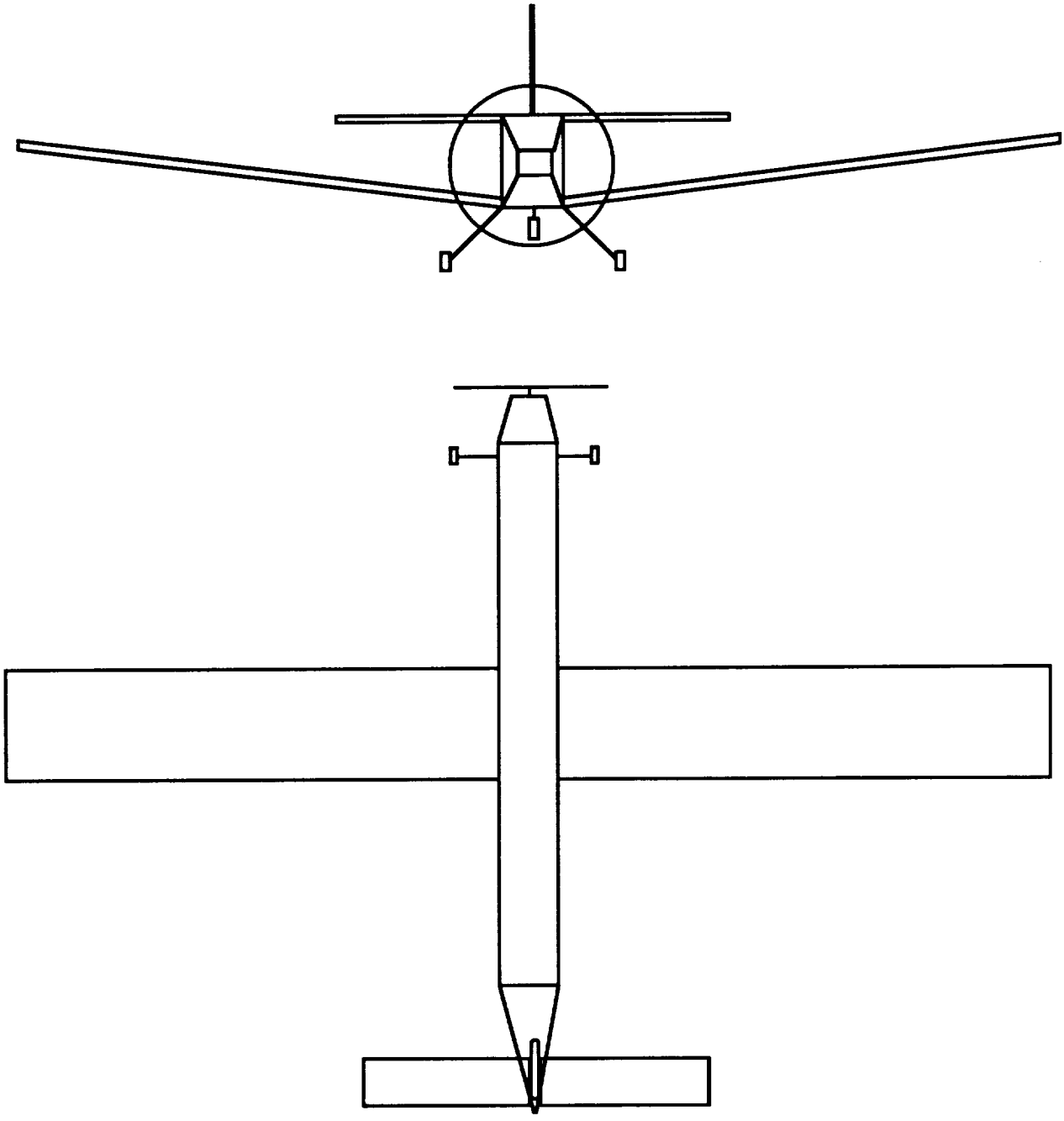

3.4 Justification of the Final Concept

A summary of the advantages and disadvantages for the three concepts considered are summarized in Table 3.4-1 below.

Table 3.4-1: Summary of Advantages and Disadvantages

Concept	Advantages	Disadvantages
Joined wing	-Cruise performance -Takeoff performance -Increased structural support	-No data base -Difficult to construct -C.G travel
Canard	-Cruise performance -Takeoff performance	-Canard too large -Canard-wing interaction -C.G. travel
Conventional	-Large data base -Simple construction -Lower weight -Less surface area	-Increased drag -Longer takeoff distance

The conventional aircraft design was selected because the benefits out weighed both the disadvantages and the potential benefits/disadvantages of the other concepts considered. This concept provides for easy construction because it consists of a rectangular cross section fuselage, a wing surface with no taper or sweep which would be mounted both at a dihedral angle and an angle of incidence through a plug-in carry through structure. The tail section would consist of flat plate airfoil section with rudder and elevator control surfaces. The conventional aircraft has less weight and surface area than the Canard configuration and Joined Wing configuration and weight is of primary concern in this design process. This concept would provide the required performance criteria, while also carrying an adequate load of cargo, again based on the abundant data base. This conventional structure provides an internal structuring conducive to practical placement of engine, servos, batteries, and most importantly cargo. The cargo is easily loaded and unloaded through a single cargo door either in the rear or top of the fuselage structure. The low wing structure was chosen even though the dihedral effects are better for a high wing configuration, because it allows for the carry through structure to remain below the internal area needed for cargo space, without disrupting the operation of the control rods and battery lines. This simple design minimizes the man hours necessary for analysis and construction and the cost of construction both important economic considerations.

4. Aerodynamic Design Detail

The aerodynamic concerns which were investigated included the design of a system with maximum efficiency while maintaining minimum weight.

4.1 Wing Design

The wing of the Hermes CX-7 was designed to provide the best mix of aerodynamic performance and structural stability. Several wing sizes were explored, with various chord and span lengths, before the final wing configuration was chosen. The characteristics of the wing which was chosen are summarized in the table below.

Table 4.1-1: Wing Geometry

Wing Area	8 $ft.^2$
Span Length	10 ft.
Chord Length	0.83 ft
Aspect Ratio	12.05
Dihedral Angle	6^o

All of these values were determined either to satisfy required performance or physical constraints. The wing area, for example, was determined to provide the required lift for the aircraft at takeoff, while avoiding the extra drag which would have been caused by a larger planform. The span length was limited by a physical constraint placed on the system. It was required that the product, when disassembled, fit within a container no longer than 5 feet. The chosen wings are to be plugged into the fuselage, and therefore the largest wing possible has a length of 5 feet, including its carry through structure. The physical structure of the wing and its carry-through is described in section 9.3.2.

In designing the planform of the wing several conflicting trends had to be compromised. To minimize induced drag, it is desirable to have as high an aspect ratio as possible. However, by increasing the aspect ratio, the bending moments of the wing are increased and a larger, heavier structure is required to handle these bending moments. Also, by increasing the aspect ratio, the chord is shortened which decreases the Reynolds number of the wing. For the low Reynolds number at which this wing operates, there is a significant increase in the profile drag of the wing when the Reynolds Number decreases. The thickness of the airfoil also effects the

performance of the wing as it permits a lighter structure to be designed but with the penalty of higher drag. Figure 4.1-1 below combines these different effects to find the optimum aspect ratio for an 8 ft^2 wing designed to carry a 5.8 lbf airplane.

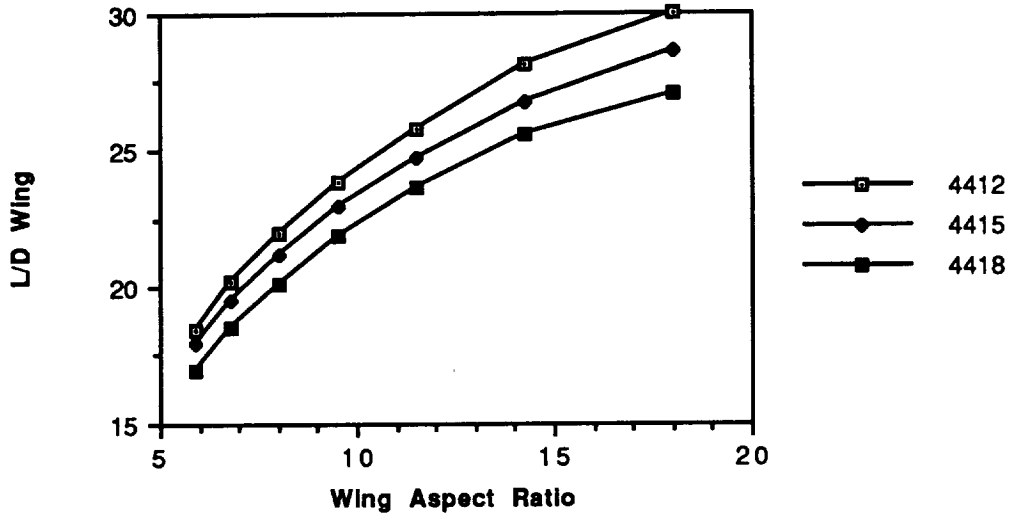

Figure 4.1-1: Aspect Ratio Effect on Lift-to-Drag Ratio of the Wing

Based on the above figure, the wing was designed for the highest aspect ratio possible while still being able to fit it in the required 2 ft. x 3 ft. x 5 ft. box with a 12% thickness airfoil. This produced a wing with a span of 10 ft. and a chord of 10 inches. The wing area of 8 ft^2 was selected based on the minimum area able to give sufficient lift at takeoff. This was based on a maximum lift coefficient of approximately 1.1.

Other important aspects of the wing are its placement, dihedral, and lack of taper. One of the unique characteristics of the Hermes CX-7 when compared to other concepts which are being constructed for the same mission is its low wing design. As was discussed above, all of the avionics and batteries, as well as the carry through structure of the wing, will be placed underneath the cargo. This will allow for easy access to the transported material through a door in the top of the fuselage. The 6^o of dihedral was chosen in order to provide roll control and stability. Since the low wing concept is not as roll-stable as a high wing, this dihedral was a critical aspect. The detailed stability considerations are presented in section 7. Finally, the wing chosen for the design was decided to possess no taper, twist, or sweep. Although a tapered wing would have better lift-load characteristics than a straight wing, it was determined that the difficulty to construct such a design outweighed any added performance.

4.2 Airfoil Selection

Several requirements were used in order make a final decision on which airfoil would be used for the system. Data from wind tunnel tests on several airfoils were explored using reference 1 in order to make a final decision. Preliminary calculations were conducted which led to the conclusion that a lift coefficient of approximately one would be required at takeoff. This necessitated choosing an airfoil which could provide a maximum coefficient of lift significantly greater than this in order to allow for finite wing effects which would decrease its performance. This was especially important since the chosen concept does not include any high-lift devices. Several airfoils in reference 1 provided this characteristic, but data was not given for all of these at a Reynolds number comparable to the 140,000 which is expected at flight conditions. A number of airfoils were determined to provide this lift requirement, among them were the GO 797, the Wortmann FX 63-137, and the NACA 6412. The drag characteristics were then explored in order to aid in the decision. This eliminated the GO airfoil since its drag was higher than the 6412, with no additional lift. Lastly, the shape of the airfoil itself was used as a determining factor. The FX 63-137 provided considerably more lift than the 6412, but it possessed a cusp at the trailing edge. This was determined to be difficult to construct effectively, and was therefore discarded.

The chosen airfoil, therefore, was the NACA 6412 shown in figure 4.2-1. This airfoil provided a maximum lift coefficient of 1.39, and does not possess unreasonable drag. Although the lower surface of the airfoil is not flat, which would have been the simplest to build, it does not possess a cusp or any other aspect which would make it difficult to construct. The shape of the airfoil, as well as its lift curve are presented below.

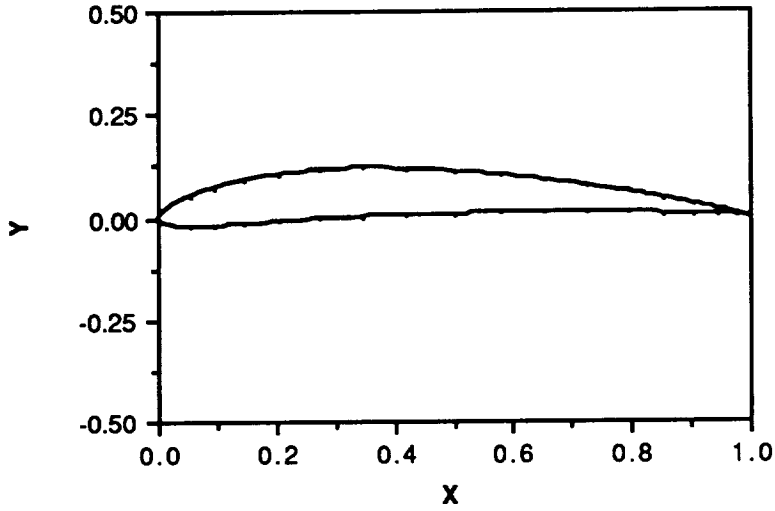

Figure 4.2-1: NACA 6412 Airfoil

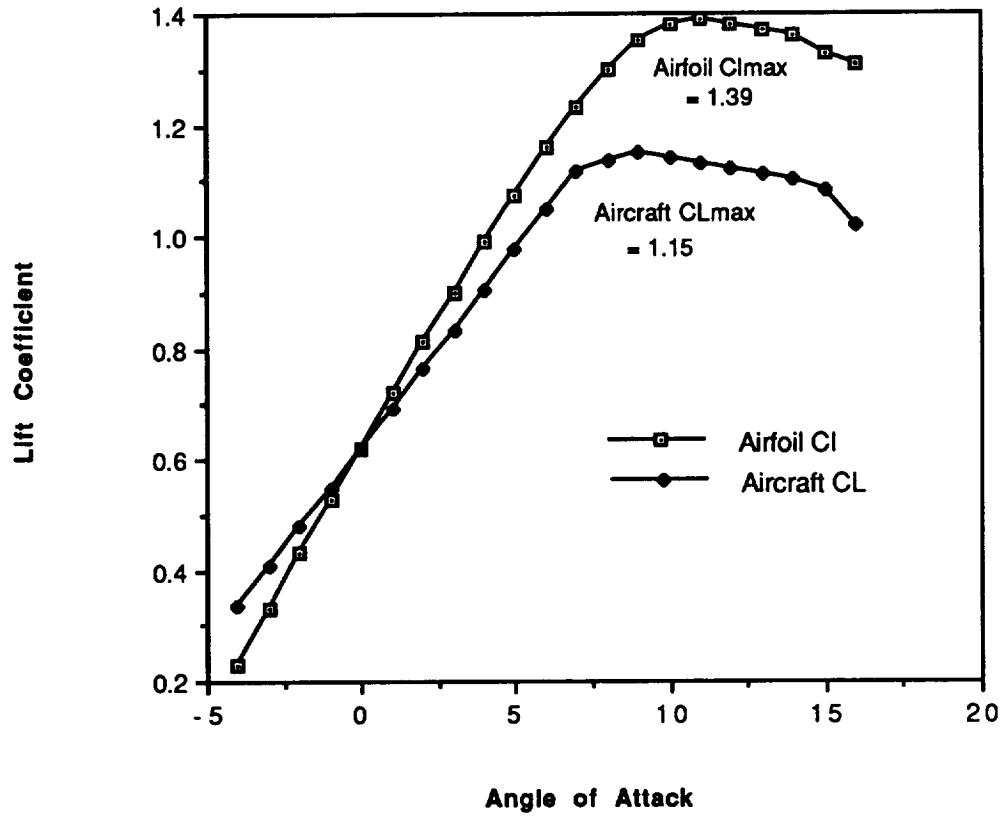

Figure 4.2-2: NACA 6412 and Airplane Lift Curves

As can be seen from the lift slope, figure 4.2-2, the maximum coefficient of lift for the finite wing was considerably lower than the ideal airfoil. This effect shows clearly that the criteria of high lift coefficient for the chosen airfoil was a critical consideration. The maximum lift coefficient provided by the wing was determined to be 1.15. This was determined through finite wing effects and lifting line theory. This basically involved determining the effects that the actual size of the wing on its performance. The reduced slope was due to losses around the tip, and the lowered Clmax was found by determining what portion of the wing would stall first, and at what lift coefficient this would occur. The lift slope for a finite wing is given by equation 4.2-1

$$a=\frac{a_o}{1+57.3a_o/\pi eAR} \qquad (4.2\text{-}1)$$

where ao is the lift curve slope for the equivalent infinite wing and e is the span efficiency factor (reference 1). These methods predicted the expected decrease in lift slope and maximum lift coefficient. Further exploration of the required lift at takeoff confirmed that the maximum C_L which would be required upon takeoff would be no greater than 1, which could be easily provided by the wing.

4.3 Drag Prediction

The drag of the aircraft was determined through a component drag breakdown method described in the masters thesis written by Daniel Jansen (reference 2). This basically required determining the relative amount each component of the aircraft would contribute to the total drag of the system. The Reynolds number for each item was used in order to make an estimate of what percentage of these components would see laminar and turbulent flow. The friction coefficient for each item was then computed, and combined to determine the total drag. The final program was completed on TK Solver, and is attached in Appendix B. This method of drag prediction was compared to an initial drag estimation, in order to check its accuracy. The initial method did not include a drag breakdown, but was simply a method to provide a basic estimate of drag. The two methods provided drag values which were within 5% of each other. The drag breakdown method was determined to be more accurate, however, since the initial method was only a basic estimate.

The drag component breakdown which was determined to find the total aircraft drag is presented below. This breakdown is based on the reference wing area. Thus yielding a total drag coefficient of .0239.

Table 4.3-1: Profile Drag Breakdown

Component	Drag Coefficient
Wing	.0152
Fuselage	.00278
Empennage	.00132
Landing Gear	.0046

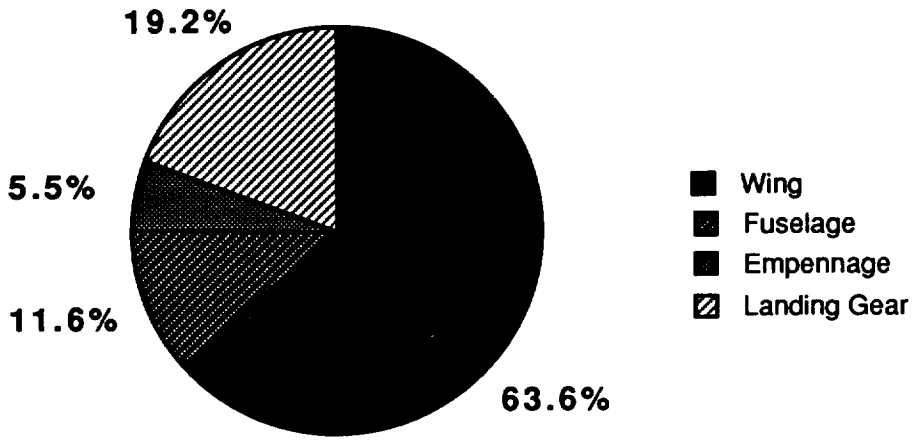

Figure 4.3-1: Component Drag Breakdown

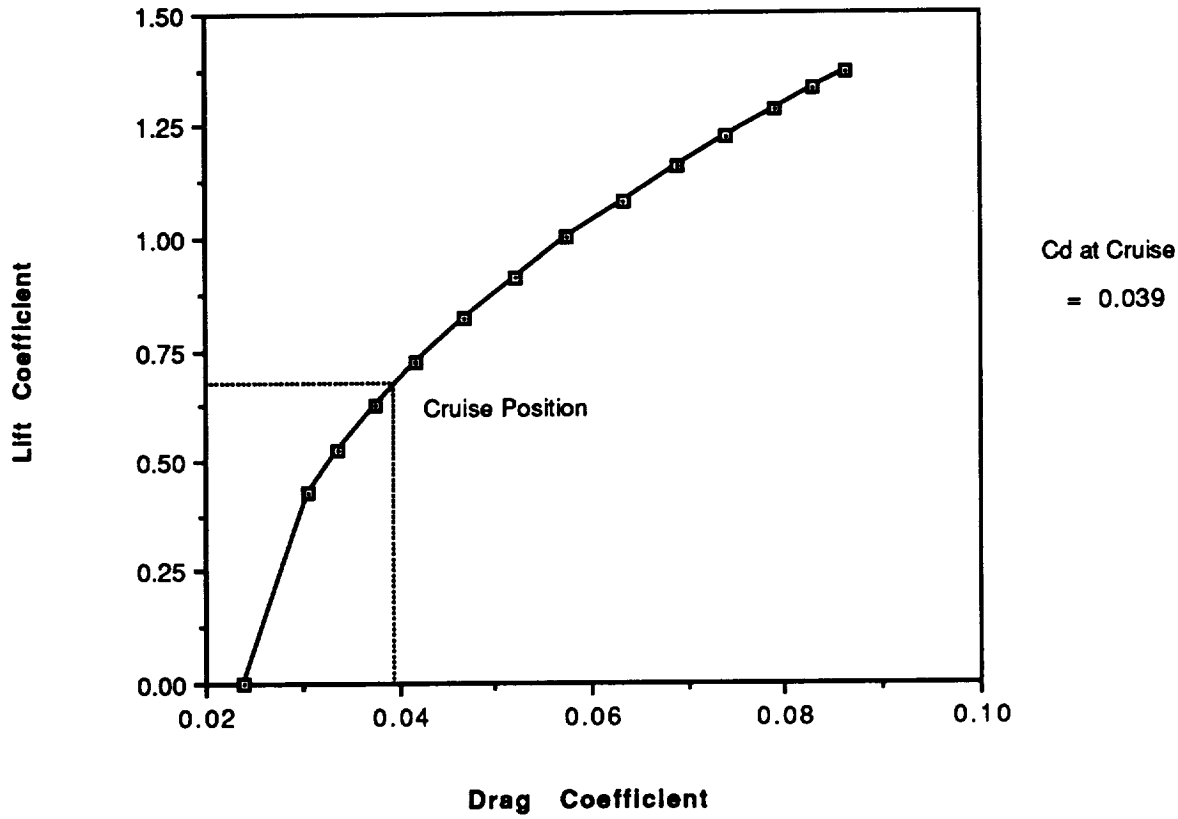

Figure 4.3-2: Aircraft Drag Polar

As can be seen from figure 4.3-1, nearly two-thirds of the total drag of the aircraft is due to the wing. It was expected that the wing provide a large amount of drag, but this was significantly higher than expectations.

Once the drag breakdown was completed, the drag polar and the lift-to-drag ratio were completed. The drag polar, figure 4.3-2, showed that the Cd_o of the aircraft was approximately .0239, while the drag coefficient which will be expected at cruise had a value of 0.039. Likewise, the Lift-to-Drag vs. Velocity, figure 4.5, showed that the maximum L/D was approximately 17.4, but at the cruise velocity of 30 feet per second, the Lift-to-Drag value was 16.84.

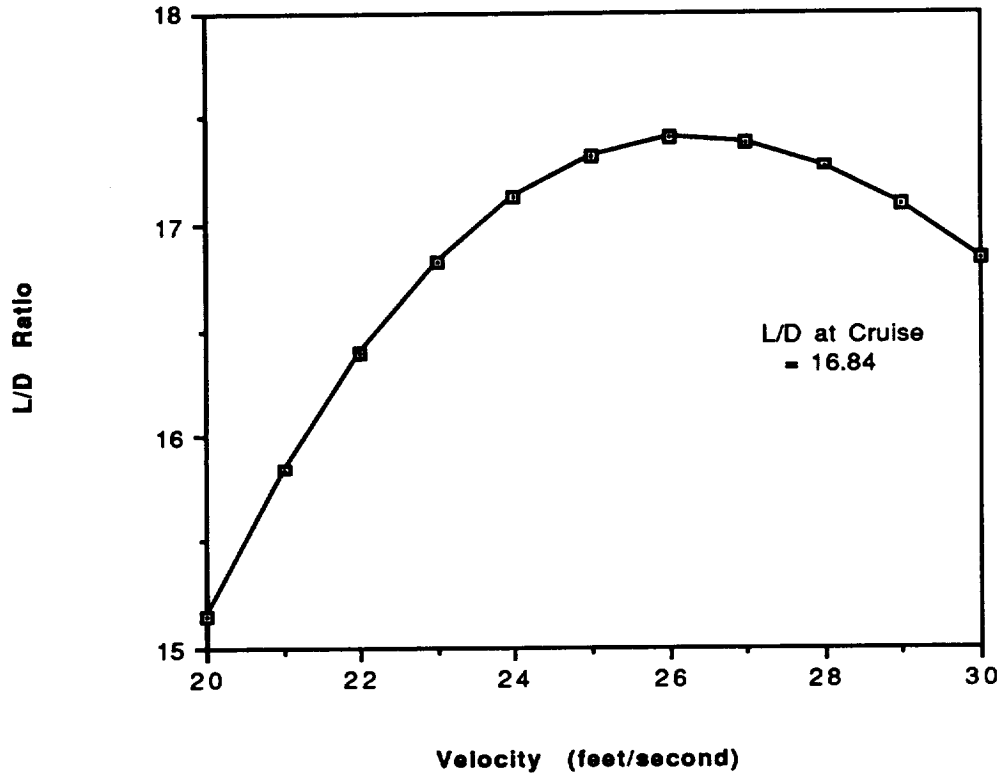

Figure 4.3-3: Aircraft Lift-to-Drag Ratio

5. Propulsion System Design Detail

The Design Proposal Requirements were the driving force in the selection of the propulsion system. After its requirements were evaluated, these propulsion goals were established:

1. The aircraft must take-off and land under its own power in less than 60 ft.
2. The aircraft's propulsion system will be an electrically powered motor with nickel-cadmium batteries, and controlled by a radio control system. This propulsion system was to be low in both weight and cost.
3. Lastly, the aircraft will be able to sustain a flight speed in cruise at 30 ft/s.

5.1 Engine Selection

As stated in the introduction, the system selection was driven by the requirement for an electric motor was included in the Design Proposal Requirements. To decide upon a specific electrically powered motor, the propulsion team found the power required at takeoff the most stringent requirement of the propulsion system. There were three engines considered to accomplish the mission at hand: the Astro 05, the Astro 15, and the Astro 25. The table below compares these engines:

Table 5.1-1 Comparison of Three Competing Engines

	Astro 05	Astro 15	Astro 25
Takeoff distance (ft)	> 300	31.7	31.6
Number of batteries (1.2 volts/batt.)	8	12	16
System weight (oz)	14.66	19.74	27.32
Gear Ratio	1.82	2.38	1.82
Battery resistance (ohms)	0.05	0.08	0.09
Motor resistance (ohms)	0.05	0.120	0.138
Current Draw, TO (amps)	4.26	12.27	8.52

The propeller used for this comparison was the Top-Flight 12-6 at a aircraft weight of 5.8 lbf,a fully loaded aircraft. From the information above, the propulsion team chose the Astro 15. This motor could accomplish the strict takeoff distance requirement and also weighed less than the Astro 25. Note from Table 5.1-1, the Astro 25 had comparable performance to the Astro 15, but the Astro 25 weighed almost one-half

pound more than the Astro 15. There was no need to carry this extra weight thus the Astro 15 was selected.

5.2 Propeller Design

The selection of the propeller was directly related to the operation of the engine. The power output of the engine depends upon the the propeller. Again, the propeller selection was dependent upon the takeoff requirements. At least a 10 inch diameter propeller was needed to satisfy the constraints. Three propellers competed for the final selection: the TopFlight 12-6, the TopFlight 10-4, and the Tornado 10-6. Since the aircraft is designed to be a cargo plane, it may carry many different cargo configurations. In order to insure the safety of the RPV, the aircraft must be able to operate at different weights. Figure 5.2-1 below shows the propulsion system performance in takeoff for different weights of the aircraft (due to varying amounts of cargo).

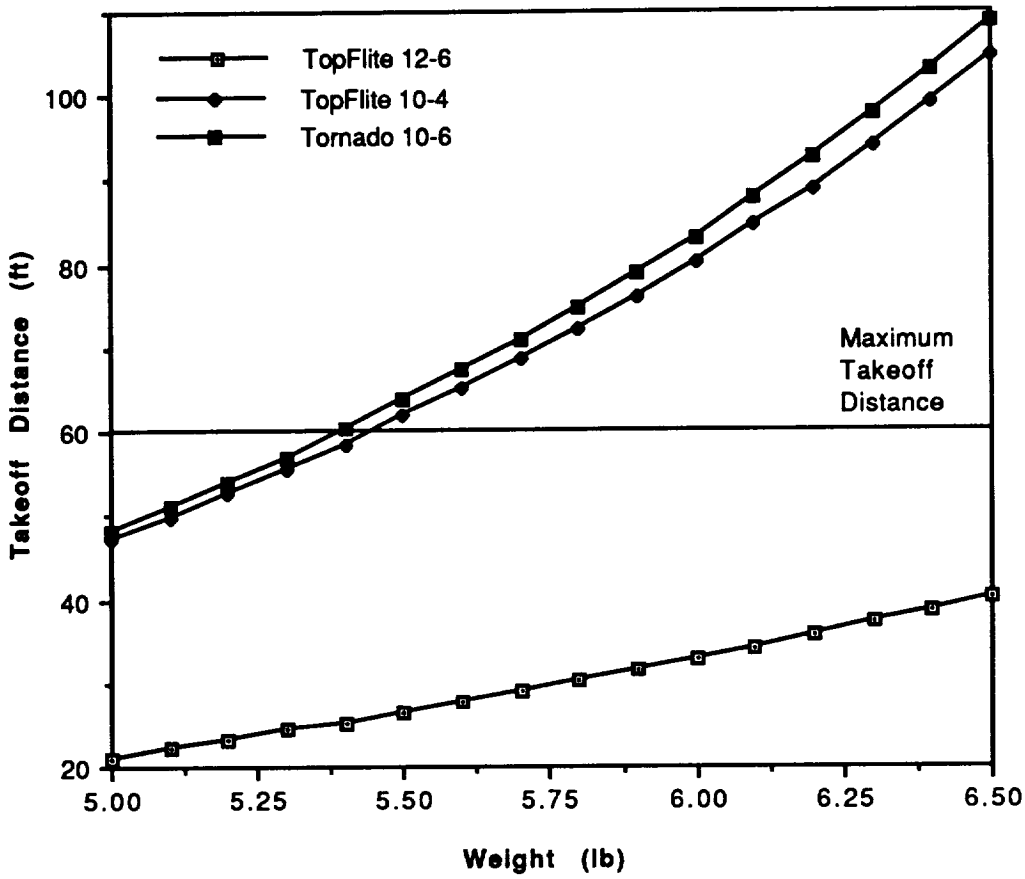

Figure 5.2-1 Takeoff Distance as a Function of Weight

As shown in the figure above, unless there were only small cargo loads in the aircraft, the TopFlight 12-6 was the only legitimate choice. This was the eventual propeller selected, however, this was not the only criterion the selection was based upon.

The best choice of a propeller would be one which has the best range of efficiencies over the widest range of power settings. At cruise, the propellers were compared for their efficiency over a range of RPMs. Note for the following two figures, the propeller data was obtained from the Apple IIe propeller analysis code.

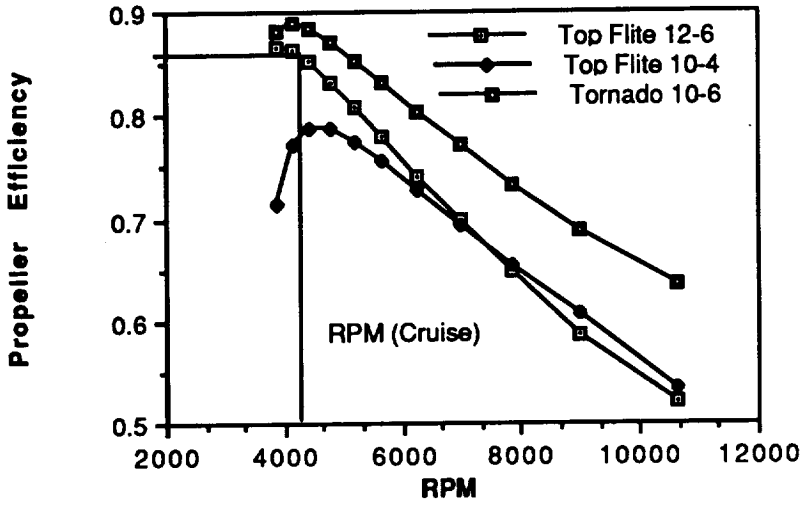

Figure 5.2-2 Propeller Efficiency vs RPM at cruise velocity

Although the Tornado 10-6 has the best propeller efficiency at the cruise RPM, this propeller would not meet the takeoff distance requirements at most operating weights. The TopFlight 12-6 performs at almost a maximum at the cruise RPM and its efficiency is slightly better than 0.85.

Similarly, Figure 5.2-3 shows these competing propellers over a range of advance ratios.

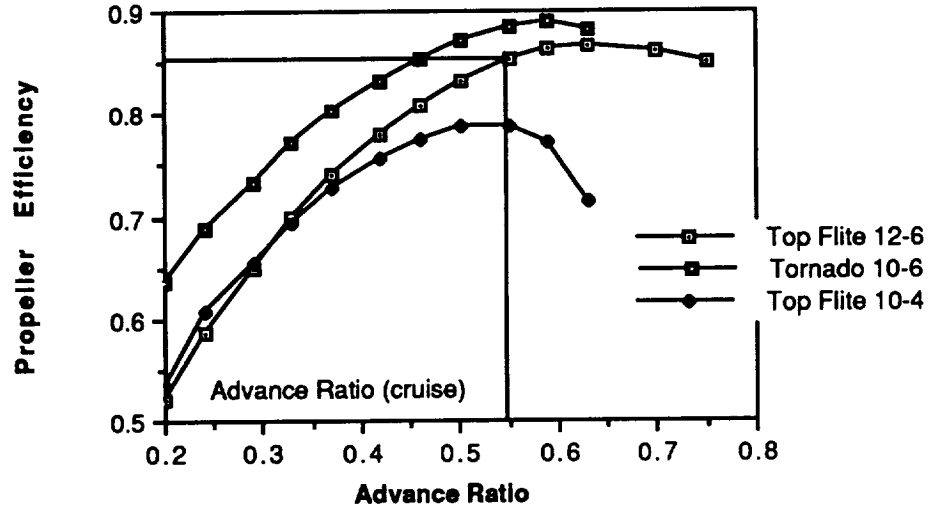

Figure 5.2-3 Propeller Efficiency vs Advance Ratio at cruise velocity

The TopFlight 12-6 shown with its cruise performance included on the previous plot, has a cruise advance ratio of 0.55. The advance ratio at cruise was determined by the propeller RPM, again taken from the propeller spreadsheet on the Apple IIe computer. Since the TopFlight 12-6 propeller was the only propeller able to provide the takeoff distance criterion, it was the propeller chosen.

5.3 Battery Pack Selection

The battery pack was chosen simply to accomplish the range and endurance of the mission at the lowest cost and weight. Furthermore, the battery replacement must take as little time as possible (this step includes recharging of the batteries).

The suggested battery load for the Astro 15 is 12 batteries at 1.2 volts per battery. These batteries placed in series produced an output voltage of 14.4 volts. This output voltage satisfied the requirements of the mission.

The next step was to choose the actual battery, and thus, pick a battery capacity (in milli-amp hours) to accomplish the mission. The range and endurance specified in the DR&O could be met with 300 mAhr. batteries. After deciding upon this battery, the P-30As, the Panasonic Corporation informed the propulsion team that this size of batteries was not available at this time. Therefore, the batteries picked are the smallest capacity, a 600 mAhr. battery. These batteries increased the weight of the aircraft, but on the other hand, provide even a longer range and endurance.

In short, the aircraft will carry a 12 pack of 600 mAhr. batteries at 1.2 volts per battery. This results in a 14.4 voltage output (at a maximum voltage setting) and carries a slight weight penalty when compared to the 300 mAhr. batteries which are not in production.

5.4 Engine Control

Speed control is needed to differentiate between the power required at takeoff and the power required in cruise. This controller allows the pilot to change the amount of the voltage supplied to the engine and hence the change in motor RPM.

The speed control will be used as part of the propulsion system shown below in Figure 5.4-1:

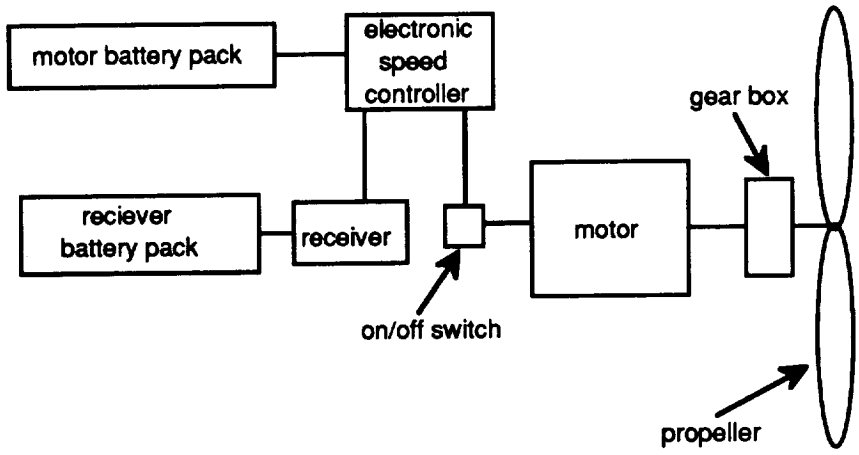

Figure 5.4-1 Schematic Diagram of the Propulsive System

The electronic speed controller, shown above, can be used to vary the voltage input into the motor, which enables the propeller speed to be changed according to pilot need and the particular flight regime.

The speed controller will be located on the Futaba 6FG radio system and a voltage setting of approximately 9 volts will be needed to maintain steady level flight. This corresponds to a current draw of approximately 5.8 Amps at cruise(see Figure 5.5-2). During takeoff, the controller is set for maximum voltage, 14.4 volts.

5.5 Performance Predictions

Using the PAVAIL program, the following predictions of the performance of the airplane at cruise can be made. First, a plot of different voltage settings for the aircraft is included below in Figure 5.5-1. This data is based on a total weight of 5.8 lbf.

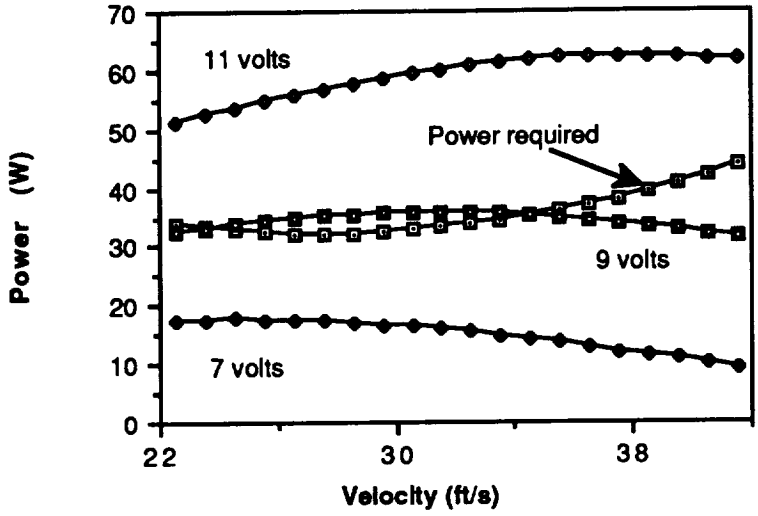

Figure 5.5-1 Power available at various voltage settings

The correct voltage setting at the cruise velocity of 30 ft/s is approximately 9 volts. At 11 volts the aircraft would be climbing and this setting may be used for climb out. On the other hand, the aircraft is descending at a setting of 7 volts. This voltage could be set for descending to land. This airplane is grossly overpowered at its cruise condition because of the stringent takeoff requirement.

Second, the effect of voltage settings on current draw was explored. This provided a "quick and dirty" estimation of the endurance of the aircraft.

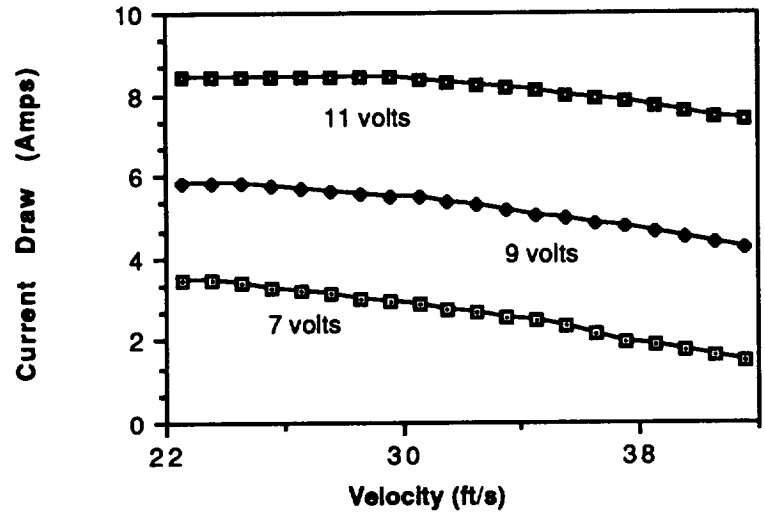

Figure 5.5-2 Current Draw at various voltage settings

At the cruise velocity the current draw is approximately 5.75 amps. Since are batteries are 600 mAhr. batteries, the endurance can be approximated at 6 minutes. This agrees with the predicted value.

Comparing the propulsion performance of the RPV with the mission requirements, the electric propulsion system meets and exceeds all requirements. Although the system provides far more power than necessary at cruise (due to the strict limitations on takeoff performance) its performance at cruise is still adequate.

6. Preliminary Weight Estimation Detail

Weight is one of the most important parameters in the design. Therefore, every effort was made to keep track of the total weight of the aircraft throughout the design process. This started with using historical data to estimate potential weight of the aircraft and concluded with a final estimate based on the designed parts of the aircraft.

6.1 Component Weights

The weight of the Hermes CX-7 was essentially determined by the route structure decided upon and the external lines needed to operate effectively in the Aeroworld market. Upon discussing the weight of the aircraft with persons knowledgeable in the field of RPV aircraft design, it was determined that, if at all possible, the weight of the aircraft should be limited to 6 pounds or less. Since the route structure relied on several derivative aircraft of the same initial mold, it was decided not to build the largest of these three derivatives, but the one more moderately sized. Since, it has been realized that the team was a little too conservative in the estimation of the maximum weight. In reality, the larger derivative aircraft, probably weighing about 7 pounds, most likely could have been constructed and flown.

The weight estimation represented the crux of the preliminary design phase, since its outcome would affect virtually the whole direction of design. It was important that the weight not be grossly underestimated, since an actual weight much greater than the estimated weight would lead to reduced performance at best and a grounded aircraft at worst. Overestimation of the weight, although more desirable, would lead to an aircraft designed about a weight that was much too heavy and would therefore never realize its full potential, since performance would again be sacrificed. Once the route structure was determined, thus deciding the optimum cargo volume to be carried, the weight estimation could be carried out in earnest.

The entire procedure of weight estimation had two possible foundations: Experience and previously compiled databases. In this case, there was no experience to rely upon, since the team had never designed or constructed an aircraft of this type before. Therefore, the foundation of the entire weight estimation were the design proposals and the aircraft built by previous design teams.

Many of the parts to be included in the Hermes CX-7 were standard on previously flown aircraft. These parts included most of the propulsion system and avionics, whose weights could then be taken directly from the database, and thus did not present a problem in the estimation.

In order to estimate the remaining parts of the aircraft, all available aircraft designed and constructed in the spring of 1991 were weighed in order to make comparisons. Because most parts of the planes could not be taken apart and weighed separately, the estimations were crude at best. The empennage and landing gear weights had to be included in the fuselage weight in this preliminary calculation. As the design progressed, these were separated and estimates were made on each item accordingly. Because each individual part could not be weighed and were thus lumped together, the initial weight estimates were made conservatively. It was hoped these estimations would account for the weights of items that were missed or unforeseen. After weighing several wings and measuring their planform areas, an average value of 0.12 lbf/sq.ft. was used to estimate the weight of the wing. Since the wing was to have a planform area of 8 sq. ft., it would then weigh an estimated 15.4 ounces. After the design of the wing was complete, the weight was reestimated at 12.4 ounces, which differed from the preliminary figure by 20%. The initial estimation of fuselage weight was over by 4 ounces, or 12%. Note that the final "design" weights are less than those initially estimated. Although these weights were overestimated, they were balanced by the underestimation of battery weight, which was 4 ounces heavier than expected due to unavailability of the desired type.

As the design developed, the original estimations were modified as parts of the aircraft were actually designed or decided upon. During the design, the previous proposals were continuously relied upon in order to make more accurate weight estimations as the configuration changed slightly.

The final estimation of weights is given in table 6.1-1, while figure 6.1-1 gives the weight breakdown of selected components and systems. The items marked by an asterisk in table 6.1-1 are items for which the actual weight is not known, and these are generally the structural parts in contrast to the avionics and propulsion system components. It is interesting to note the final weight estimation of 91.65 ounces (5.73 lbf) compares favorably with the first weight estimation of 93.75 ounces (5.86 lbf). The proximity of the final estimate to the initial was probably due to luck as much as skill, and the actual weight of the prototype will no doubt differ slightly from both of these estimates.

The percentage of the payload weight to the total weight of the aircraft is low in comparison to other groups, but this again relates to the fact that the team decided to build a more conservative aircraft. The larger derivative planned will no doubt have a much higher payload to total weight ratio.

Table 6.1-1 Preliminary Weight Estimate
(* Denotes Estimated Weight)

	Part:	Estimated Wt (oz)	Actual Wt (oz)
	Wing:		
2	Leading Edge Spar	.42*	
2	Trailing Edge Spar	.37*	
2	Longerons	.19*	
32	Ribs	1.70*	
2	Top Spar Cap	1.92*	
2	Bottom Spar Cap	1.44*	
2	Spar Web	1.11*	
	Monokote (1150 sq. in.)	4.15*	
	Other (Glue & Unaccountables)		
	=10% Wing Weight	1.13*	
	Wing Total Weight	12.42*	14.1
	Avionics:		
	Receiver	0.95	0.95
	System Battery	2.0	2.0
2	Servos @ .6 oz each	1.2	1.2
	Speed Controller	1.9	1.9
	Avionics System Weight	6.05	6.05
	Propulsion:		
	Engine (Astro 15)	7.5}	
	Mount	1.2}	9.9
	Gearbox	1.6}	
	Prop	1.0*	0.7
12	Batteries @ 1.02 oz each	12.24*	13.2
	Wiring Harness	2.0*	1.0
	Propulsion System Weight	25.54*	24.8

Fuselage:			
	Vertical and Horizontal Tails	4.0*	
	Landing Gear		
	Forward	4.3*	
	Aft	1.5*	
	Attachment Support	0.51*	
	Truss Structure (F.E.M.)	5.2*	
	Bulkheads		
	Engine Firewall	1.35*	
	Aft Cargo Support	.39*	
	Floors		
	Cargo Floor	2.08*	
	Battery Floor	.42*	
	Avionics Floor	.42*	
	Monokote (1700 sq. in.)	3.06*	
	Avionics Support	1.0*	
2	Control Pushrods (total)	1.53*	
	Carry-Through Support	2.7*	
	Fuselage Total Weight	28.46*	26.25
Cargo:			
	(640 cubic in. @ .03 oz/cubic in.)	19.2*	19.2
Total Weight:		**91.65***	**90.4**

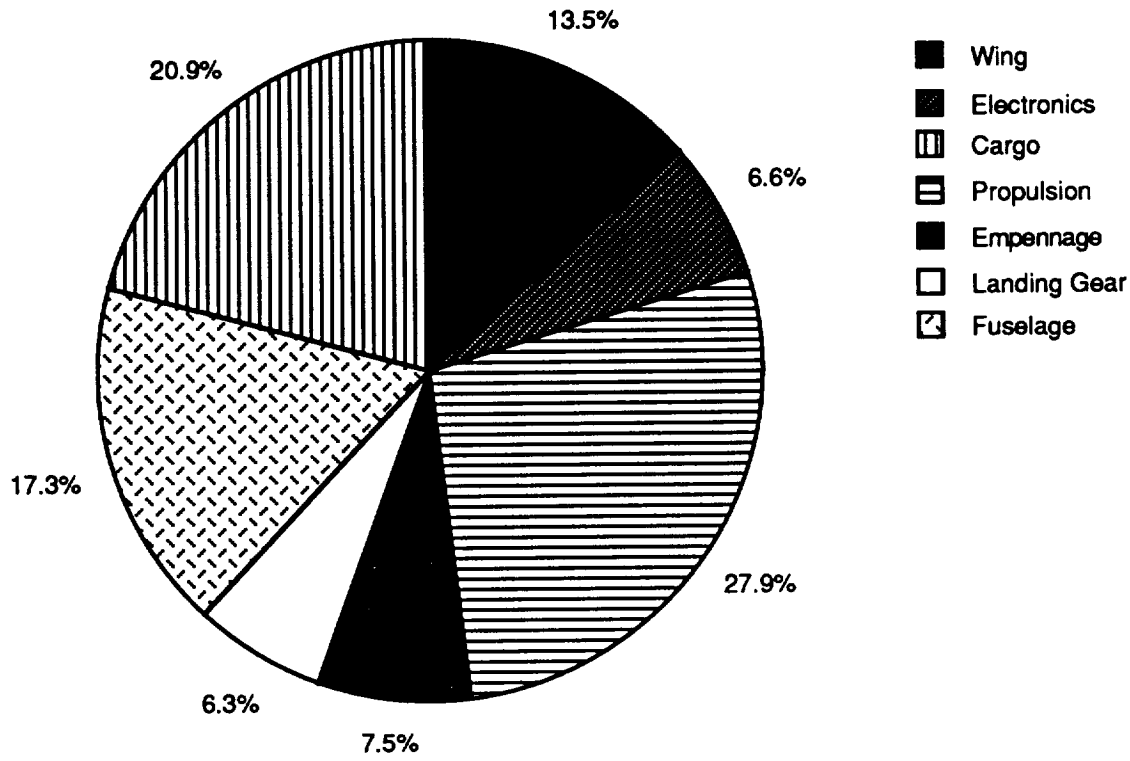

Figure 6.1-1: Ratio of Selected Component Weights to Total Weight

6.2 C.G. and Moments of Inertia

In order to facilitate the calculation of the center of gravity as the weights and positions of the various components of the aircraft were changed, the coordinates and weights were placed in a spreadsheet that also used this information to calculate the moments of inertia about the center of gravity of the aircraft. In this way, the placement of the components needed to facilitate the correct c.g. location was made much easier, and the effect of moving a given item could be determined.

6.2.1 Moments of Inertia

The moments of inertia were calculated by separating the aircraft into its many parts and then finding the moments of inertia for each component about the c.g. of the aircraft using the parallel axis theorem, equation 6.2.1-1:

$$I_{c.g.} = I_{c.g.\,component} + m_{component}\, r^2 \qquad (6.2.1\text{-}1)$$

where r is the distance from the component center of gravity to the aircraft center of gravity.

This procedure mentioned thus far is entirely correct, except that in order to make the analysis much easier, several assumptions were made that introduced error. First, the wing and tail sections were divided into sections (48 wing sections, 12 sections in the horizontal tail, 6 in the vertical tail), and then it was assumed the moment of inertia of these sections with respect to the term added by the parallel axis theorem were negligible. The error introduced by this assumption was less then 5%, since the individual wing and tail sections are quite small, while the distance from these sections to the aircraft c.g. were usually much larger.

The assumption concerning the fuselage was necessary but introduced approximately 10% error. In this case, the entire weight of the fuselage was lumped into the longerons of the fuselage. This effectively increased the moment of inertia about the longitudinal axis, essentially specifying that the roll control of the aircraft would have to be slightly larger than it would normally have been. It will be almost impossible, due to time restrictions, to test the validity of the model and the resulting moments of inertia until the prototype tests. The only way to properly validate the results with a computer would involve building the model and recording the weight and c.g. location of each part or assembly.

A final cause of error will be the anticipated difference in weights of some of the parts from the predicted values. It is not anticipated this error will have as great an affect on the difference between actual and design values as the first two causes of error mentioned above.

6.2.2 C.G. Location

Figure 6.2.2-1 shows the placement of the major components and their c.g.

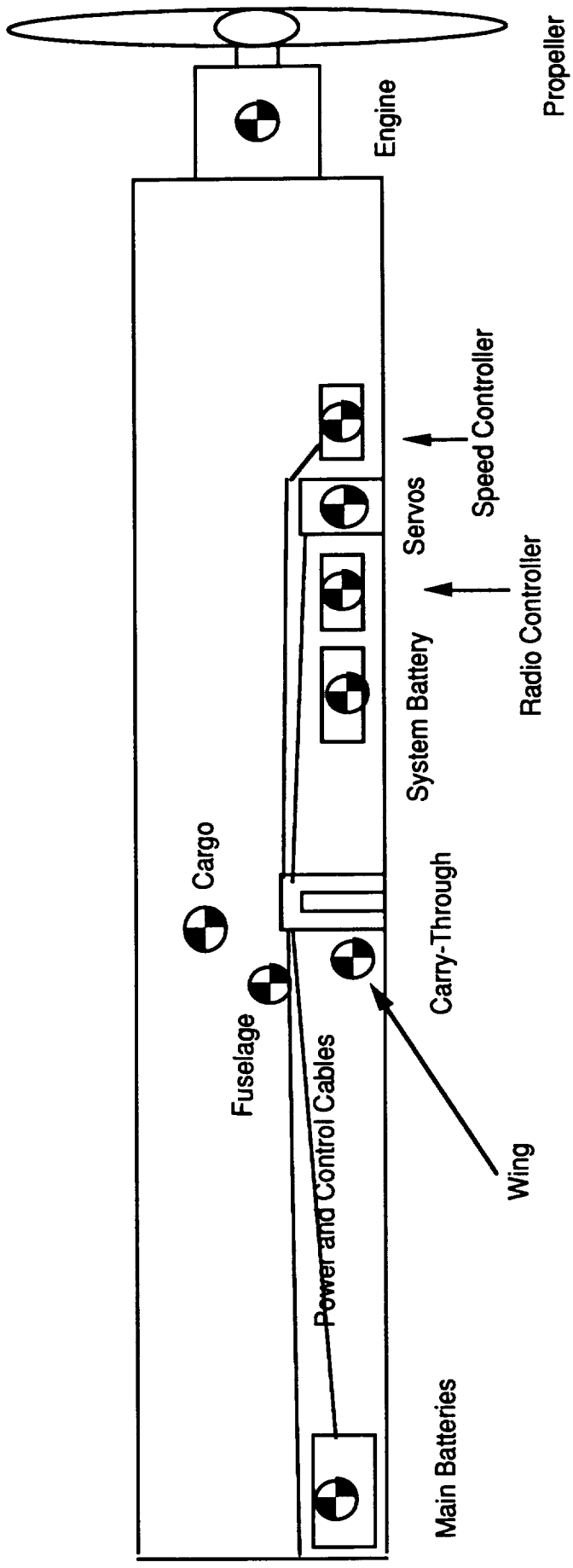

Figure 6.2.2-1: Internal Layout & C.G. Location of Major Components

locations. The following requirements had to be met in the placement of the avionics package:

1) The servos are to be placed so as not to be interfered with by other electrical components., and so the control rods may be placed for adequate control of the aircraft.
2) All items should be in as close proximity as possible so the connections between components can be as short as possible. All the components should fit on a balsa floor that measures 4 in. by 8 in. so the entire package can be moved easily at one time. Thus, weight and complexity will remain low.
3) Sufficient space must exist to run the battery power cord to the speed controller and then to the engine, and also for the anchoring of the control units to the floor.

The batteries will be placed side by side in the longitudinal direction in an aft location and will be removed for recharging through a door in the top of the fuselage. The power cord and the control rods may be run over the top of the wing carry-through structure and under the cargo floor above the wing carry-through structure. There is approximately 3/8 inch in which to run the control rods and the power harness. The main concern is that the diameter of the power harness will be greater than 3/8 inch, but it is felt that this is not a likely possibility.

6.2.3 C.G. Travel

Probably the most important aspect of the c.g. location involves the stability and control of the aircraft with changing cargo weights. Because the cargo is a relatively heavy item, it has a great affect on the moments about the center of gravity of the aircraft. Great concern was expressed over the stability and control of the aircraft upon the removal of the cargo or when given a maximum payload condition. Obviously, the aircraft must have the ability to be controlled and to be stable regardless of cargo weight. In addition, the aircraft must be able to tolerate a variety of loading configurations, in the event that the cargo would be improperly loaded. To this end, the Hermes CX-7 has been designed so that the c.g. position of the cargo along the length of the fuselage is equivalent to that of the airframe. The only difference the addition or removal of cargo would make is in the vertical direction: the c.g. of the aircraft moves higher when more cargo is present, and lower as the aircraft is emptied.

The rudder, whose moment arm is directly affected by such a shift has been designed to take the worst case scenario into account. In this case, the pilot would experience a slight difference in the response of full and empty aircraft, but the ability to control the plane is in no way affected.

Although the difference between the design weight and actual weight will have a small effect the values of the moments of inertia, the control surfaces have been sized taking into account the possibility for error in the inertia calculations, and therefore the error will have to be quite large before adequate control is lost. However, if the c.g. moves even a small amount from the desired location, the entire static and dynamic stability of the aircraft may be placed in jeopardy. To remedy this possible problem, the c.g. of the aircraft may be changed by moving the engine batteries and the avionics. These components may be moved to place the c.g. at the desired location.

7. Stability and Control System Design Detail

Stability of the aircraft comes from the empennage and dihedral of the wing. Since the aircraft is remotely piloted, a radio receiver is incorporated into the system to receive the commands from the pilot and convert these commands into control surfaces deflections and engine speed changes.

7.1 Ground Handling

Although the main goal of aircraft design is to produce an airplane with proper handling capabilities during flight, handling of the aircraft through ground maneuvers is also extremely important and often overlooked. To ensure adequate ground maneuvering for this aircraft, a steerable tail wheel was incorporated into the design. This allows excellent handling at any speed independent of forces caused by control surface deflections without detracting from flight performance.

7.2 Longitudinal Stability and Control

The aircraft empennage was designed for longitudinal static and dynamic stability. This was accomplished by properly sizing the horizontal tail as well as computing the necessary distance from the center of gravity of the airplane to the quarter chord of the wing. An analysis for static pitching stability was performed for the aircraft according to reference 1 (pp.44-48). The pitching moment contributions for the wing, body, and fuselage were computed for both the zero lift and the angle of attack dependent contributions. It was determined that the fuselage contributions were negligible(as determined from eq. 2.31&2.32 of ref 1), therefore the tail needed to be large enough to produce a negative slope for the entire pitching moment curve. From figure 7.2-1, it can be seen that the aircraft is statically stable for all c.g. locations. It was also desirable to have the trim point coincide with the cruise C_l, since that would mean that the pilot could fly the plane "hands off" when at cruise. Setting the tail at an incidence angle of -1.1 degrees with the predetermined geometry characteristics gave the desired slope and trim point as well as a static margin of approximately 15%.

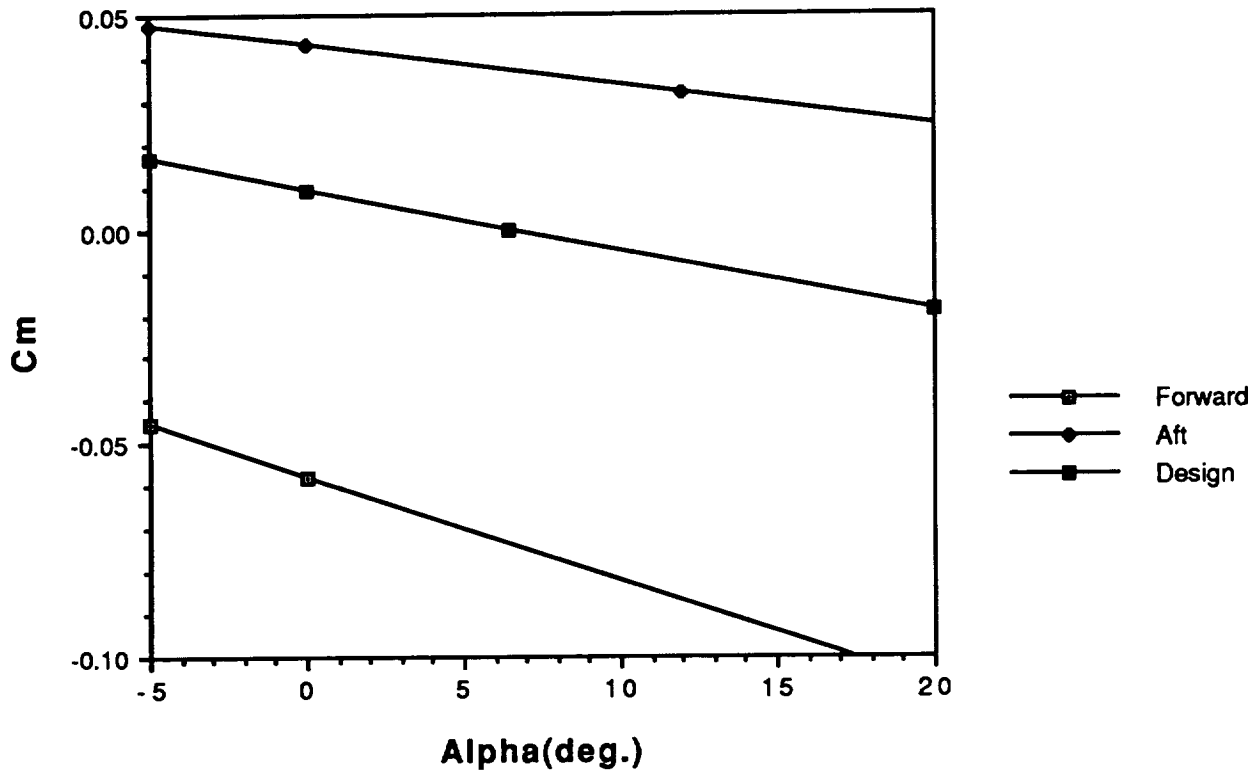

Figure 7.2-1: Aircraft Pitching Moment vs. Angle of Attack

In addition to the static stability analysis, a FORTRAN program was written which computed matrix elements for the longitudinal stability matrix from given design geometry values. The eigenvalues of the resulting matrix were computed, and both the tail area and distance from the aircraft center of gravity were varied until the eigenvalues were of the proper form (as given in Fig. 4.13 of reference 1). This form consists of two conjugate pairs with negative real components, one pair near the imaginary axis and one pair further out with larger imaginary components. The longitudinal roots were to be of the form of two pairs of conjugate roots on the negative side of the imaginary axis, and Table 7.2-1 indicates that such is the case for the final design values for the aircraft.

Table 7.2-1 Longitudinal Roots

phugoid roots	-.003348 +/- 1.05405i
short period roots	-7.14239 +/- 4.74859i

Any movement of the center of gravity will affect the static stability of the aircraft. Therefore, it was undesirable to produce a "point design" for stability given the fact that cargo, batteries, etc. may need to be moved, thereby altering the center of gravity location. Thus a study was done concerning the sensitivity of longitudinal stability to center of gravity movement. It was found that the center of gravity could move 10% of the chord forward or 5% rearward of the design location of 24 inches from the nose of the aircraft (Figure 7.2-2). Outside of this c.g. travel envelope, the eigenvalues were of the proper form outside of this envelope but the damping ratios became unacceptable.

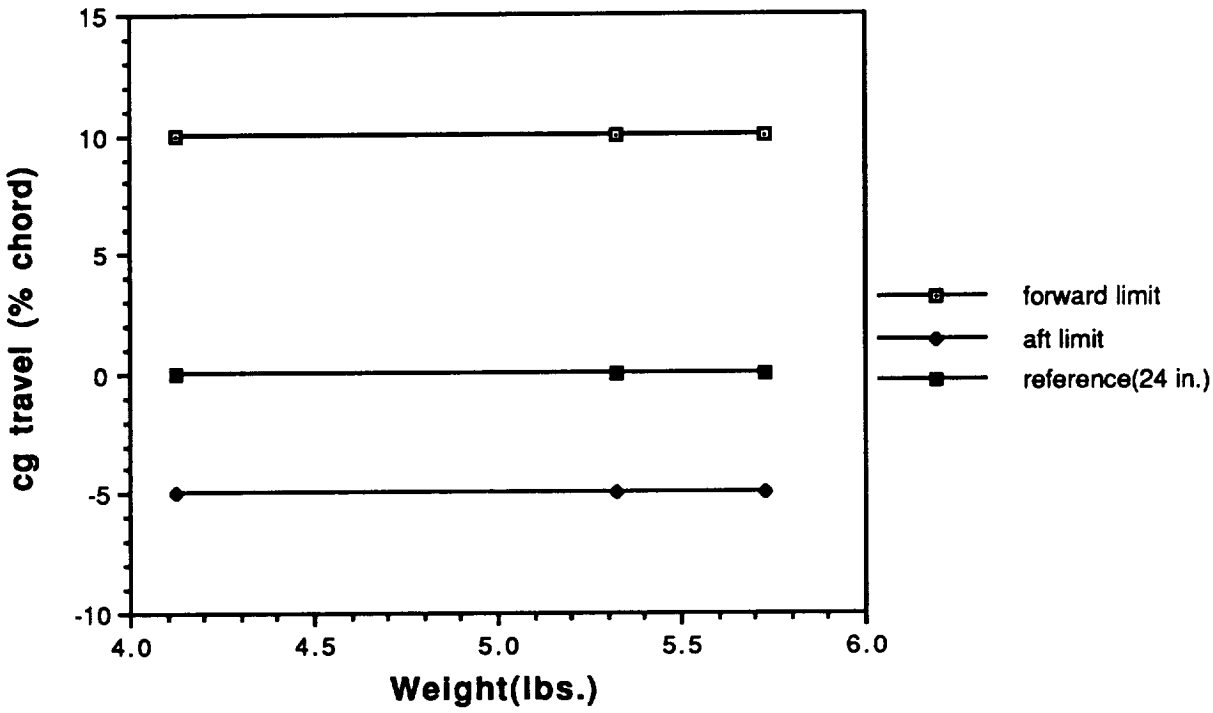

Figure 7.2-2: Center of Gravity Travel

Working closely with the structures team to keep updated on the center of gravity location and moments of inertia lead to a design quantity of 1.2 ft^2 for the horizontal tail area. The horizontal tail aerodynamic center location was set at 28.5 inches from the center of gravity. Whereas the cargo area ends 20 inches from the center of gravity, it was found that this extra length on the empennage was needed not only for stability, but also for control system concerns. In order to string the control actuators from the servos at the bottom of the aircraft to the control surfaces at the top,

a distance greater than 22 inches was necessary so that the actuators would not be crimped and, therefore, unreliable when actuated.

7.3 Lateral/Directional Stability and Control

It was also necessary to have lateral static and dynamic stability. This was important because the aircraft was designed to fly and maneuver without ailerons. Such a design shifts maneuvering dependence from the ailerons to the vertical tail and wing dihedral. Therefore proper estimation of these values was critical.

Lateral static stability is usually easy to maintain since most aircraft are designed to be symmetric about the lateral control axis. Since this was true in this case, analysis showed that dynamic stability concerns far outweighed those of static stability. Thus the FORTRAN code was expanded to compute derivatives and matrix eigenvalues for the lateral stability matrix. The design variables were vertical tail area, distance from the center of gravity to the tail, and dihedral angle of the main wing. The eigenvalues were to be of the form of one pair of conjugate roots and two real roots, all located on the negative side of the imaginary axis. Once the eigenvalues appeared in this form, the design variables were varied to find the ideal location according to structural and fabrication concerns. The final design values were .67 ft^2, 24 inches, and 6 degrees for the vertical tail area, distance from c.g. to tail, and dihedral angle, respectively. The eigenvalues for this configuration are given in Table 7.3-1 for the design c.g. location. As can be seen from this table, the spiral root is unstable, but this is acceptable by FAA standards. It is not expected that this instability will in any way hinder the flight of the aircraft.

Table 7.3-1: Lateral/Directional Roots

dutch roll roots	-1.16799 +/- 4.36621i
spiral root	.167428
roll root	-62.2277

7.4 Control Mechanisms

Once the sizes and locations were determined, the next point of action was to determine the control surface sizes. The elevator area was computed according to the method shown in reference 1 (p.60). This gave an elevator size of approximately 30% of the horizontal tail area. The horizontal tail was designed for a span of 2.45 feet, which was limited by the constraint of the aircraft being able to fit in a 2' x 3' x 5' box for

storage. This gave a tail chord of 5.9 inches, of which 1.75 inches would be for elevators. This size elevator provides adequate ability to trim and maneuver the aircraft in all flight regimes and c.g. locations

The rudder size and main wing dihedral were determined using a simple analysis for turning the aircraft. Since ailerons were deemed too expensive both in the aspect of additional manufacture time and also the need for an additional servo, it was decided that the aircraft would be able to turn by using the rudder and wing dihedral. The data base of past aircraft supported this idea, so the dihedral was chosen to be 6 degrees while the rudder was sized at 50% of the vertical tail. The dihedral angle was determined from the lateral stability matrix, while the rudder size was calculated from a simple analysis of power needed to turn the aircraft. The dimensions of the vertical tail were chosen to be 8 inches long by 12 inches high because any higher would again violate storage requirements. All calculations were made based on the facts that both tail surfaces were to be flat plates for simplicity, that elevator and rudder deflection would be 15 degrees or less, and that the tail efficiencies were chosen to be equal to one since it was hoped that downwash effects would be negligible with a low wing and high tail combination.

Control of the aircraft is maintained through the use of a remote control system. The parts of the system that are contained in the aircraft are shown in figure 7.4-1.

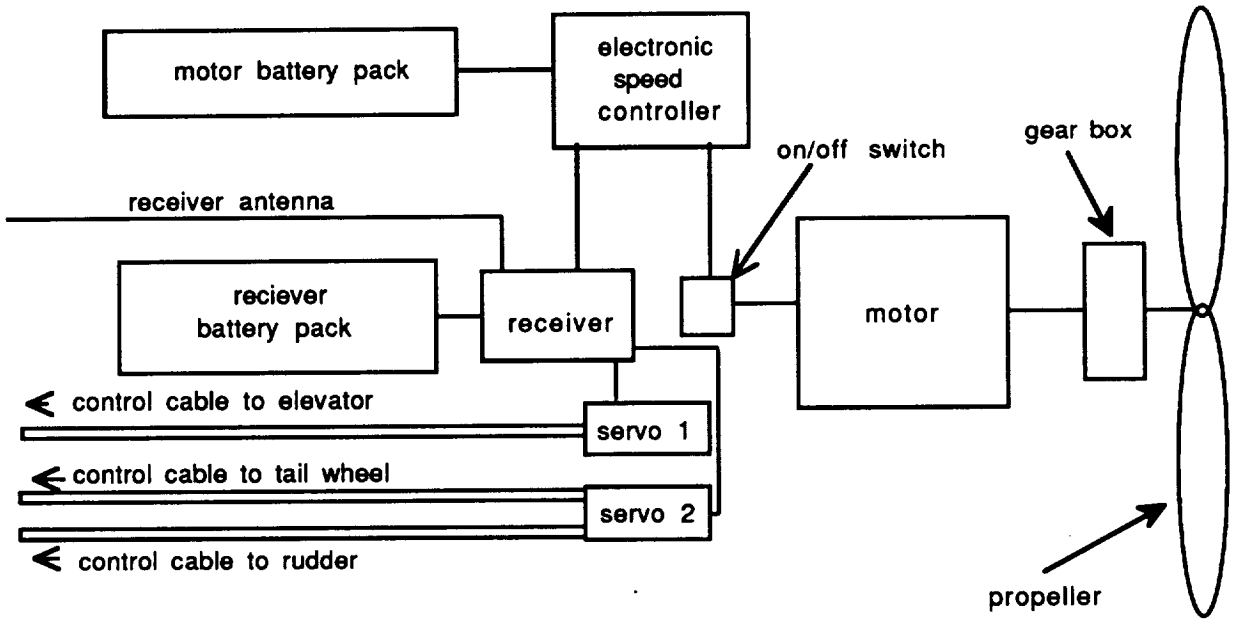

Figure 7.4-1: Aircraft Control System

All components shown in figure 7.4-1 are located forward of the wing carry through structure under the cargo with the exception of the motor battery pack which is aft of the carry through structure. The empennage was designed so that the servos in the front of the aircraft would connect to the tail surfaces through actuation cables which would travel the distance of the utility space underneath the cargo area and then angle up through the hollow empennage structure to their respective tail surfaces.

8. Performance Estimation

In the process of designing the Hermes CX-7, performance criteria were established by the constraints of the mission and by the criteria set by the market conditions. Thus these parameters are crucial to the success of the design project. The table 8-1 contains a summary of the performance data for the final design and the constraints on that data.

Table 8-1: Summary of Performance Characteristics

Max Velocity	>30 ft/s	max- 30 ft/s
Stall Velocity	23 ft/s	----
Takeoff Velocity	27 ft/s	max-30 ft/s
Takeoff distance	32 ft	max- 60 ft
Landing distance	47 ft	max- 60 ft
Range(cruise)	10,655 ft	min- 6500 ft
Endurance(cruise)	355 sec.	
Max Range	10,655 ft	
Max Endurance	356 sec.	
Max rate of climb	10 ft/s	
Min.glide angle	3.8 deg.	
Cruise Velocity	30 ft/s	max- 30 ft/s
takeoff angle	1 deg.	
Catapult range	970 ft.	

** All numbers are based on a fully loaded aircraft.

8.1 Takeoff and Landing Estimates

The engine and propeller selection are greatly influenced by the desired takeoff characteristics. They must supply sufficient power to allow the aircraft to takeoff in a distance less than 60 feet as constrained by the smallest runway serviced by the company. Further analysis of the takeoff performance may be found in the section discussing Propulsion. The takeoff distance was determined to be 37 feet well within the constraints.

The landing performance is influenced by the weight of the aircraft, the wing sizing, the maximum coefficient of lift and the drag and lift at 1.3 times the stall velocity, 29.9 ft/s, and the coefficient of friction. The maximum coefficient of lift occurs at the

stall velocity 23 ft/s, and its value is 1.28. The landing distance is determined from the using equation 8.1-1 (found in ref. 1)

$$X_{land} = \frac{1.69W^2}{g\rho Cl_{max}[D+\mu(W-L)].7Vt} \qquad (8.1\text{-}1)$$

where Vt = 1.3 Vstall. The resulting landing distance for the design in 47 feet. This also is well below the constrain of 60 feet.

8.2 Range and Endurance

Determined from the maximum distance flown in one flight in the route system, the maximum range needed is 4500 feet. An additional 2000 feet are added to this value to allow for flight to the nearest alternate airport and loiter time of one minute for safety in the event that an aircraft cannot land at any of the serviced airports. Thus the maximum needed range is 6500 feet and endurance of 4.6 minutes. These requirements could be easily meet with the use of 300 milli-amp hour batteries. As was discussed in the propulsion section, these batteries were unavailable so 600 mAhr. batteries were utilized thus the resulting range and endurance values well exceed those required for the design mission. A TK Solver program was utilized for the analysis of range and endurance. These values were dependant on the following parameters, cruise velocity, wing sizing, engine, propeller, and batteries. The table 8.2-1 lists the parameters used in the program inputs and the values used.

Table 8.2-1: Parameters Used to Compute Range and Endurance

input variable	input value	input variable	input value
cruise velocity	30 ft/s	gear ratio	2.385
wing area	8 sq. ft.	propeller diameter	1 ft.
aspect ratio	12	Kt	1.08
aircraft weight	5.6 lb.	gear efficiency	.95
load factor	1	battery capacity	.6
Kb	.1058	Cdo	.03
Ra	.12		

The range at cruise conditions as listed above was calculated to be 10,655 feet and the endurance 355 seconds. The maximum range value was determined to be at the maximum velocity, 30 ft/s. As shown in Figure 8.2-1, the range increases with

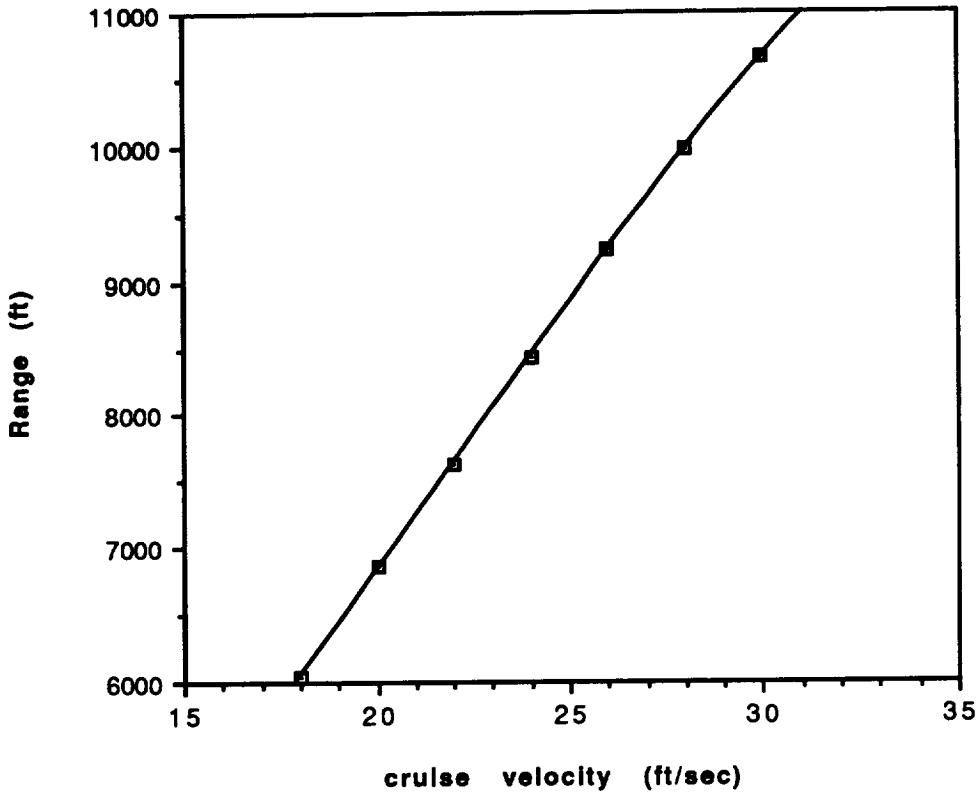

Figure 8.2-1: Aircraft Range at Maximum Payload

increasing cruise velocity thus the maximum velocity optimizes the range giving a maximum range of 10,655 feet. The endurance maximizes at a lower velocity of 28 ft/s as shown in Figure 8.2-2. The endurance value at this velocity is 356 seconds with a

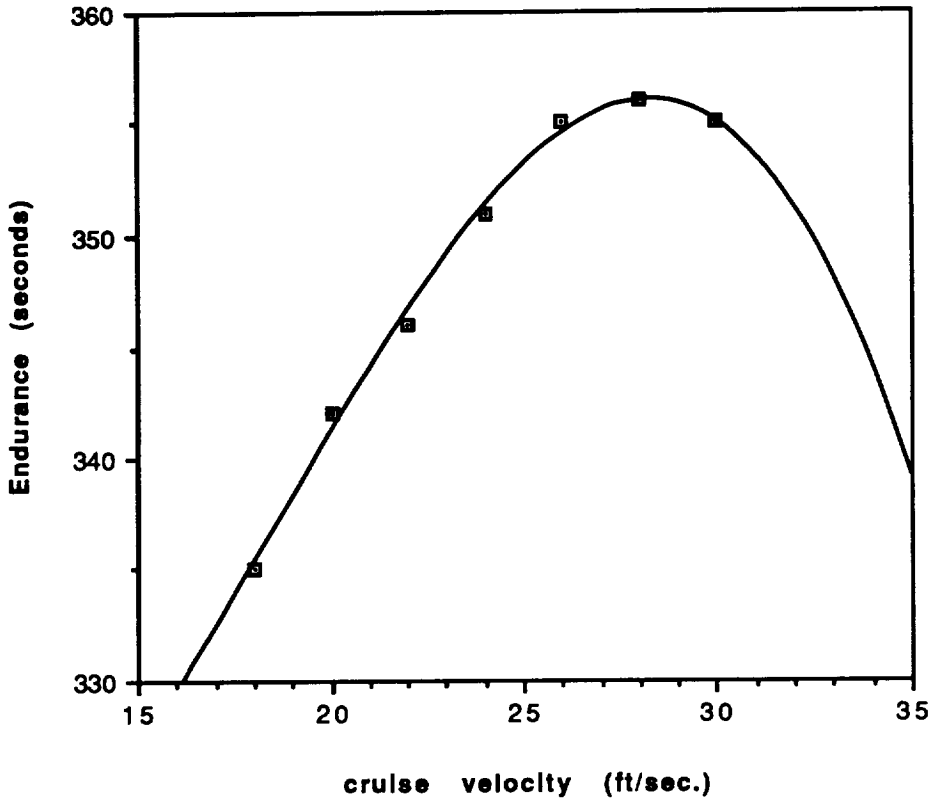

Figure 8.2-2: Aircraft Endurance at Maximum Payload

corresponding range of 10,252 feet. The cruise velocity was set at 30 ft/s because the loss in endurance of only one second increases the range by 400 feet. The range and endurance also vary with the payload weight. As shown in Figure 8.2-3, as the

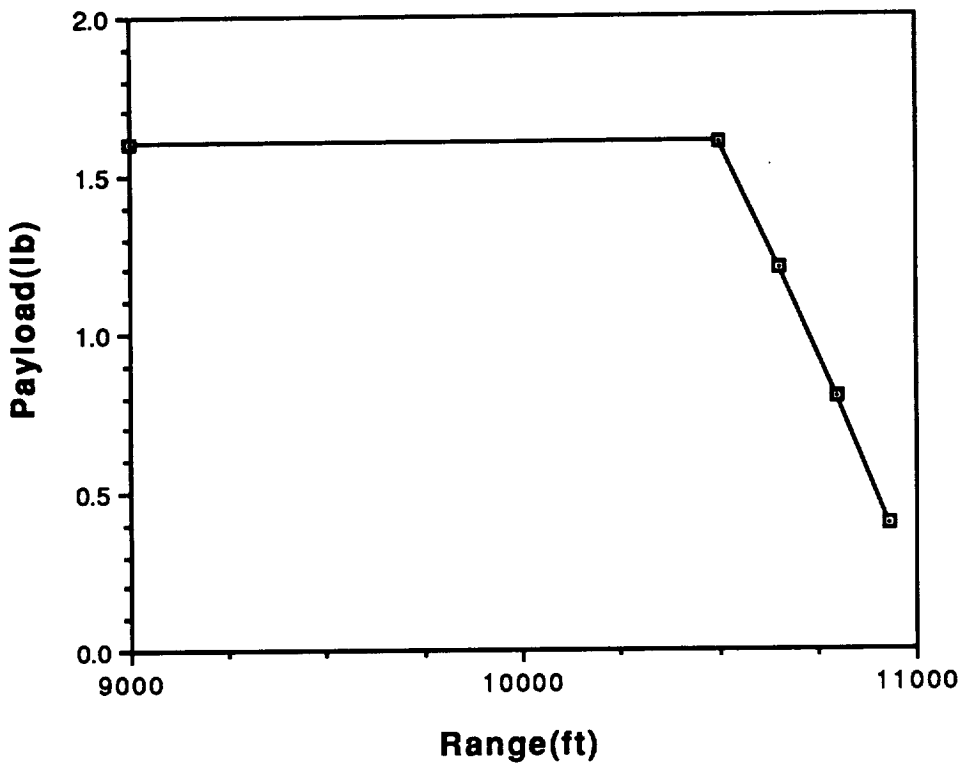

Figure 8.2-3: Aircraft Payload vs. Range

payload increases the range decreases. But because of the additional battery power, the range of the aircraft at all payloads from a minimum of 0 lb to a maximum of 1.6 lb is still well above the desired range. Note as indicated in this graph that while the aircraft was designed to carry only 1.2 lbs. of cargo, it is actually capable of carrying 1.6 lbs. This is due to the fact that the aircraft had to be over-designed because of the unavailability of parts in the proper sizes.

8.3 Power Required and Power Available

Analysis of power available and power required may be found in the propulsion section 5.5 of this report.

8.4 Climb, Glide, and Turn Performance

The data from that analysis is important to the climb performance of the aircraft. The rate of climb is determined from the excess power and the aircraft weight. The maximum rate of climb occurs at a velocity of 30 ft/s and has a value of 21 ft/s.

The glide angle of the aircraft is determined from the lift to drag ratio. The minimum glide angle occurs at the maximum L/D which is 17.78. This yields a minimum glide angle 3.22 degrees.

The turning performance is determined by the bank angle which determined the load force on the aircraft and by the velocity of the plane. At a bank angle of 30 degrees, thus aircraft has a load factor of 1.155 as determined by

$$n=\frac{1}{\cos(\alpha)} \tag{8.4-1}$$

The turn radius is then determined from the equation

$$R=\frac{V^2}{g(n^2-1)^{.5}} \tag{8.4-2}$$

Thus the turn radius is 48 feet which is within the required 60 feet.

8.5 Catapult Performance Estimate

Preliminary catapult estimates indicate that the aircraft will travel approximately 970 ft. from a launch height of 50 ft. Using these numbers, a rough estimate of the L/D of the aircraft can be made and this estimate indicates that the maximum L/D may be as high as 19.4. The catapult program did not indicate any potential problems such as instability or a tendency to stall. The trajectory of the aircraft is shown as figure 8.5-1.

Figure 8.5-1: Catapult Trajectory

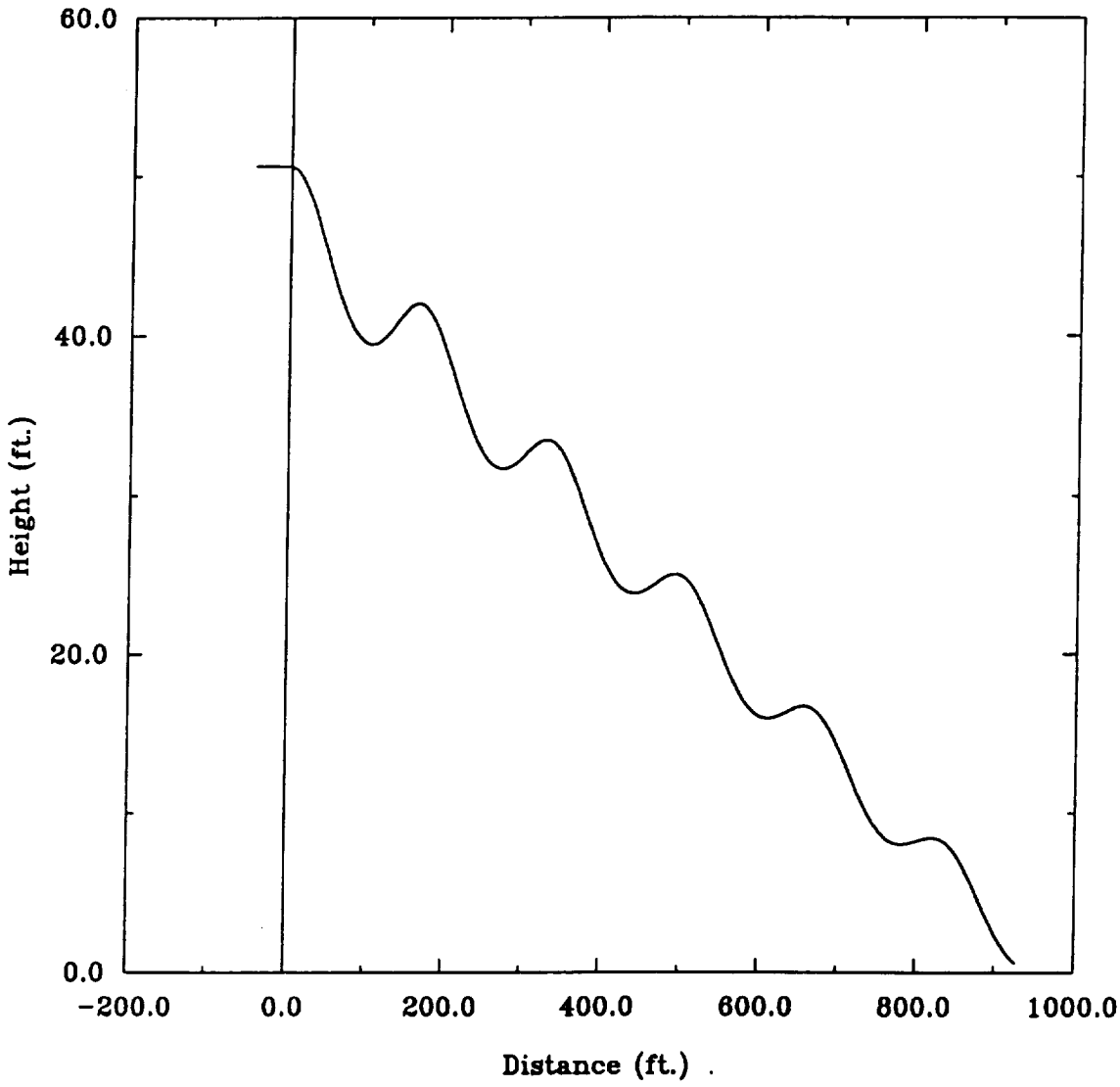

9. **Structural Design Detail**

9.1 Flight and Ground Load Estimation

In order to analyze the wing and the fuselage in flight, some estimation of the loads on these structures were necessary. The structural components of the wing were designed to carry the shear and bending moments during flight. The wing carry-through structure was designed to carry off the wing shear, bending and pitching moments during flight, as well as the weight of the wing when the aircraft was on the ground. The fuselage also had to carry the bending moments and shear associated with the horizontal and vertical tail sections.

The loads acting on the wing were lift, drag, and the pitching moment under normal flight conditions. In addition to being able to carry the loads associated with flight, the wing also had to be designed to carry the inertial loads due to a severe catapult launch. From the analysis of the wing structure, the critical loads which sized the structural members of the wing were the bending moment due to lift and the bending moment due to the inertial loads when the airplane is catapult launched. The bending moment due to lift was estimated by using lifting line theory to estimate the lift distribution across the wing. The lift distribution could then be integrated to find the bending moment at a given location based on equation 9.1-1. In computing the bending moments, no credit was taken for the weight of the wing as it would have only decreased the bending moments by less than 15% and in retrospect would have had no effect on the size of the structural members chosen. The bending moment due to the inertial loads was computed by integrating the distributed weight of the wing to find the bending moment at a given location.

The loads acting on the wing carry-through structure are the shear load due to lift, and the shear load due to weight. The shear load due to drag was neglected because of its small magnitude. The bending moments acting are the bending moment due to lift, the bending moment due to weight and the pitching moment of the wing. The bending moment due to drag was neglected. The forces and moments acting on the empennage due to the horizontal tail are the shear load due to tail lift and the bending moment due to tail lift. The vertical tail also applies a shear force and a bending moment at times. The forces and moments due to tail weight and drag were neglected. In all cases, the loads on the fuselage and wing were calculated at the cruise velocity of the Hermes CX-7 and a safety factor of 1.5 was then applied in order to determine if the structure would adequately support a multiple of the applied loads.

The shear load acting at the wing root is exactly equal to the lift. At cruise, this becomes the weight of the aircraft, or 2.85 lbf on each side of the fuselage. The shear force on each side due to the weight of the wing was determined to be .3875 lbf, since this is half the wing weight. The bending moment due to lift may be calculated from:

$$dM = y(dL) \tag{9.1-1}$$

where dM is the differential moment due to lift, y is the coordinate from the root out along the span, and dL is the differential lift at the y coordinate. Since

$$dL = Cl\ q\ dS = Cl\ q\ c\ dy \tag{9.1-2}$$

where Cl is the section lift coefficient at the spanwise location y (Cl=.68 at cruise), q is the dynamic pressure (q = 1.07 lbf/sq ft. at cruise) and dS=cdy is the differential area at the spanwise location (c represents the chord which is 10 in.). Substituting equation (9.1-2) into (9.1-1) and integrating from the root to the wing tip (0 to 57.5 in.), it is found that the bending moment due to lift is 82.3 lbf in. The moment of the wing due to weight, assuming uniform mass distribution, is just the weight of the wing (12.4 oz) acting at the midpoint of the wing on each side. This moment was determined to be 11.6 lbf in. The moment due to pitch of the wing may be found by using:

$$M=C_{Mwing}\ q\ S\ c \tag{9.1-3}$$

where C_{Mwing} is the coefficient of moment for the wing, and is equivalent to -0.156 for the NACA 6412 at cruise. Therefore, the bending moment on the carry-through due to the pitching moment of the wing was found to be -6.7 lbf in. for each side of the fuselage, with the negative sign representing a pitch down moment.

In an analogous fashion, the shear load due to lift from each horizontal tail was found to be -4.59 oz = -.287 lbf where the sign is negative because of the downward load on the tail. The bending moment due to lift was determined to be 2.39 lbf in. for each side. It was assumed that the rudder would apply these same loads in deflection at cruise.

In addition to these loads applied at the carry-through structure, there is the distributed weight of the cargo and the fuselage itself. For the design cargo weight, the combined load totals 2.81 lbf. There are also loads due to the weights of the controls and batteries, and these were assumed to be point loads equal to the weights of the

items. A summary of the flight loads applied at cruise on the wing and the fuselage can be found in table 9.1-1.

Table 9.1-1 Flight Loads

Load: (In All Cases, Loads Were Computed @ the Root Chords of the Applicable Lifting Member)	Magnitude:
Shear Load Due to Wing Lift	2.85 lbf / wing
Shear Load Due to Wing Weight	.3875 lbf / wing
Bending Moment Due to Wing Lift	82.3 lbf in. / wing
Bending Moment Due to Wing Weight	11.6 lbf in. / wing
Torsion Due To Wing Pitching Moment	-6.7 lbf in. / wing
Shear Load Due to Horizontal Tail Lift	-.287 lbf / side
Bending Moment Due to Horiz. Tail Lift	2.39 lbf in. / side
Distributed Weight of Cargo & Structure (@ Design Weight)	2.81 lbf
Battery Weight (Point Load)	.765 lbf
Avionics Weight (Point Load)	.378 lbf

The ground loads applied are due to the weight of the wing (.3875 lbf / side) and the bending moment of the wing due to weight (11.6 lbf in. / side). In addition the distributed weight of the aircraft minus the wing acts at the c.g., and there are equivalent normal forces acting through the landing gear to balance the weight. Generally, the forces on the ground are much less than those encountered in the air, however the forces encountered during landing may be quite severe due to inertial loads. These loads and conditions will be talked about in section 9.3.7, Landing Gear Design. Besides the normal flight testing of the prototype, a catapult launch to determine the validity of the aerodynamic predictions provides an additional load environment, which will be discussed in section 9.3.3.

9.2 Material Selection

The selection of the materials involved choosing materials that met the stress requirements, were readily available at low cost and had a low weight. The stress requirements were determined through preliminary calculations involving the flight load estimates, while the material cost and availability was determined through

several visits to local stores. In essence three types of materials were considered for use: woods, plastics and light metals. Table 9.2-1 shows how the three compared in the four important categories. A one indicates that the material was the best in that particular category, whereas a three indicates the material was the worst of the three choices.

Table 9.2-1: Materials Comparison

Material	Strength	Cost	Weight	Availability
Woods	3	1	1.5	1
Plastics	2	2	1.5	2.5
Light Metals	1	3	3	2.5

The table clearly indicates that if the values are added, wood receives the lowest score, which makes it the choice of material for the aircraft. Actually, since all three materials would have met the stress requirements, that category could have been deemed as not applicable, and thus wood would have been chosen by a wider margin. Wood, in addition to having the lowest weight also was the most readily available. It was difficult to find metals and plastics of the right strengths and shapes while maintaining a low weight. Also, since wood is the choice of many knowledgeable modelers, and since most of the past planes have been constructed from wood, it was felt that the large existing database for wood was a great reason to choose that over plastics or metals, whose existing databases are much smaller in the modeling field.

Basically, there were five types of wood available in many sizes for construction the aircraft: Spruce, balsa, birch, plywood, and basswood. Table 9.2-2 lists the relative strengths and weaknesses of each material where one is a desirable rating, five is undesirable.

Table 9.2-2: Comparison of Different Woods

Wood	Strength	Cost	Availability	Weight
Balsa	5	1	1.5	1
Spruce	3	2	1.5	3
Basswood	4	3	3	2
Birch	2	4	4.5	4
Plywood	1	5	4.5	5

Balsa is the best material to use unless the strength requirements are too great. In that case, spruce is the next best choice. They were both available in a variety of cross sections and lengths, as well as in panels. The availability of the other three woods severely limits their use. The basswood is available mostly in larger cross sections, to be use for areas of large stresses. Birch came only in panels and is normally used for the webs of the wing spar and perhaps bulkheads. The plywood also was available in panels only and it is usually used for the engine firewall or in small amounts in highly stressed areas. Table 9.2-3 lists the properties of each material used.

Table 9.2-3: Material Properties

Material	E (psi)	ρ (lbf/in.^3)	σ xx (psi)	σ yy (psi)	τ xy (psi)
Balsa	65.e3	.0065	400	600	200
Spruce	1.3e6	.016	6200	4000	850
Birch	1.6e6	.022	7100	4880	1080
Birch Plywood (3-ply)	2.01e6	.025	2500	2500	2500

These properties are somewhat difficult to find. The data on balsa is taken from Reference 4, while the data on the remaining three woods is taken from reference 5. The actual combination of materials depended on the stress requirements at the location in question. The structural design was essentially a trade-off between strength and weight, and will be discussed in section 9.3

9.3 Design of Structural Components

The design of the aircraft's structural components centered around finding a combination of materials and geometries that met the stress requirements at as light a weight and as low a cost as possible. In addition, the aircraft was designed so that its manufacture could be simple and require as little time as possible.

The entire aircraft structure was designed to be capable of handling a load factor of 3.0 over the lifetime of the aircraft. This was determined from a stall load factor of 2 multiplied by a safety factor of 1.5. Since the aircraft was designed for 650 ground-air-ground fatigue cycles, a new aircraft would need to be designed to sustain an ultimate load factor of 3.75. The ultimate load factor calculation took into the actual load factor, a safety factor, and the stress reduction factor due to fatigue. It was seen that at a cruise velocity of 30 ft/s, the aircraft would stall at a load factor of 2. A factor of safety of 1.5 was assigned, and the stress reduction factor at 650 flights was .8, from figure 2 in the request for proposals from G-Dome Enterprises. Then

$$\text{Ultimate Load Factor} = \frac{(\text{Stall Load Factor @ Cruise})(\text{Factor of Safety})}{(\text{Stress Reduction Factor @ 650 Cycles})}$$

$$= \frac{(2.0)(1.5)}{(.8)} = 3.75 \qquad (9.3\text{-}1)$$

In the design analysis, the aircraft structure was loaded for a load factor of 1 (cruise condition) with the flight loads calculated previously. If the stresses in the all of the materials were less than 1 / 3.75 of the ultimate stress of the material, then the structure would be able to achieve an ultimate load factor of 3.0 over the life of the aircraft. The aircraft was also designed to be able to fly at a load factor of -1 after 650 fatigue cycles. This load factor was assumed to be the largest negative load factor the aircraft would experience for the desired mission. It was assumed that the aircraft would rarely need to engage in maneuvers involving higher negative load factors.

9.3.1 V-n Diagram

The V-n diagrams for the design weight, maximum weight and minimum weight configurations may be seen in figures 9.3.1-1 through 9.3.1-3 respectively. The solid lines

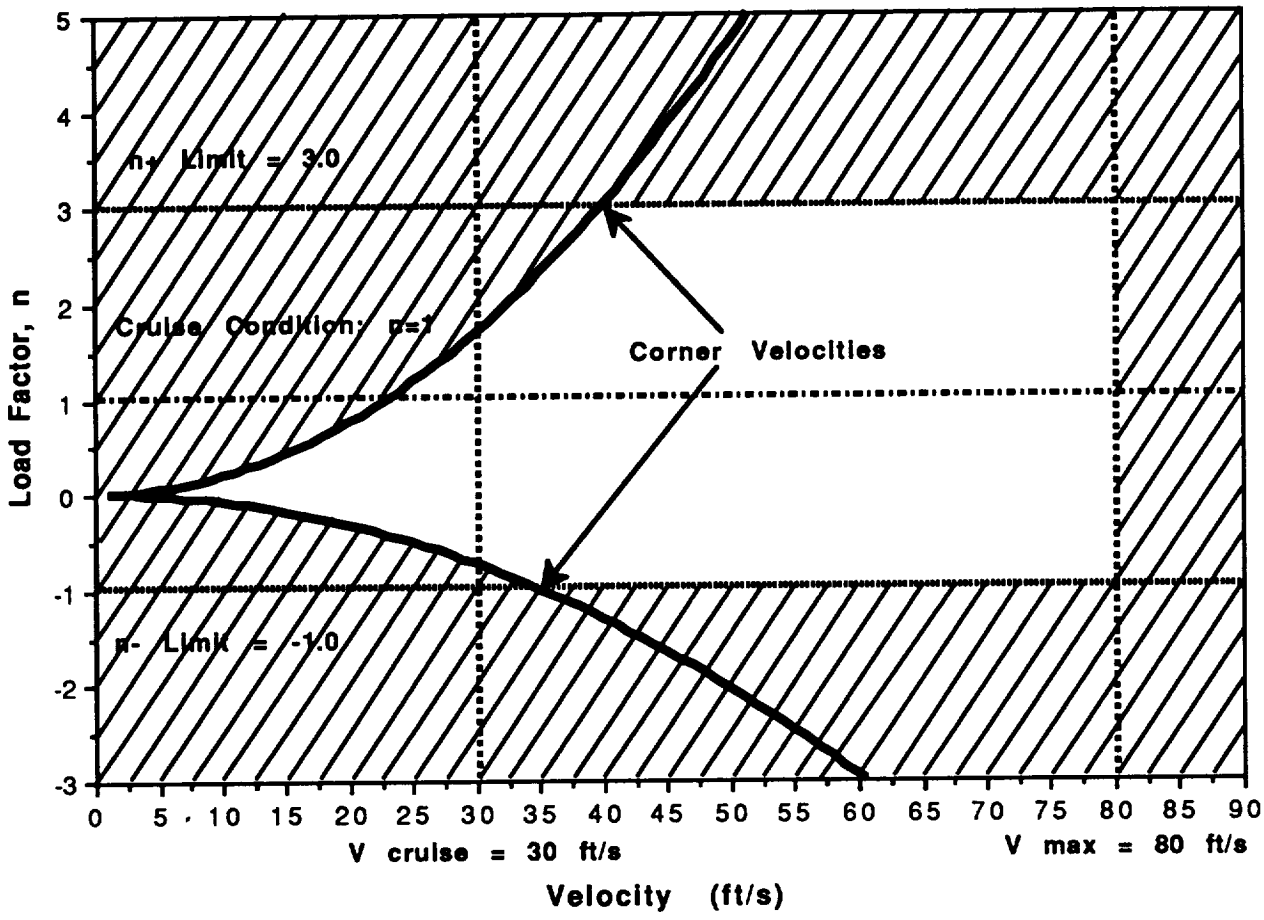

Figure 9.3.1-1: V-n Diagram at Design Weight

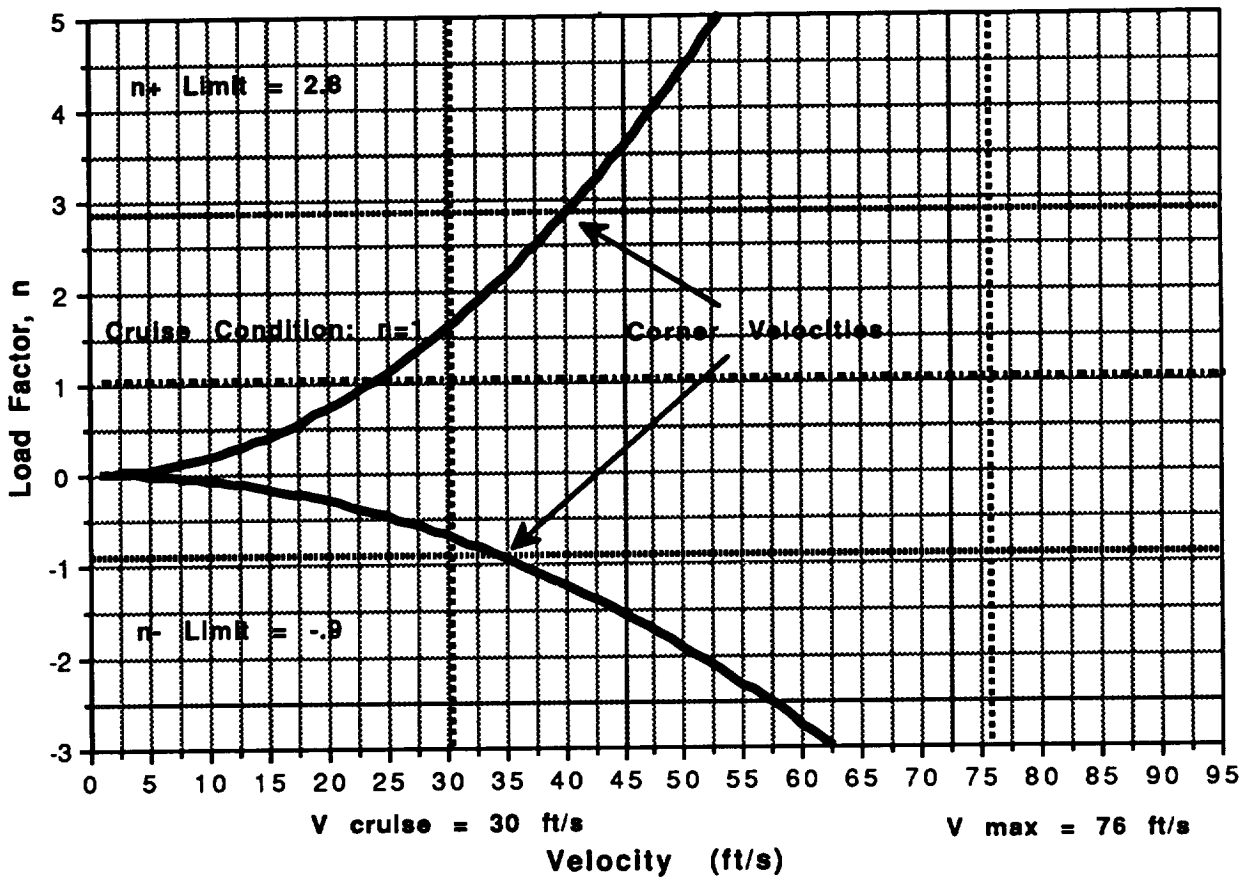

Figure 9.3.1-2: V-n Diagram at Maximum Weight

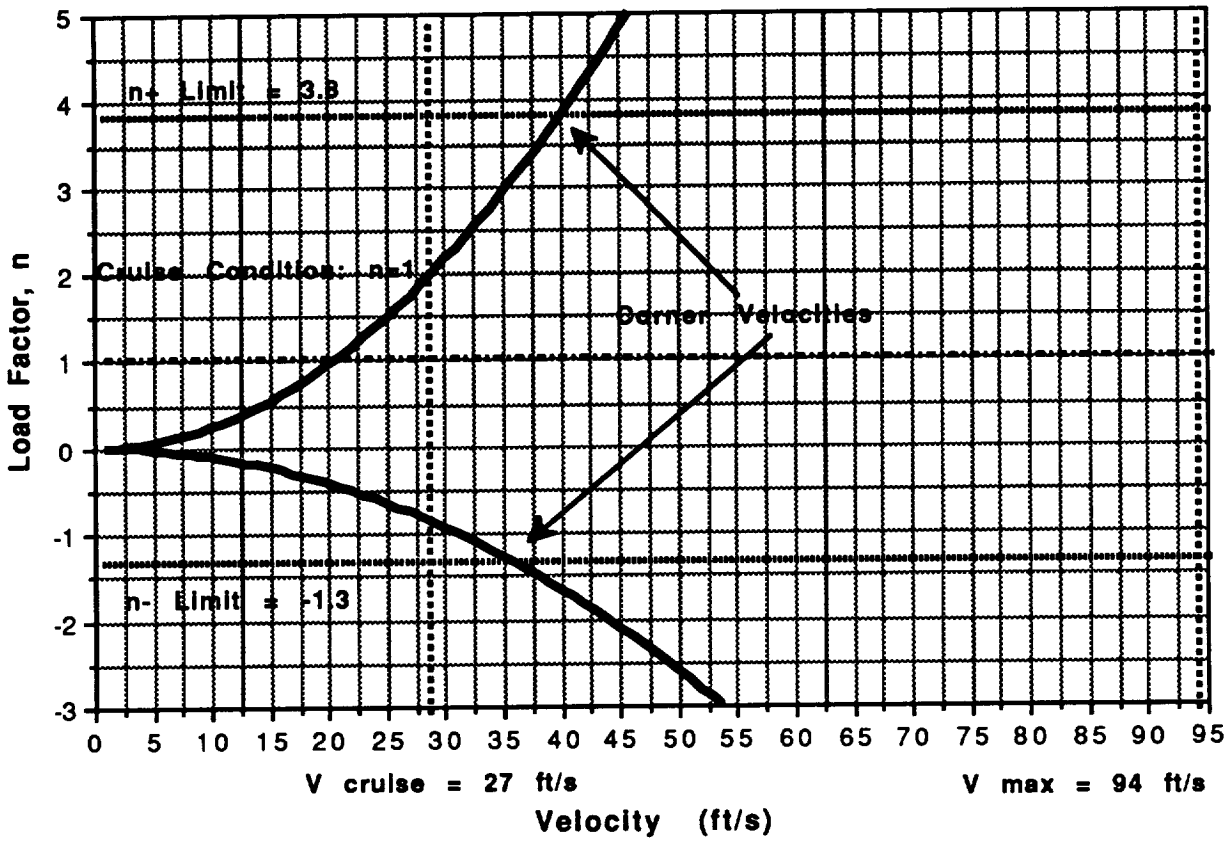

Figure 9.3.1-3 V-n Diagram at Minimum Weight

represent the stall curves of the aircraft. At any point above the upper curve or below the lower curve, the aircraft is stalled. The upper and lower limits on the load factor are represented by the horizontal dotted lines. If the aircraft flies at a point above the n+ limit or below the n- limit, the aircraft structure will be in danger of failing. The cruise and maximum velocities are denoted by the vertical dashed lines, and the cruise condition is denoted by the horizontal dot-dashed line at n=1. Note that a weight increases, the maximum velocity achievable decreases, as does the cruise velocity. Also note that the n limits decrease in magnitude with an increase in weight.

An important point on the V-n diagrams are the corner velocity points. At these points (shown on the diagrams) the stall curves meet the n limit lines. If the aircraft maintains a velocity below the corner velocity, it will stall before getting into a region where the plane could fail. Because the n limit lines and the stall curves both change

with weight, it is somewhat interesting that the corner velocities are practically equivalent for all three weight configurations. The cruise velocity is the maximum allowable by law, since the aircraft is required to fly below Mach 1, which was defined as 30 ft/s. However, in an emergency the aircraft has the ability to fly at Mach 2.3. At 30 ft/s, the aircraft will always stall before a point where failure may occur. If the airplane must exceed 35 ft/s (40 ft/s for a positive load maneuver) then the pilot must be careful what kinds of maneuvers the plane attempts.

9.3.2 Wing Design

As previously mentioned, the loads which sized most of the structural members of the wing were the bending moments due to lift and the inertial loads. The basic layout chosen for the wing, figure 9.3.2-1, was a three spar design with spars located

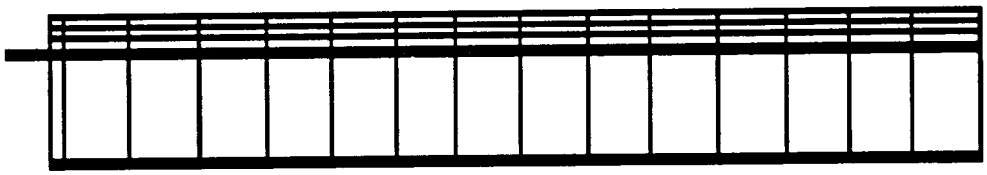

Figure 9.3.2-1: Wing Layout

at the leading and trailing edges and the main spar located along the 30% chord line. Ribs were placed every four inches and longerons were placed at the 10% and 20% chord lines to help maintain the shape of the monokote skin. There wasn't sufficient time to analyze several different potential designs. Therefore, the designs of several past aircraft were studied and the best aspects of each design were incorporated into the layout discussed above. In order to facilitate construction of the wing, the spars will have a constant spanwise cross section. As a result of this decision, all members were sized based on the maximum load in the member which usually occurs at the root. The only exception to this rule pertains to the situation where the shear web on the main spar was eliminated on the outboard two-thirds of the wing because it would both reduce weight and make the wing easier to build.

The primary purpose of the main spar is to carry the shear and bending moments due to lift. The main spar of the wing is made of two spruce spar caps to carry the bending moment and a shear web to carry the shear force. The analysis indicated that the shear web need not carry the shear forces because there was

enough material in the spar caps to carry off the shear. However, the shear web is included on the inboard 20 inches of the spar to stiffen it.

The leading and trailing edge spars were sized by the inertial loads experienced during the catapult launch. These members also carry much of the torsional load acting on the wing and stabilize the leading and trailing edges of the ribs. Both the leading and trailing edge spars are made from balsa because the loads acting on them are much smaller than those for the main spar. The leading edge spar is made from a 3/16" x 1/4" piece of balsa which will be sanded to round the front corner. The trailing edge spar is made from a 1/2" wide x 1/8" high triangular piece of balsa.

The two longerons were sized by the shear forces acting on them. Their primary purpose is to stabilize the upper monokote skin. The monokote has a tendency to sag in between the ribs especially on the upper surface between the leading edge and the main spar which decreases the aerodynamic efficiency of the wing. This can be counter either by placing the ribs closer together or by using longerons. Longerons were used for this airplane because they are a lighter alternative. These two longerons are 1/8" x 3/32" and are made of balsa.

The primary purpose of the ribs is to give shape to the airfoil. The forces acting on these members are very low, therefore, they will be cut from 1/16th inch thick balsa sheets which are the thinnest available. No lightening holes will be added to these ribs because the weight savings does not offset the cost to add the holes. The root and tip ribs will be made of 1/32nd inch plywood because they will be subject to more abuse from being bumped than the interior ribs. In addition, a screw will placed through the root rib to help fasten the wing to the fuselage. This screw will produce a high-stress region which balsa would not be able to handle.

One of the biggest problems encountered with designing the wing is the availability of materials in the appropriate sizes. Most of the desired wood could only be purchased with dimension in increments of 1/16th of an inch, as a result some members of the wing are capable of handling loads much larger than needed. The net result of this is that the wing will be able to lift 9.1 lbs if necessary. This allows the payload to increase beyond design limit. The only advantage for this is that the wing will not have to be structurally redesigned for any heavier derivative aircraft.

9.3.3 Fuselage Design

The final fuselage design is seen in the isometric view of the aircraft shown in figure 9.3.3-1. The fuselage design began with the definition of the external lines of

Figure 9.3.3-1: Isometric View of the Final Design

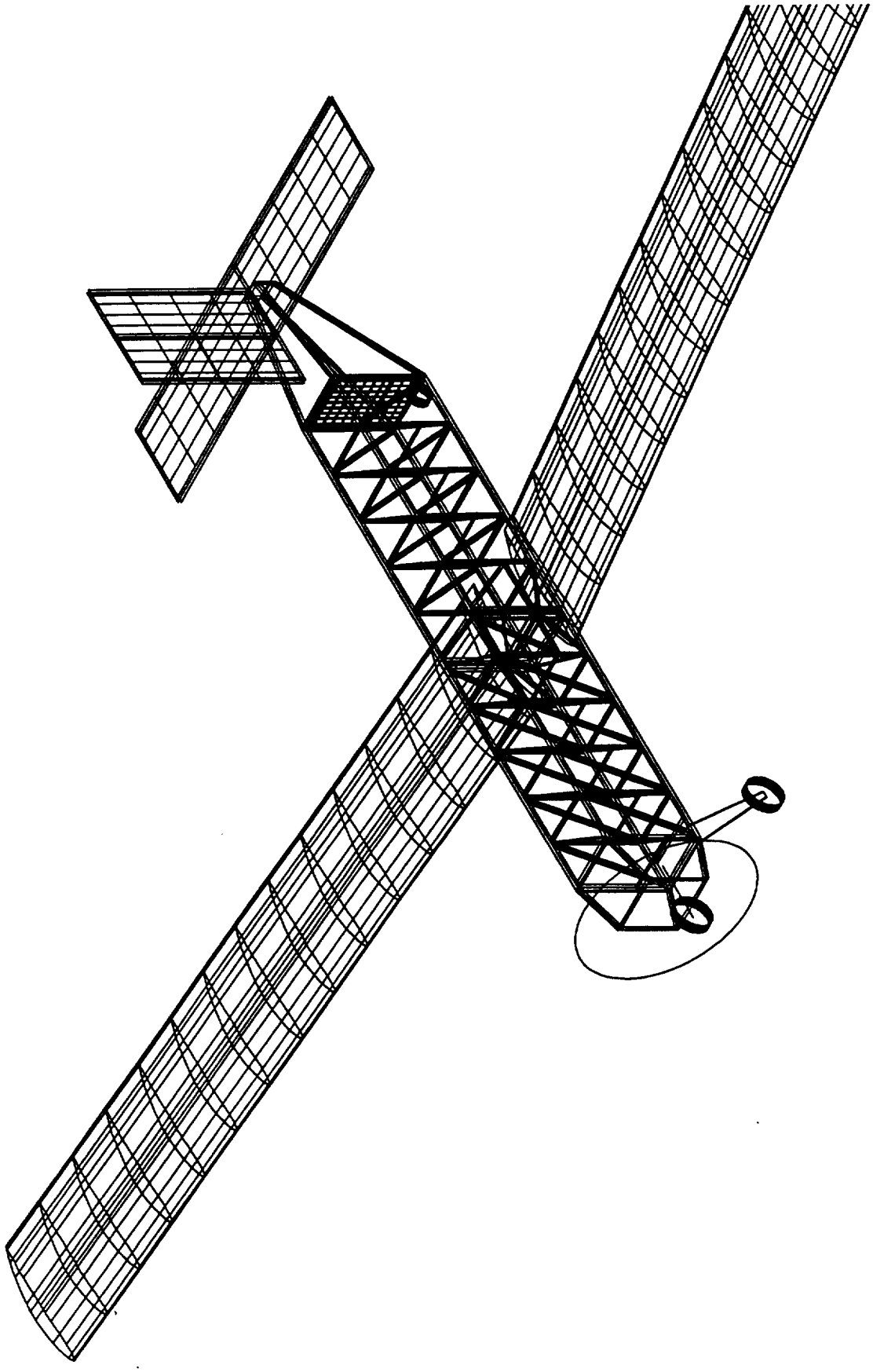

the aircraft. In order to carry 640 cubic inches of cargo in the most efficient manner possible, the cargo will be carried in a block that measured 4 in. by 4 in. by 40 in., running longitudinally through the aircraft. This configuration would result in a high fineness ratio and thus in lower fuselage drag. In order to carry cargo that is 4 in. wide, the fuselage will be 4.625 inches wide, including the two longerons which are .25 in. wide each. This will allow 1/16 in. on each side of the fuselage between the cargo and the longerons. This allowance will yield the minimum fuselage width while giving a reasonable manufacturing tolerance.

In order to place the avionics, controls, and the wing attachment structure so that they did not interfere with the cargo bay, two inches are added to the bottom of the cargo bay. This space will extend the entire length of the cargo bay (40 inches), and will contain the avionics batteries and the wing carry-through structure. For this reason, the fuselage needs to be 6.875 in. high. This figure allows for the two longerons, the cargo floor support (1/8 in. thick), the cargo floor (1/16 in thick), the 4 in. high cargo and a 1/8 in. manufacturing tolerance. This configuration gives a cross section of 6.875 in. x 4.625 in., or slightly over 31 square inches.

The length of the fuselage was restricted by the storage requirements of the aircraft, which specified that the aircraft be stored in a space no larger than 2 ft. x 2 ft. by 5 ft. This meant that the fuselage would have to be less than five feet, or 60 inches long. Slightly over four inches were needed for the engine and its support, which was mounted directly in front of the forward end of the cargo bay. Stability and control needs dictated the need for an empennage of 11 inches, which meant that the entire fuselage would be 54 inches long. The fineness ratio for the fuselage was then calculated as:

$$\text{Fineness Ratio} = L/D_{eff} = .5(L / (A_C/Pi)^{1/2}) \qquad (9.3.3\text{-}1)$$

where A_C is the cross-sectional area of the fuselage, and L is the length. Equation (9.3.3-1) gives a fineness ratio of 8.72.

In the case of derivative aircraft that have larger cargo capacities, there are two possible design paths. First, if the storage restrictions were lifted the fuselage could be extended to greater lengths. However, if the cargo capacity was doubled, it would not be feasible to double the lengths of the fuselage, since the stresses involved would be disproportionately high. It seems that a larger cross-sectional area would be the best expansion path, especially since the fuselage drag was not a major percentage of the

drag breakdown. In the original configuration, the fuselage drag accounted for 11% of the total drag. Even if the fuselage cross-section were changed to 6.75 in. x 8 in. in order to place two rows of cargo side-by-side (essentially double the cargo volume) the fuselage would still account for only 20% of the total drag. If a larger derivative aircraft were to be made, the fuselage should not be made longer, but wider.

In the first approximation, the fuselage was modeled as box beam, and the applied loads gave a maximum bending moment in the longerons of 787 oz in. Under this load, with a safety factor of 5, balsa longerons of 1/4 in. x 1/4 in. cross section were needed to satisfy the stress requirements.

Once design began in earnest, the fuselage was modeled using the finite element program SPACETRUSS written by Dr. Stephen Batill of the University of Notre Dame. The process involved the input of nodal coordinates and loads at cruise condition. The materials and cross-sectional areas were varied in order to find a lightweight fuselage structure that satisfied the stress requirements. In addition, the deflections of the nodes were to be held to less than .2 inches, especially in the wing area, since a large deflection there could affect the lifting capabilities of the wing The entire fuselage design centered around the efficient transfer of the high stresses in the wing carry-through to the rest of the structure without overstressing any of the members while respecting the ultimate safety factor of 3.75. Finally it was felt that every member should have a cross-section of at least 1/8 in. x 1/8 in. or the equivalent cross sectional area. Dealing with parts smaller than this would lead to difficulty in construction and in handling. An important point to remember is that although the members are designed to be capable of the flight loads placed on them, the loads encountered during handling, packaging, and transport of the aircraft may be quite different and possibly more severe. Availability of materials was a concern, since exotic cross sections would most likely not be available in large quantities. Therefore, cross-sections were chosen to meet all of the above concerns. For these reasons, the fuselage is slightly heavier than need be, and a bit over designed for the flight loads, which is are necessary results of the stated restrictions.

At first, to save weight and initial cost, an entire structure of balsa was modeled. It was found that the balsa did not have enough strength to sustain the high loads from the wing, and so spruce was tried instead. The balsa model with the spruce carry-through satisfied all the stress requirements and was the model which was chosen for the final design because of its light weight. Spruce could have been used in the longerons or for the entire structure, but the strength of balsa in all areas except the carry-through was all that was needed and balsa saved weight. Either plywood or

birch panels had been considered for use in the design of the carry-through, but the panels could not be modeled in the finite element code, and so spruce members were used instead.

Note that the balsa longerons are of 1/4 in. x 1/4 in. cross section, which is approximately the same cross-section needed to support the stresses when the fuselage was modeled as a box beam and the axial stress due to bending was found by using the relation:

$$\sigma_{xx} = M_y / I \qquad (9.3.3\text{-}2)$$

where M is the maximum bending moment, y is the distance from the neutral axis of the beam, and I is the moment of inertia of the beam perpendicular to the plane of bending. This check validates the finite element code, since radically different results were not seen.

The final analysis of the fuselage consisted of applying proper loads to simulate the catapult launch. The information given to us specified that an acceleration of twice the gravitational acceleration would likely be required to launch the aircraft. This corresponded to a load of twice the weight of the aircraft applied where the catapult was attached. For this reason, and because of the way the catapult system is set up, it was decided to attach the catapult hook on the underside of the fuselage directly between the front landing gear. During analysis, the landing gear support proved more than capable of bearing the 11.4 lbf load, and this configuration would allow the catapult to release freely during launch. Elevator deflection will be necessary to maintain stability.

9.3.4 Wing Carry-Through Design

Two possible wing attachment configurations were considered. In both cases, it was necessary to attach the wing so that it did not interfere with the cargo bay, since a continuous cargo bay was desired. It was also necessary to construct the wing in sections five feet or less in length due to the storage requirements already stated. One choice would have involved attaching the wing to the top of the fuselage. One advantage of this design was that the center of the wing would have been constructed in one continuous section. Another was that since this was a high-wing, the roll stability of the configuration would have been better than average. With this design, the center of the wing would have no dihedral angle, but outside plug-in sections would have a dihedral angle, thus making the wing a polyhedral. One worry with this

design was that the wing would interfere with cargo placement and therefore the fuselage would have to be enlarged. The main reason this configuration was not chosen was because it lacked structural efficiency. In this design the structure must not only transfer loads from the wing to the fuselage at the root of the wing, but would also have to transfer loads between sections of the wing where there would otherwise be no buildup of support material.

The configuration eventually chosen involved plug-in wings, with the wing carry-through being situated in the lower part of the fuselage underneath the cargo bay. Since this part of the fuselage would have been built up already, it was felt that this design was more structurally efficient. Figure 9.3.4-1 shows a diagram of the wing carry-through and its components. Besides being structurally efficient there were only two identical wing sections to be made for this configuration , as opposed to three sections that were not identical. Another advantage was that the carry-through would not interfere with the cargo placement in any manner. Although the low wing is susceptible to poor roll stability, this aspect was helped considerably by the dihedral. However, this configuration carried with it higher stress concentrations in the wing carry-through, since the wing attachment now consisted of a spar extension being plugged into a sheath-like hole in the side of the fuselage.

As figure 9.3.4-1 shows, the sheath is 3/8 in. wide to allow for the spar to plug-in, and runs to the center of the fuselage from each side- a distance of 2 5/16 in. The spar is 1.2 in. high

The carry-through is also responsible for aligning the wing to the correct incidence angle of attack at cruise, and also to give the wing the correct dihedral angle. Therefore, the entire carry-through must be tilted to an incidence angle of about 1 degree, and the internal design of the carry-through must be tilted 6 degrees. These alignments can also be seen in figure 9.3.4-1.

Figure 9.3.4-1: Wing Carry-Through Structure
(note: all dimensions are in inches)

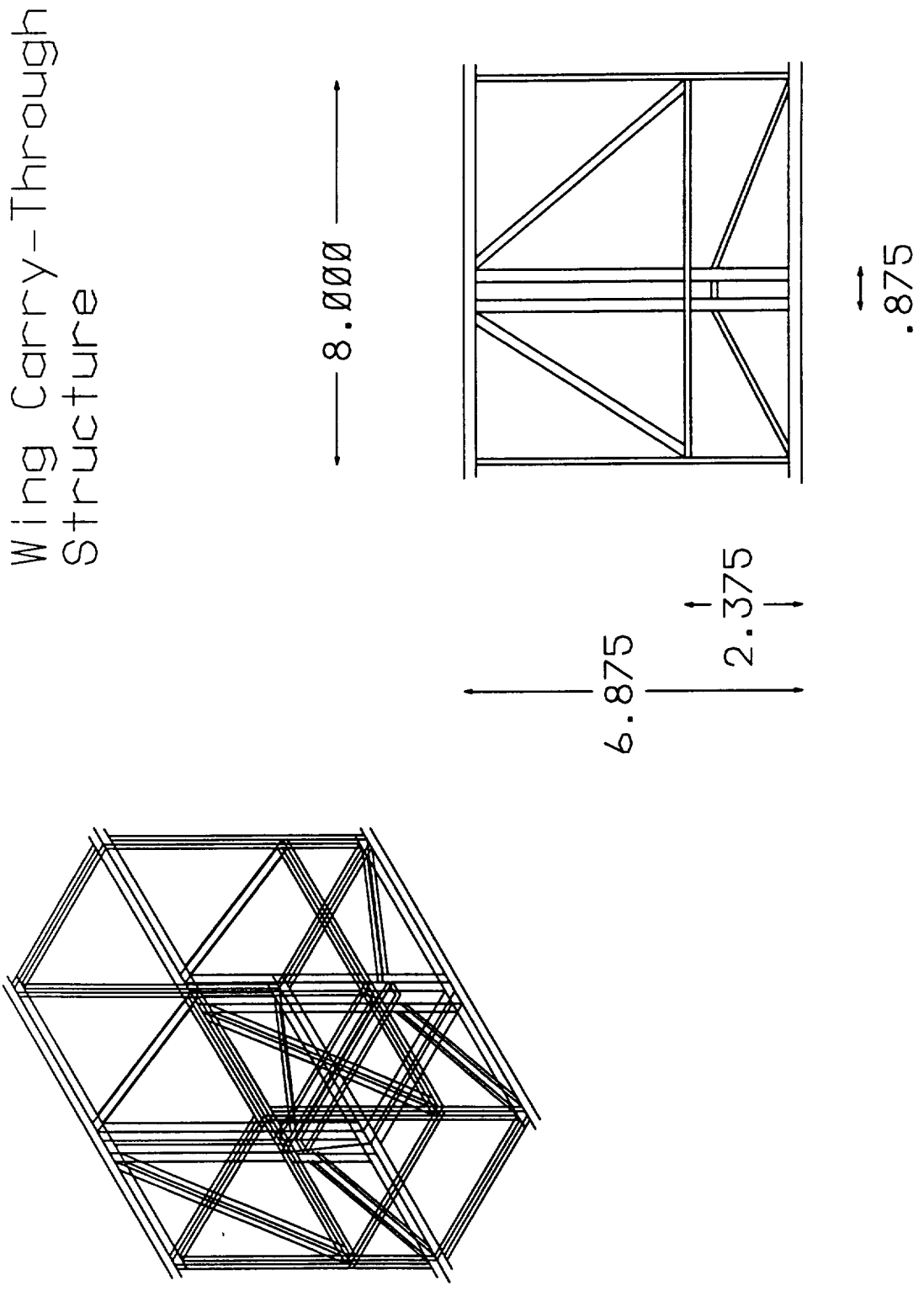

Figure 9.3.5-1: Empennage Design

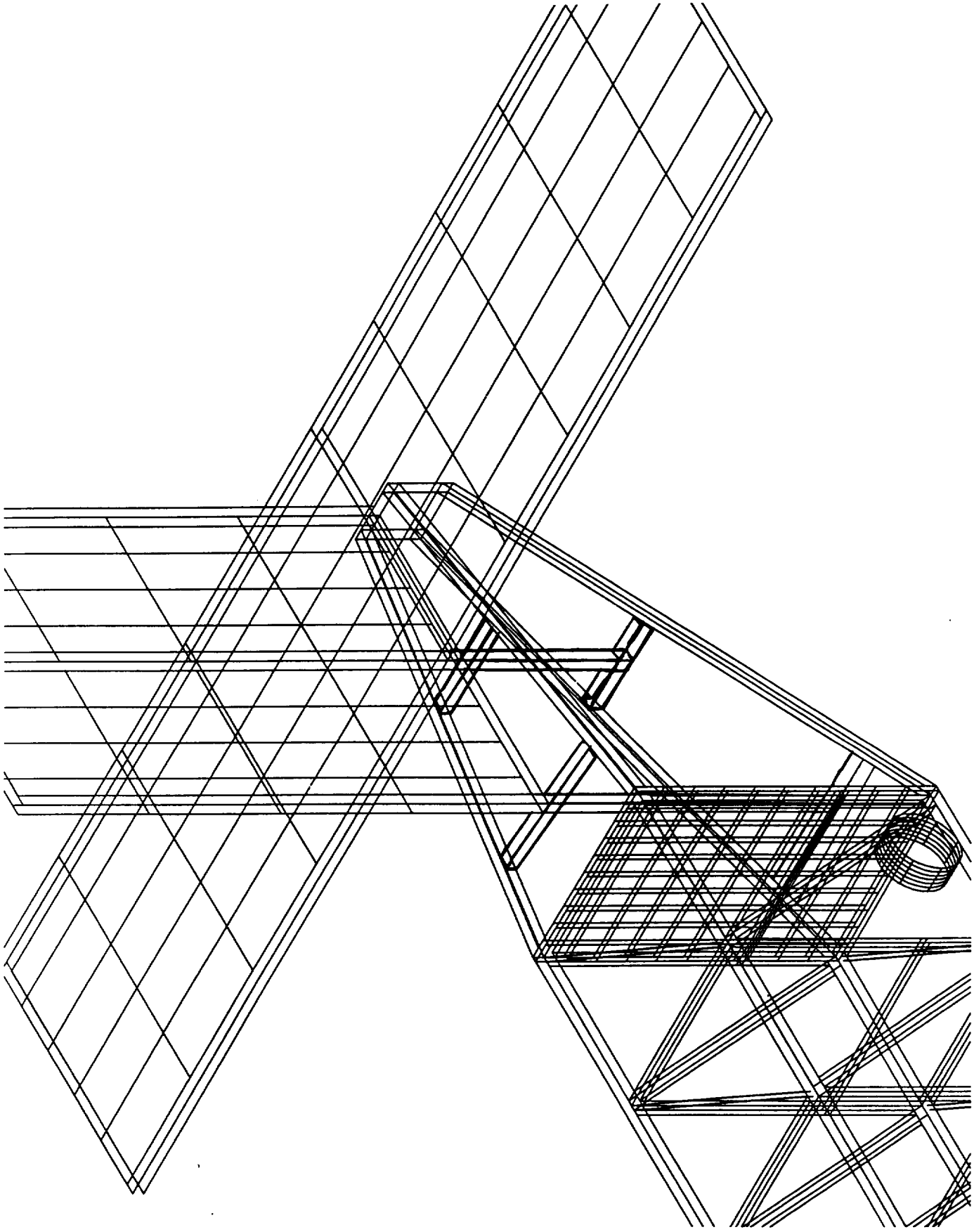

9.3.5 Empennage Design

The empennage, shown in figure 9.3.5-1, consisting of the part of the fuselage aft of the cargo bulkhead and the tail sections, will be constructed entirely from balsa. The tail sections will be rectangular flat plates 3/16 in. thick. The vertical tail is 8 in. long by 12 in. high and the horizontal tail, which will be mounted above the fuselage. will have a span of 2.4 feet and a 6 in. chord. Each control surface will have two spars and ribs spaced every three inches. The rudder and elevator will be designed similarly and be connected to the vertical and horizontal stabilizers via hinges. Control horns will be attached to the rudder and elevators and the control rods will actuate these surfaces through the control horns.

9.3.6 Engine Support Structure

The engine is a relatively heavy piece of equipment (for this structure) and its stabilization is of the utmost importance since an unstable engine could easily rip the fuselage apart if it came free from its mount. Therefore, the engine will be mounted on a 1/8 in. thick piece of plywood that also acts as the forward wall for the cargo bay and electronics bay. This type of support structure has worked well in past designs and so it will be utilized for the Hermes CX-7.

9.3.7 Landing Gear Design

Time did not permit an in depth analysis to design the landing gear. Therefore, a complete, ready-made system which is designed for aircraft in the same weight class as the Hermes CX-7 will be acquired from an outside contractor. The main landing gear chosen has a footprint (width) of 12 inches with wheels attached. The tail gear, which is steerable, is mounted so that the angle of attack of the wing when the aircraft is preparing to takeoff is the required angle to achieve 120% of the stall velocity, which is adequate to give the CX-7 a safe liftoff. This arrangement will reduce takeoff roll by eliminating the usual need for lifting the tail off the ground before takeoff and then rotating to achieve the required lift.

10. **Construction Plans**

From the beginning of the design sequence, the manufacturing process for the airplane has been considered. No part of the aircraft has been designed without asking the question: How will it be built? Consequently, the Hermes CX-7 is airplane which has been optimized both for its mission and the ease with which it can be constructed.

10.1 Major Assemblies

There are five major assemblies to be completed: wing, fuselage, empennage, landing gear, and control/propulsion systems support. The wing, fuselage and empennage will be drawn out in full scale on posterboard, and the assemblies will take place right on the drawing. This will provide the basis for an accurate assembly at relatively low cost and little time spent. The control and propulsion systems support will then be integrated into the fuselage.

10.2 Complete Parts Count

Throughout the project, the group tried to reduce the total number of parts needed to construct the full airplane, since a decrease in parts would mean a decrease in the time needed to build the aircraft, and thus a decrease in labor costs. The final design consisted of a total of 354 separate parts. Table 10.2-1 gives a complete breakdown of the parts count for the Hermes CX-7

Table 10.2-1: Parts Breakdown

System/Part:	Number:
Wing	
Ribs	32
Spar	4
Spar Web	12
Longeron	4
Leading Edge	2
Trailing Edge	2
Fuselage	
Carry-Through	32
Longerons	4
Floor Support	11
Sides	36
Top & Bottom	34
Floors	4
Bulkheads	2
Engine Cowling	8
Empennage	
Vertical Tail	17
Horizontal Tail	29
Tail Support	20
Longerons	2
Propulsion	16
Propulsion Support	20
Avionics	8
Avionics Support	20
Landing Gear	5
Miscellaneous	30

10.3 Assembly Sequence

Each half-span of the wing will be assembled following the full-scale drawing. The ribs will be cut using a hardwood template, and these will be connected at four inch intervals by the spar caps. The spar web will then be fitted, as well as the leading and trailing edges. The leading edges, which will initially be of rectangular cross-section, will have to be rounded to conform to the rib shape of the 6412 airfoil section. The spars will extend 2 in. beyond the last rib in order to facilitate the plug-in to the fuselage. Next, the smaller longerons will be fitted, and the finished wing will then be coated with monokote.

The fuselage sides will be constructed from the full-scale drawing, and then connected using the wing carry-through and the two major bulkheads fore and aft of the cargo bay. Next, the top and bottom of the fuselage will be constructed, allowing

room for the two doors in the top of the fuselage. The doors will then be constructed, and the cargo floor installed followed by the engine cowling and the floors for the avionics and the batteries. At this point the landing gear supports will be fitted to the appropriate locations on the fuselage. Finally, control rod supports will be installed, as well as the supports for the avionics package and the batteries.

The empennage will be constructed from full-scale drawings, with the horizontal and vertical tails having separate drawings. The rudder and elevators will be attached with monokote hinges. The vertical tail will be mounted to the lower part of the empennage by extending the vertical spars of the tail. The completed horizontal tail will be mounted on top of the lower section of the empennage. The supports for the control rods and the control horns themselves will be installed. Finally the empennage will be attached to the fuselage just aft of the aft cargo bay bulkhead.

The front landing gear will be installed on its support, and the back landing gear will then be properly installed so as to give the fuselage the proper angle when on the ground. Then the entire fuselage/empennage sections will be covered with monokote.

Once the avionics, batteries and engine are installed, the plane will be ready for taxi tests, after which certain structural adjustments may have to be made.

11. **Environmental Impacts and Safety**

In an efforts to minimize the environmental impact of this airplane, every effort was made to design this aircraft so that it could be built with recyclable materials. It was designed so that it would not impact the lives of those living near airports through undue noise or unsafe operation.

11.1 Disposal Costs

In an effort to prevent further damage to the environment, Group C anticipates that most, if not all, of the Hermes CX-7 will be made of recyclable or reusable materials. The majority of the Hermes CX-7 is composed of wood. All balsa, spruce, and plywood components of the structure will be recycled. The only costs will be for transporting the wood to the recycling center. It may also be possible to use the wood for other projects in the area. The skin of the aircraft has been designed out of monokote. Investigations have shown that monokote may have reusable applications or recyclability. Again, the only costs would be minor costs for shipping. All metal components will likewise be removed from the aircraft and recycled. The NiCad batteries are perhaps the most toxic component of the aircraft. However, companies can be contracted to take used batteries and recycle the materials at their facilities. These companies look for organizations like AE441, Inc. and G-Dome Enterprises to provide the raw materials for their work. No substantial charge, if any, is foreseen from these companies. In fact, it may even be possible to work a deal where these companies pay us for the batteries as is done with car batteries. All other components of the aircraft (i.e. landing gear, control rods, etc.) can be divided into recyclable groups and distributed.

11.2 Noise Characteristics

The Astro-15 engine and TopFlight 12-6 propeller used in the propulsion system meet noise requirements for operation. The RPM and tip speed will not reach excessive values and cause undo noise. Group C anticipates no problems with the noise either while the aircraft is near cities or for the pilot. Both have been used on past aircraft without incident.

This airplane does have the ability to exceed the speed of sound if the pilot chooses to do so. This is not recommended however over populated areas as the residents will surely complain about the sonic booms. The plane and route structure were designed so that it will be unnecessary for the pilot to exceed Mach 1 under

normal circumstances as the plane operates efficiently at subsonic speeds and the route system provides sufficient time for him to reach his destination without exceeding the speed of sound.

11.3 Waste and Toxic Materials

As the construction process is refined, Group C anticipates minimizing the amount of waste material. As all of the components of the aircraft are recyclable, the waste material will be sent out as well.

The Hermes CX-7 has been designed to fly at 30 ft/s at an altitude no greater than 25 ft. Any impact of the aircraft due to system or pilot failure will not generate the forces necessary to break the batteries and spill the toxic material in them. When the batteries have been exhausted, they will be sent to a used battery handling facility. The only other toxic material used on the aircraft is the adhesive. The only problems with the adhesive will occur when it is in large quantities during construction. Group C will be using the adhesive in a well ventilated area. Employees will not be allowed to work alone, and any employee who abuses the adhesive will be dismissed immediately.

11.4 Flight Safety

As previously mentioned, this airplane has been designed so that it is statically and dynamically stable in all flight regimes. Thus, unless the pilot should attempt an ill-advised maneuver for which it was not designed, there will be no problems controlling the aircraft.

The only potential problem would be if the batteries ran out. If the main batteries which power the motor run out, there will be no problem controlling the airplane as the flight control system operates on a separate set of batteries. The only thing the pilot will have to do in the event of a main battery failure is find a suitable landing site nearby. It is not expected that flight control system battery will fail suddenly. The only thing which could cause a sudden loss of power in the flight control system is if the battery wires are cut. However, there is little chance that this will happen. If this battery becomes low, the pilot should notice because the response of the aircraft will become erratic. When this happens, he will have to find a place to land immediately before power is completely lost and he loses control of the aircraft.

12. Economic Analysis

12.1 Production Costs

Group C estimates the unit production cost of the Hermes CX-7 at $390,000.00. This amount can be divided into cost of prototype and cost of labor. The cost of prototype can be more specifically described in terms of direct materials costs, propulsion costs, and avionics costs. Table 12.1-1 shows a complete breakdown of the total cost for production of a single aircraft.

The direct materials costs of $50,000.00 is based on initial purchases. Designers of past aircraft have had a wide range of direct materials costs, and Group C may find it necessary to make additional purchases of direct materials. $100,000.00 went towards the purchase of the propulsion system. Firm quotes have been received from the propulsion subcontractors, and all of the propulsion components have been ordered. The total cost for aircraft avionics of $90,000 has also been set by quotes from the subcontractors. Group C also estimates $150,000.00 for labor based on the number of person hours needed to construct an aircraft of similar design in past years. The set rate for labor costs is $1000 per person hour.

As in all things, the first time is always the most difficult and, often, the most expensive. Group C anticipates the unit production cost to decrease as the construction process is refined. In addition to reducing the amount of direct materials needed, the construction process may require fewer person hours per aircraft. Group C anticipates that as much as $25,000.00 or more could be saved through the improvements gained by experience. This would lead to a 6.5% reduction in unit production costs, a substantial savings.

With only 22 aircraft necessary to service the entire commercial cargo transportation system, G-Dome Enterprises would make a relatively small initial investment of $8,580,000.00 to begin operation.

Table 12.1-1: ESTIMATED UNIT PRODUCTION COST

PROTOTYPE COST			
Direct Materials			
	balsa, spruce, plywood	$20,000.00	
	monokote	$10,000.00	
	fasteners & adhesives	$10,000.00	
	landing gear	$10,000.00	
Total			$50,000.00
Propulsion			
	engine	$50,000.00	
	propeller	$2,000.00	
	batteries	$20,000.00	
	speed controller	$28,000.00	
Total			$100,000.00
Avionics			
	radio & receiver	$50,000.00	
	servos	$30,000.00	
	control rods	$10,000.00	
Total			$90,000.00
TOTAL			$240,000.00
LABOR COST			$150,000.00
UNIT PRODUCTION COST			$390,000.00

12.2 Flight Costs

The average flight cost was based on the daily performance of the 22 aircraft system. The 88 flights have an average range of 2500 ft covered in 1.5 minutes. The flight cost consists of four different expenditures: fuel, operation, maintenance, and

depreciation. Figure 12.2-1 illustrates the dependence of the flight cost on these four values.

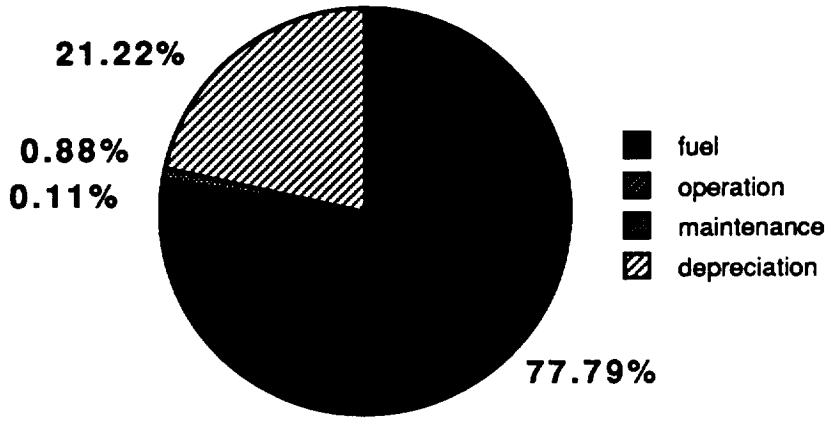

Figure 12.2-1: Cost Breakdown

While fuel costs span a range from $5 to $20 per milliamp-hour, all cost estimates have been made using an average fuel cost of $12.50 / mAhr. For a flight of 2500 ft, the Hermes CX-7 will consume 176 mAhrs. of fuel at a cost of $2200. Due to the fluctuation in fuel costs, the cost of fuel consumed on an average flight can vary from $880 to $3520. Fuel costs, therefore, makes up 60% to 85% of the total flight cost.

The Hermes CX-7 has two control surfaces, the rudder and elevator. By minimizing the number of control surfaces, and hence the number of servos needed, the aircraft has an operation cost of only $2 per minute in flight.

Group C has designed the aircraft for easy access to the batteries. At a cost of $50 per person-minute, one member of the ground crew will be able to perform a complete battery change on the Hermes CX-7 in one half of a minute.

The Hermes aircraft has been designed for 650 ground-air-ground cycles before decommissioning. Using a simple depreciation over the life of the aircraft, the economics group has included a $600 depreciation cost per flight to cover the unit production cost.

The cost of an average flight will total $2828.00, based on all four of these cost components. Each mission's range affects the flight cost. Increased flight time increases the operation cost slightly; however, greater fuel costs will have a much

greater impact on the flight cost. The effort throughout the project's development has been to reduce costs. The primary method of achieving this has been to reduce the amount of fuel consumed to deliver the packages.

12.3 Fleet Economics

The distribution network set up by Group C's economic team requires a total of 22 aircraft to satisfy the demand for overnight package delivery to and from all of the cities in the northern hemisphere of Aeroworld. As described in section 12.1., the aircraft will have a unit production cost of $390,000.00 for a total fleet cost of $8.58 million. To complete the 88 missions required daily, each aircraft will make four flights every night. With an average cost of $2,228.00 per night, daily fleet expenses will be $196,064.00. Over the 162 day life of the fleet, the fleet life cost will be just over $40 million.

G-Dome Enterprises believes that the demand for cargo delivery will produce 29,400 in^3 each day for the network. Over the life of the fleet, this amounts to over 4.75 million cubic inches of cargo. The fleet will cover 197,512 ft per night and 32 million feet in 162 days. Therefore, the average unit volume cost equals $6.70.

The economics group sees cargo being delivered at an average rate of $10.50 per cubic inch for a daily revenue of $308,700.00. At a profit of $112,636.00 per day, G-Dome Enterprises will break even on its initial investment 76 days, less than half of the fleet's life. With continuous operation, G-Dome Enterprises will have a net yearly income of nearly $22 million.

13. Compliance With Design Requirements and Objectives

All the design requirements and objectives presented in Appendix A were met or exceeded with one exception. The requirement for the aircraft to be able to fit into a 5 ft. x 2 ft. x 2 ft. box was eased to a 5 ft. x 3 ft. x 2 ft. box.

When designing the empennage, it was desirable to reduce the induced drag due to the tail. To do this, an aspect ratio of 5 was specified for the horizontal tail. However, this aspect ratio was impossible because the span of the tail would exceed two feet. One alternative discussed was to build extensions for the tail which would give the necessary span but be removable so that the span could be reduced to less than two feet so that the airplane could fit into the required package. However, to do this, it was estimated that the weight of the horizontal tail would be increased by 50% and this large weight penalty was determined to be too high. After consulting with the program manager (Dr. Batill), it was determined that the requirement for the package size could be relaxed.

In many cases, the aircraft exceeds its design performance. In all cases, this is by no fault of the designers. Rather, it is due to the fact that materials and equipment were unavailable in the required sizes. Therefore, the next larger size had to be used if the minimum design requirements were to be met.

14. **Results of Technology Demonstrator Development**

14.1 Complete Configurational Data, Geometry, Weights, and C.G.

A complete listing of the final configurational data, geometry, weights, and C.G. is compiled in the CDS. A summary is included below.

Span:	10 ft.
Chord:	10 in.
Length:	56.25 in.
Empty Weight:	4.45 lbf
Static Margin:	20%
Vertical Tail Area:	0.67 ft^2
Horz. Tail Area:	1.25 ft^2
Prop:	TopFlight 12x6
Engine:	Astrro 15
Cargo Volume	640 in^3

14.2 Flight Test Plan and Test Safety Considerations

The flight testing of the technology demonstrator will be conducted in a controlled and low risk manner. Before the aircraft is allowed to move under it own power, a complete set of system checks will be made to insure that the propulsion system and flight control system are fully operational. In addition, the center of gravity location will be checked to insure that it falls within the prescribed limits.

Once the ground checks have been completed, the aircraft will be taxied. The purpose of the taxi tests will be to insure that the aircraft has adequate ground handling characteristics and to attempt to identify any potential problems which might occur in flight. Once the aircraft can be successfully taxied without problems, it will be cleared for flight with no cargo on board.

Initial flights will be conducted without cargo on board. The reason for this is that no cargo is required to place center of gravity within prescribed limits and because flying empty will minimize risk because the stresses in the airframe and the stall speed will be lower. The purpose of these flights will be to evaluate the handling characteristics throughout the flight envelope and identify any problems. Once these tests are completed, cargo will be added to the aircraft and the flight envelope will again be expanded.

To insure the highest level of safety possible, the testing will be conducted in the order set forth above. The testing will not progress to the next step until the current set of tests has been successfully completed.

14.3 Flight Test Results - Taxi, Catapult, and Controlled Flight Tests

Taxi testing was completed on April 28, 1992. At such testing the aircraft propulsion and control systems were checked. All systems were in working order. Upon testing the ground handling ability of the craft, it was determined that the aircraft had sufficient ability to maneuver on the ground and to maintain a straight takeoff path to aid in takeoff performance. The aircraft achieved liftoff without difficulty, at a power level less than full throttle. The aircraft was then brought down immediately and landed with no damage to the landing gear or aircraft structure. No corrections were deemed necessary prior to the flight tests.

Flight testing was completed on May 1, 1992. The aircraft successfully lifted off in less than 30 feet and flew several laps of the Loftus center test sight. The plane was than brought down smoothly to change the setting on the rudder control actuator to allow the pilot greater rudder deflections. The plane was then flown again successfully. Group C is completely satisfied with the results of the flight tests and recommends production of the Hermes CX-7 for G-Dome enterprises.

14.4 Manufacturing and Cost Details

Table 14.4-1 below outlines the actual production costs for the technology demonstrator. With 22 aircraft in service, the commercial cargo transport system would require an initial investment of $8,338,000.

Table 14.4-1: Actual UNIT PRODUCTION COST

PROTOTYPE COST

Direct Materials			
	balsa, spruce, plywood	$20,000.00	
	monokote	$15,000.00	
	fasteners & adhesives	$6,000.00	
	landing gear	$10,000.00	
Total			$51,000.00
Propulsion			
	engine	$50,000.00	
	propeller	$1,300.00	
	batteries	$20,000.00	
	speed controller	$28,000.00	
Total			$93,000.00
Avionics			
	radio & receiver	$50,000.00	
	servos	$30,000.00	
	control rods	$5,000.00	
Total			$85,000.00
TOTAL			$229,000.00
LABOR COST			$150,000.00
UNIT PRODUCTION COST			$379,000.00

C-2

References

1. Anderson, John D., Introduction to Flight, McGraw-Hill Book Company, New York,1989.

2. A Catalog of Low Reynold's Number Airfoil Data For Wind Turbine Applications. Department of Aerospace Engineering, Texas A & M University, College Station, TX. Feb. 1982.

3. Jensen, Daniel., A Drag Prediction Methodology for Low Reynolds Number Flight Vehicles, Department of Aerospace and Mechanical Engineering, The University of Notre Dame, 1990

4. Nelson, Robert C., Flight Stability and Automatic Control

5. Swift, Richard A. Application of Finite Element Methods to the Preliminary Structural Design of Lifting Surfaces. University of Notre Dame, 1989.

6. ANC Bulletin, Design of Aircraft Wood Structures, War Department, Navy Department, Department of Commerce, 1944.

Appendix A: Design Requirements and Objectives

Date: February 4, 1992
To: G-Dome Enterprises
From: AERO 441 Group C
Mr. Brian Amer
Mr. Jack Barter
Mr. Jay Colucci
Miss Caryn Foley
Mr. James Kockler
Mr. David Rapp
Mr. Matthew Zeiger

Subject: **Design Requirements and Objectives**

The following requirements, constraints and objectives have been set by Group C concerning the design of an aircraft in response to the RFP by G-Dome Enterprises for an aircraft to exploit the market for overnight parcel delivery by air.

External Configuration:

- The aircraft shall be designed such that all required cruising and maneuvering can be accomplished while flying at a height of no greater than 25 feet above ground level.
- The aircraft will be designed so that it can be disassembled for transportation and storage and will fit in a storage container no larger than 5 ft. X 2 ft X 2 ft.
- The aircraft will have the ability to be catapult-launched.

Internal Configuration:

- The aircraft will have at least 640 cubic inches of payload volume.
- The aircraft will be designed to carry 1.2 pounds of payload cargo.
- The cargo space will be configured so that the aircraft will have the ability to carry both two (2) inch cubes (8 cubic inches) and four (4) inch cubes (64 cubic inches) that serve as parcel packing containers.
- The aircraft will have the ability to carry a specialized instrument package as specified by the instructor or AERO 441.

Propulsion:

- The aircraft and its derivatives will use one or a number of electric propulsion systems currently available.

Fuel Storage:

- Fuel storage will be accomplished through the use of nickel-cadmium batteries, which have the ability to be recharged in no more than 1/4 of an AeroWorld day. This constraint will mean that each plane will require multiple (up to 6) battery packs for use during one night of flight.

Flight Control System:

- The pilot will have the ability to control the velocity of the aircraft under normal circumstances.
- The radio control system and the instrumentation package must be removable, and installation will be accomplished in one AeroWorld day or less.
- The prototype will be designed so that stability and control of the aircraft can be maintained with the fewest number of servos possible.

Airframe Structure & Materials:

- The airframe will be designed so that it can (barring accidents) safely withstand 650 ground-air-ground cycles without being overhauled.

Performance:

- The aircraft will service all cities presented in the RFP except C, D, E & O. All of the cargo requirements from these cities will be met overnight (18.75 minutes)
- The aircraft will have an optimum range of 4500 ft. when carrying its maximum cargo weight at 30 ft/s.
- The aircraft will have the ability to fly to the nearest alternate airport and maintain a loiter for one (1) minute.
- The aircraft will takeoff and land in 60 ft. or less.
- The aircraft will have the ability to carry 640 cubic inches of cargo based on an average of .03 ounces per cubic inch. If the average weight of the cargo exceeds this limit, the aircraft will carry a lesser volume.
- The aircraft will have the ability to perform a sustained, level 60 foot radius turn.
- The aircraft will have the ability to takeoff and land under its own power.

Landing Gear & Ground Control:

- The nose gear will be able to rotate so that the aircraft can be turned while taxiing.

Safety & Environmental Considerations:

- All FCC and FAA regulations concerning the operation of RPV's and other safety constraints imposed by the instructor of AERO 441 will be complied with.
- A complete safety analysis will be performed for each subsystem of the in order to discern if a component's failure will compromise the integrity of the aircraft.
- The pilot will have the ability to maintain full aerodynamic control of the aircraft upon shutdown of engine power.
- The aircraft will not have the need to fly at speeds greater than Mach 1 (30 ft/s).
- All material used in the aircraft structure will be biodegradeable except the surface covering (monokote). All other materials used in the structure or propulsion of the aircraft will be reuseable or recyclable. The nickel-cadmium batteries will be rechargeable but have a finite life.

Manufacturing:

- The time required to complete construction of the prototype will not exceed three weeks in real time.
- The cost of materials used in manufacture of the prototype will be equal to or less than $100,000 in AeroWorld dollars.
- The number of man-hours required to complete prototype constuction will not exceed 210 in real time.

Costs:

- The total cost for the construction of the prototype, including materials cost and labor shall not exceed $310,000 in AeroWorld dollars.
- The maintenance cost of the aircraft shall not exceed $25 per flight, based on 1/2 minute needed for a complete battery exchange.
- The operation cost for the airplane will not exceed $3 per minute.

- In order to break even, G-Dome Enterprises shall not have to charge in excess of 28 cents per cubic inch of cargo per 100 feet delivered, based on a fuel cost of $12.50 per milli-amp hour.

Appendix B: Drag Breakdown Method Routine

TK Solver Program to Solve for Drag

cd = cdo + cdp + (1+d)*((cl^2)/(ar*pi))

cdo = (1/sref)*(cff*fff*swf + cfe*ffe*swe + .031 + .0078)*1.15

cff = (2.73*(1.328/(ref^.5)) + .84175*(log(ref))^(-2.58))/4.58

ref = (.00233*v*lfus)/3.82e-7

cfe = 1.328/(ree^.5)

ree = (.00233*v*ce)/3.82e-7

fff = 1 + (60/(ld^3)) + (ld/400)

ffe = (1 + (.6/xcm)*(tce) + 100*(tce^4))*(1.34*(M^.18))

M = v/ss

cdp = cdmin + k*cl^2

swf = lfus * 2*(hfus + wfus)

swe = 2*(sht * cht) + 2*(hvt * cvt)

cl = .6239 +(.098849*aoa)-(5.8818e-4 *aoa^2)-(1.8859e-4 *aoa^3)

clcd = cl/cd

d = (1/e) -1

cdn = cdo + cdmin

	cd	.03654561	coeff. of drag
	cdo	.01008232	modified drag coeff.
	cdp	.01524023	wing profile drag
	d	.08695652	planform efficiency factor
	cl	.6239	
12.8	ar		
3.142	pi		
7.8	sref		wing reference area
	cff	.00273152	skin frict. coeff. - fuselage
	fff	1.1100447	form factor - fuselage
	swf	7.6028	wetted area - fus.
	cfe	.00439042	skin frict. coeff - empennage
	ffe	.82873838	form factor - empennage
	swe	3	wetted area - emp.
	ref	838068.06	fuselage reynolds number
30	v		velocity
4.58	lfus		length of fuselage
	ree	91492.147	empennage reynolds number
.5	ce		empennage mean chord
8.8	ld		fuselage fineness ratio
.3	xcm		chordwise location of max thickness -
.09	tce		ave. thickness ratio - emp.
	M	.02678571	Mach number
1120	ss		speed of sound
.9	e		wing efficiency factor
.0138	cdmin		minimum drag coefficient
.0037	k		airfoil efficiency factor
.5	hfus		height of fuselage c-section
.33	wfus		width ""
2	sht		span of horiz. tail
.5	cht		chord of horiz. tail
1	hvt		height of vert. tail
.5	cvt		chord of vert. tail
0	aoa		angle of attack
	clcd	17.071816	cl/cd
	cdn	.02388232	

Appendix C: Required Figures and Tables

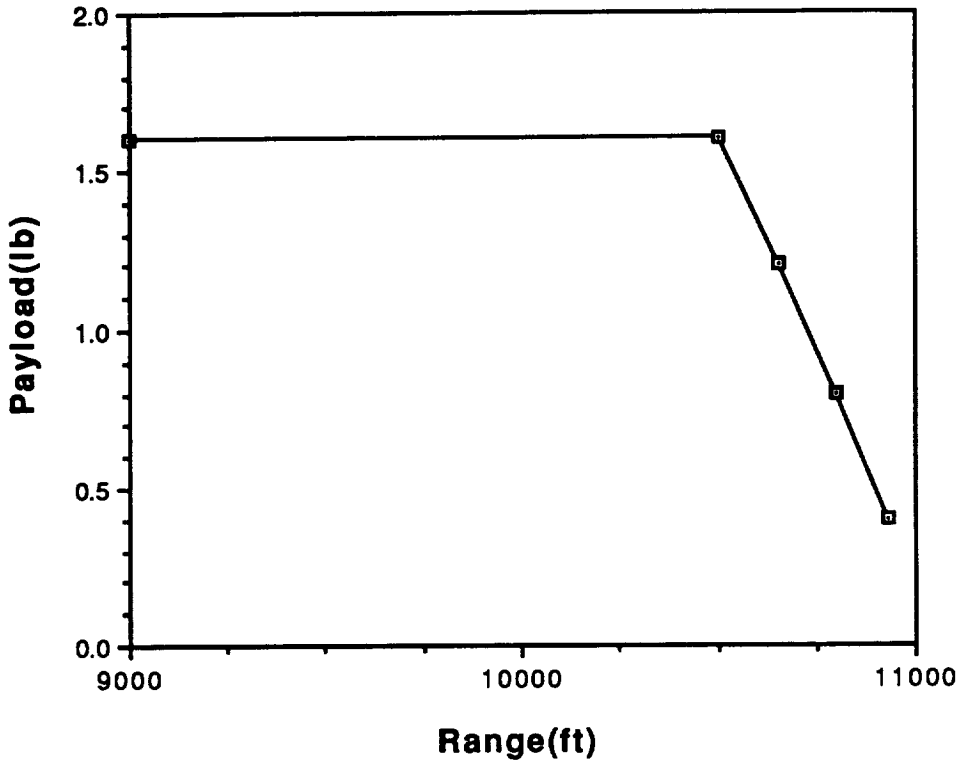

Figure 8.2-3: Aircraft Payload vs. Range

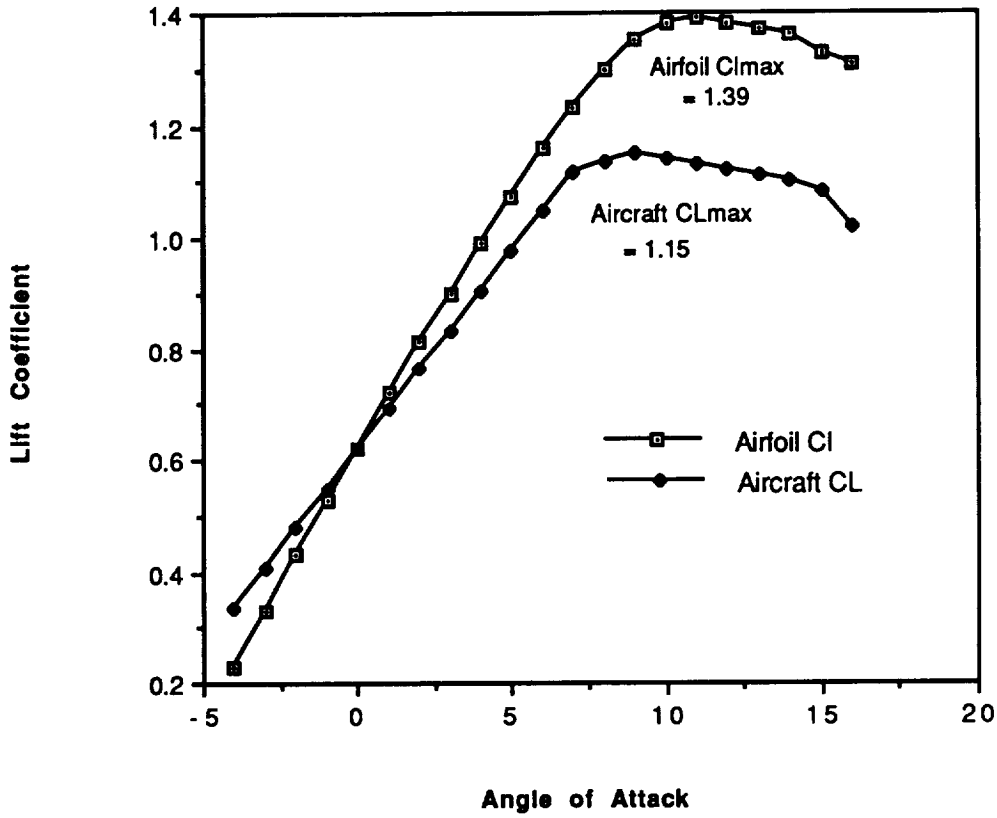

Figure 4.2-2: NACA 6412 and Airplane Lift Curves

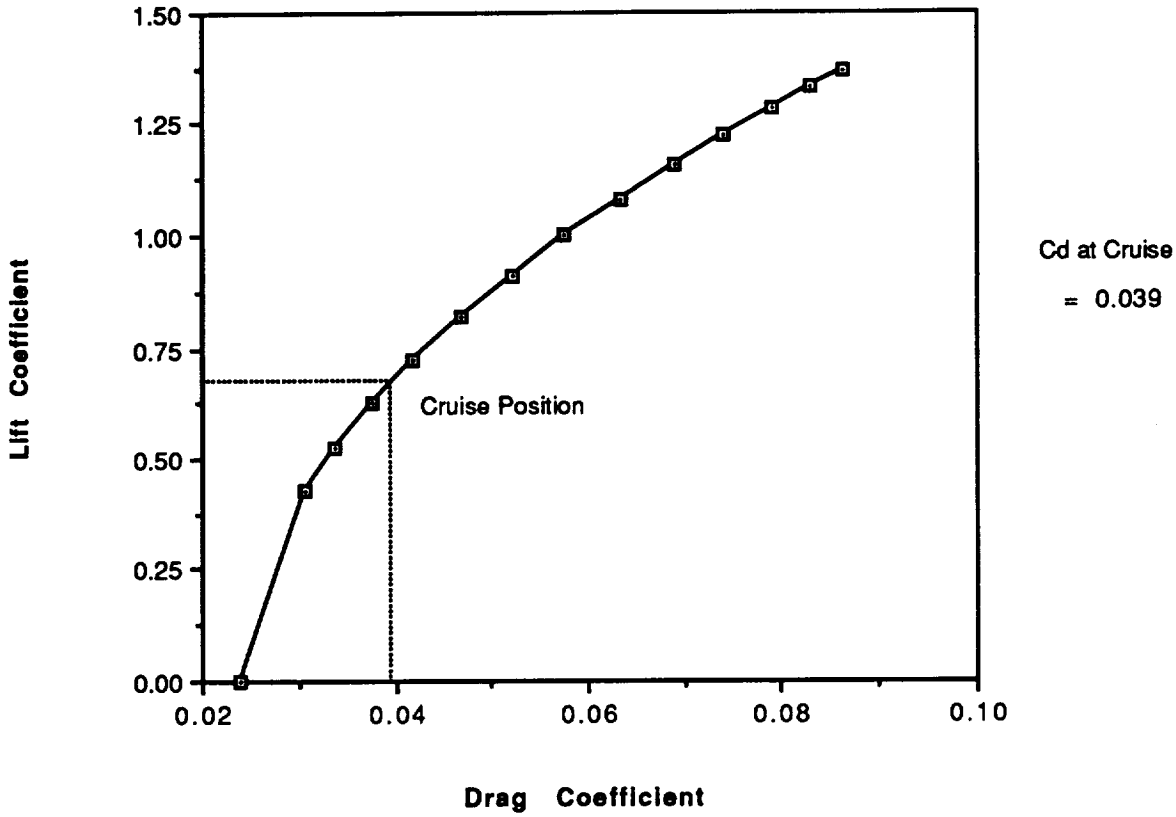

Figure 4.3-2: Aircraft Drag Polar

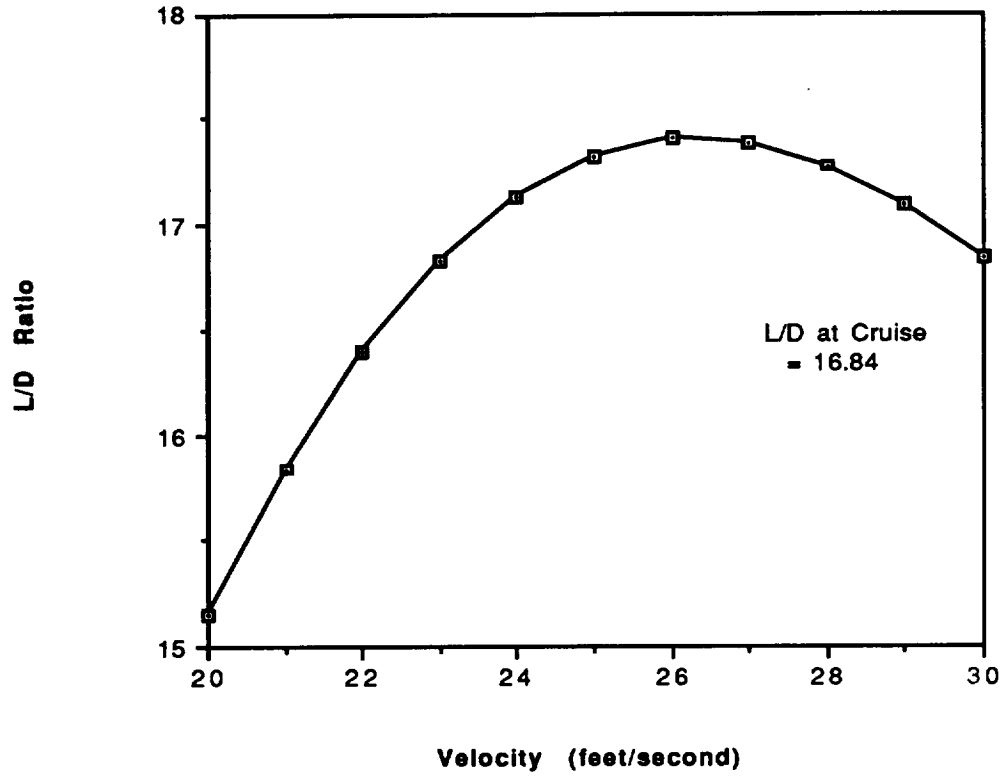

Figure 4.3-3: Aircraft Lift-to-Drag Ratio

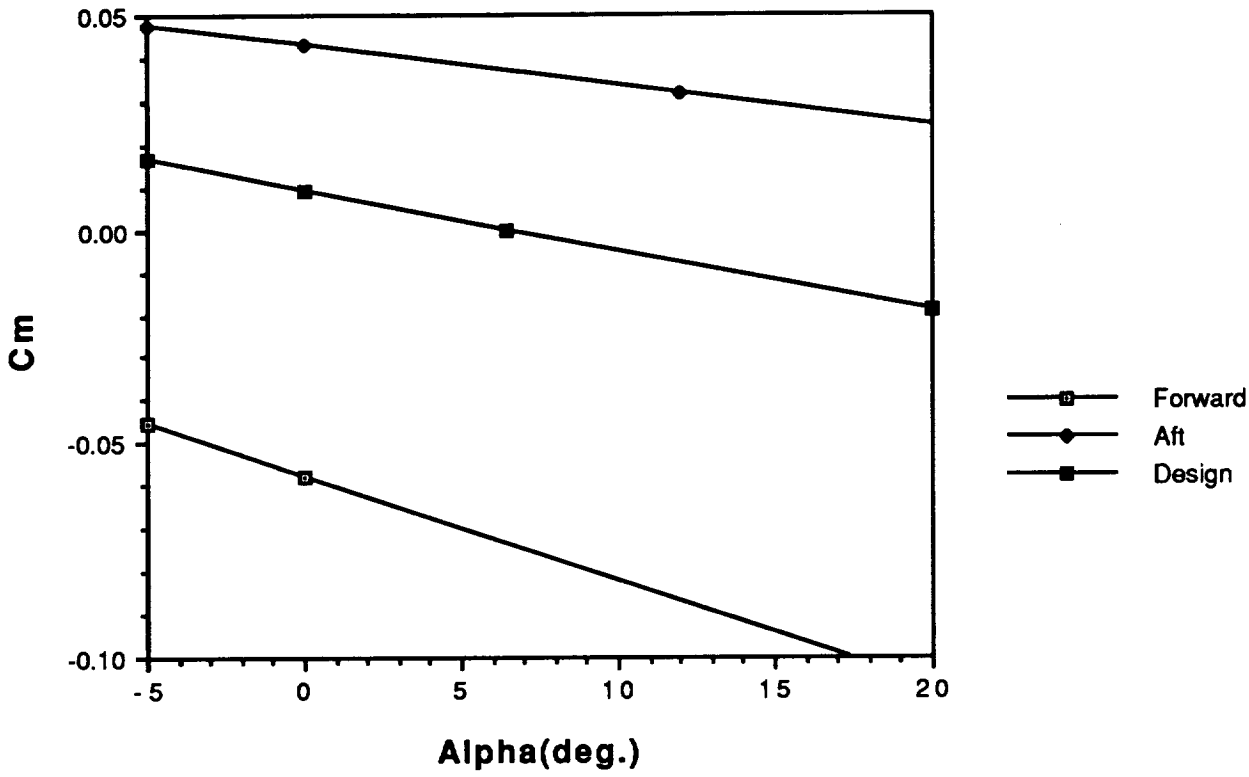
0.05
0.00
-0.05
-0.10
Cm
-5
0
5
10
15
20
Alpha(deg.)
Forward
Aft
Design

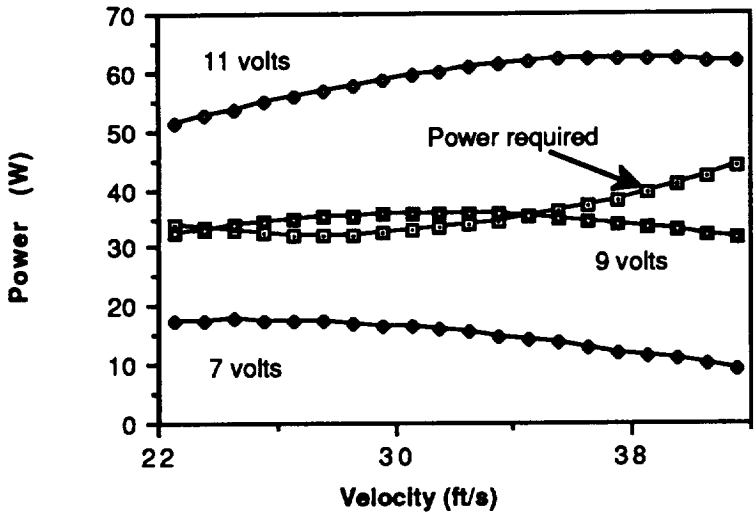

Figure 5.5-1 Power available at various voltage settings

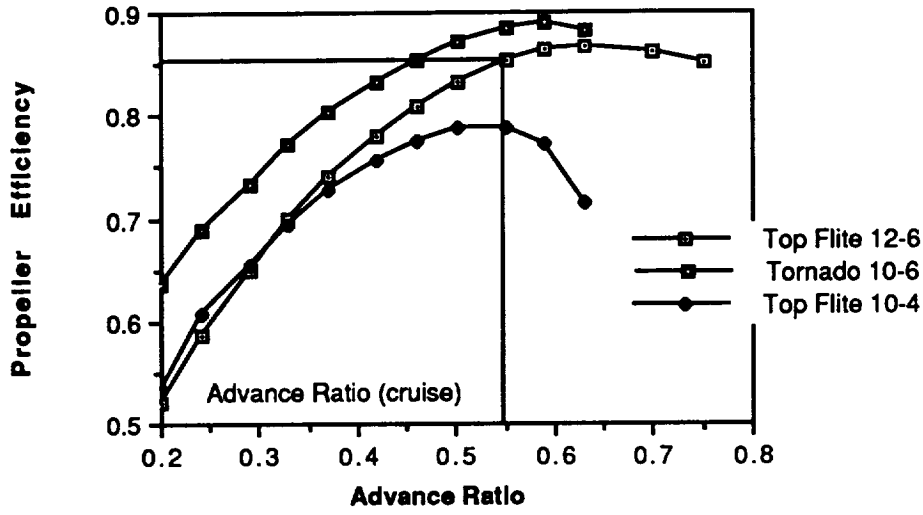

Figure 5.2-3 Propeller Efficiency vs Advance Ratio at cruise velocity

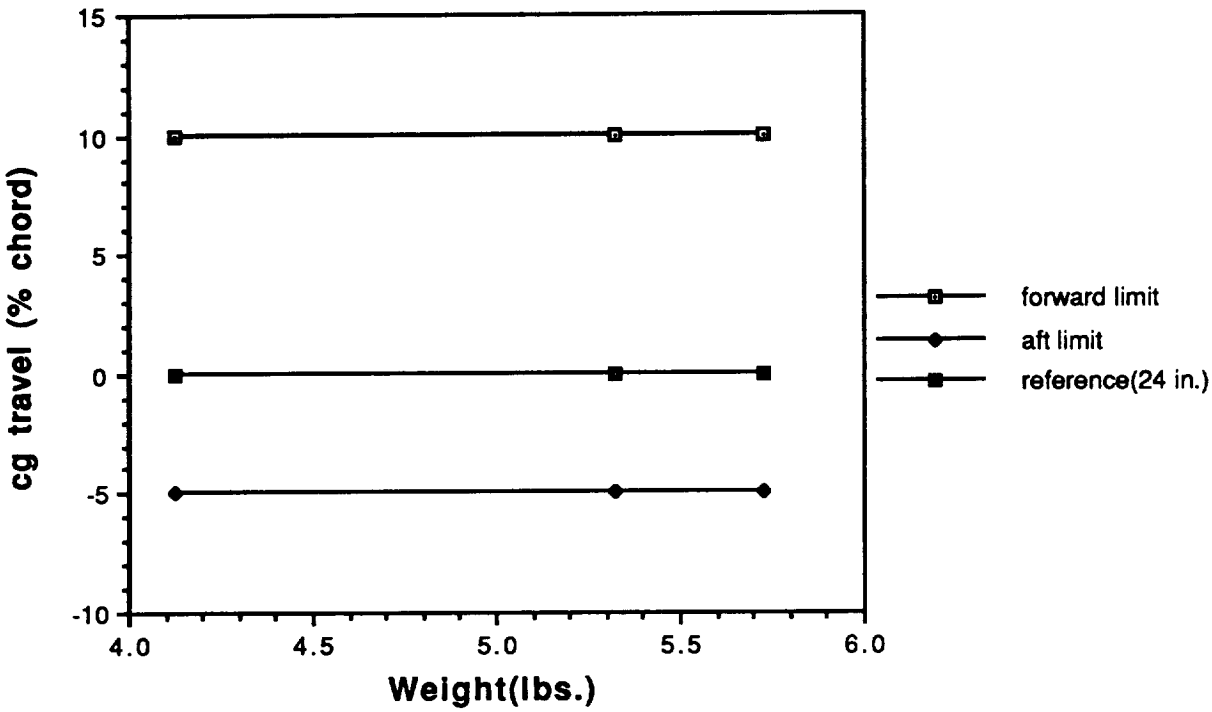
15
10
5
0
-5
-10
cg travel (% chord)
4.0
4.5
5.0
5.5
6.0
Weight(lbs.)
forward limit
aft limit
reference(24 in.)

Table 6.1-1 Preliminary Weight Estimate
(* Denotes Estimated Weight)

	Part:	Estimated Wt (oz)	Actual Wt (oz)
	Wing:		
2	Leading Edge Spar	.42*	
2	Trailing Edge Spar	.37*	
2	Longerons	.19*	
32	Ribs	1.70*	
2	Top Spar Cap	1.92*	
2	Bottom Spar Cap	1.44*	
2	Spar Web	1.11*	
	Monokote (1150 sq. in.)	4.15*	
	Other (Glue & Unaccountables)		
	=10% Wing Weight	1.13*	
	Wing Total Weight	12.42*	
	Avionics:		
	Receiver	.95	
	System Battery	2.0	
2	Servos @ .6 oz each	1.2	
	Speed Controller	1.9	
	Avionics System Weight	6.05	
	Propulsion:		
	Engine (Astro 15)	7.5	
	Mount	1.2	
	Gearbox	1.6	
	Prop	1.0*	
12	Batteries @ 1.02 oz each	12.24	
	Wiring Harness	2.0*	
	Propulsion System Weight	25.54*	

Fuselage:		
	Vertical and Horizontal Tails	4.0*
	Landing Gear	
	Forward	4.3*
	Aft	1.5*
	Attachment Support	.51*
	Truss Structure (F.E.M.)	5.2*
	Bulkheads	
	Engine Firewall	1.35*
	Aft Cargo Support	.39*
	Floors	
	Cargo Floor	2.08*
	Battery Floor	.42*
	Avionics Floor	.42*
	Monokote (1700 sq. in.)	3.06*
	Avionics Support	1.0*
2	Control Pushrods (total)	1.53*
	Carry-Through Support	2.7*
	Fuselage Total Weight	28.46*
Cargo:		
	(640 cubic in. @ .03 oz/cubic in.)	19.2*
Total Weight:		**91.65***

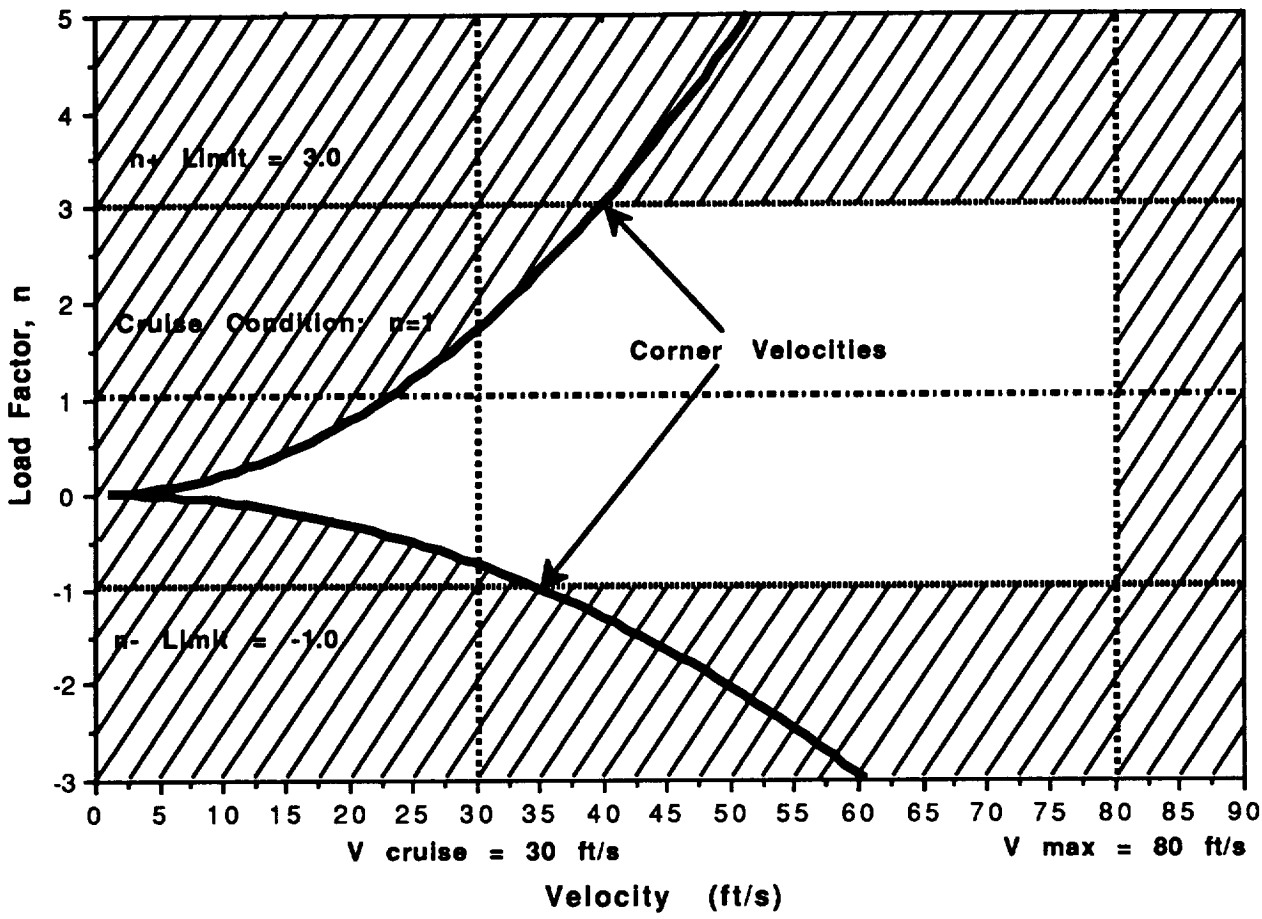

Figure 9.3.1-1: V-n Diagram at Design Weight

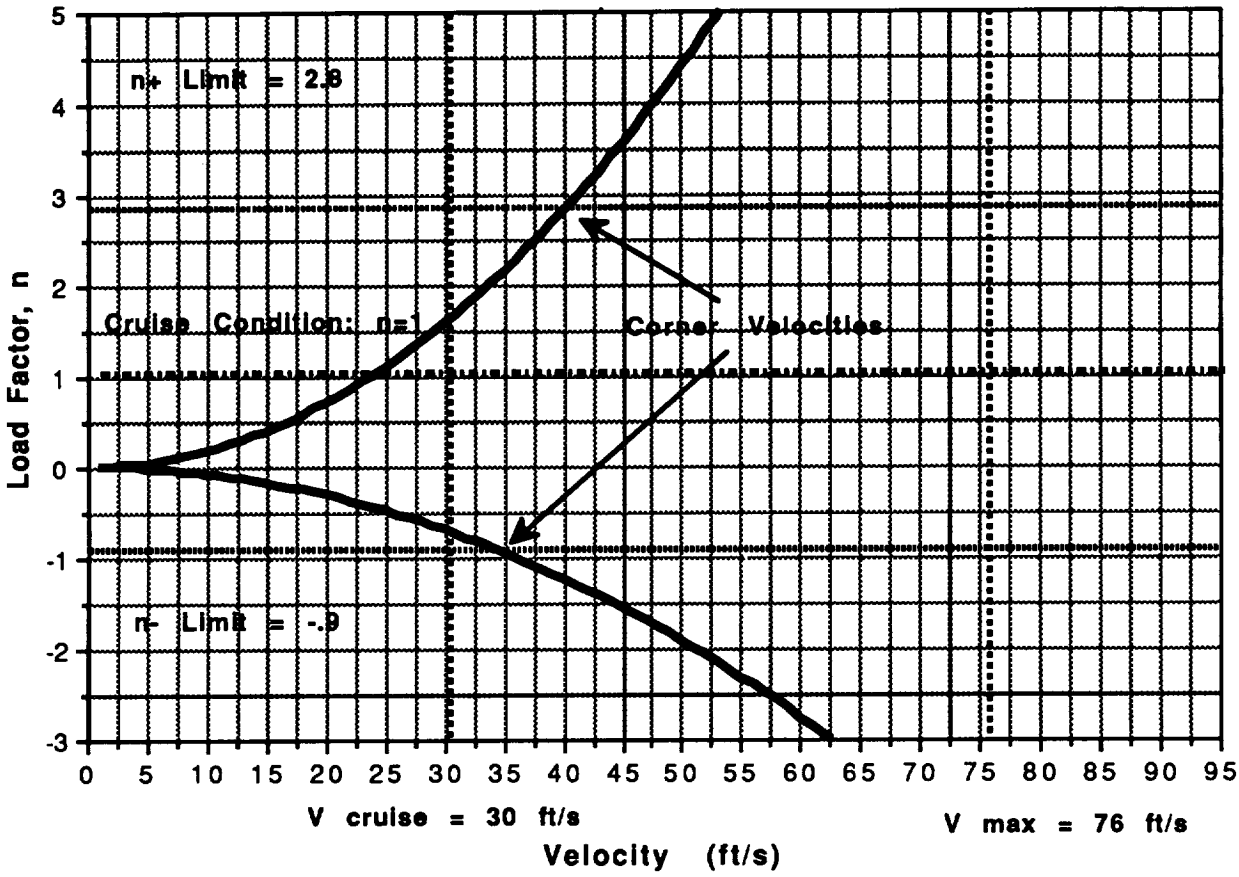

Figure 9.3.1-2: V-n Diagram at Maximum Weight

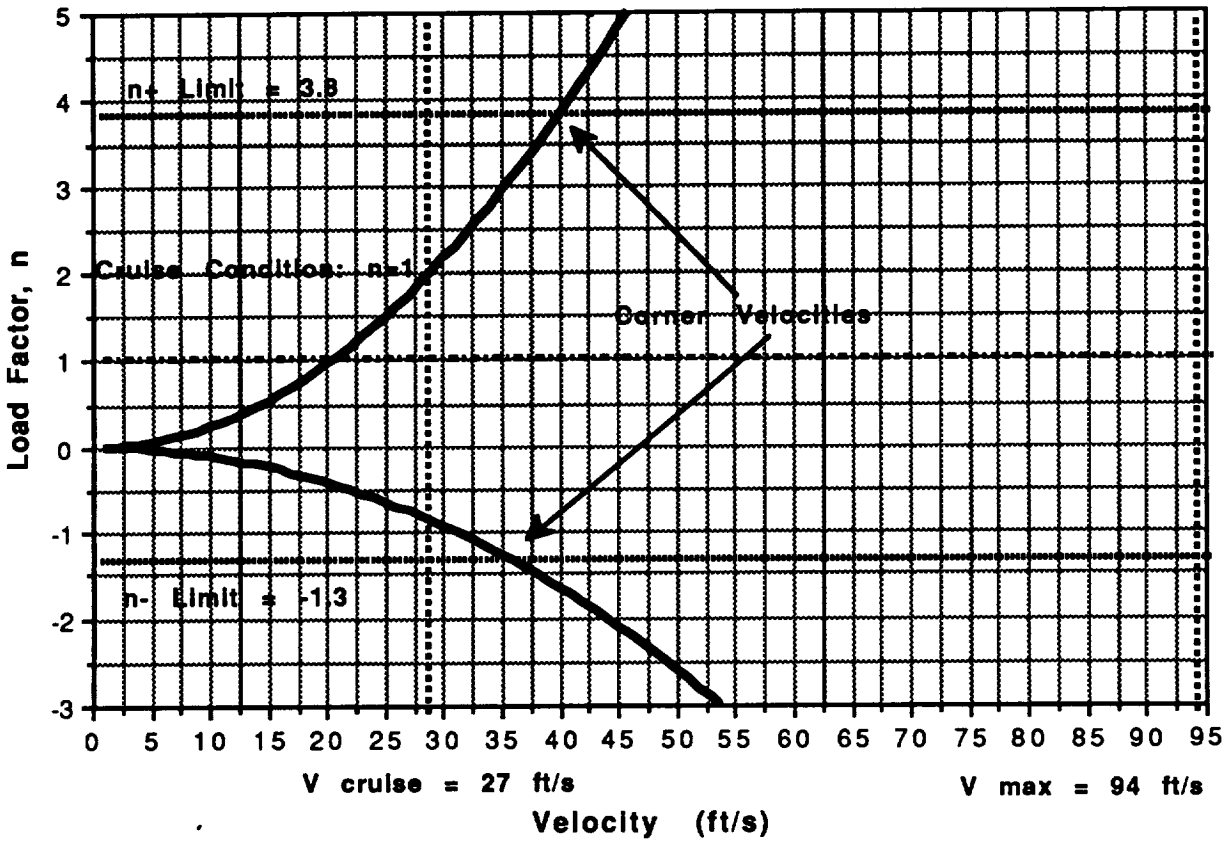

Figure 9.3.1-3 V-n Diagram at Minimum Weight

Table 12.1-1: UNIT PRODUCTION COST

PROTOTYPE COST			
Direct Materials			
	balsa, spruce, plywood	$20,000.00	
	monokote	$10,000.00	
	fasteners & adhesives	$10,000.00	
	landing gear	$10,000.00	
Total			$50,000.00
Propulsion			
	engine	$50,000.00	
	propeller	$2,000.00	
	batteries	$20,000.00	
	speed controller	$28,000.00	
Total			$100,000.00
Avionics			
	radio & receiver	$50,000.00	
	servos	$30,000.00	
	control rods	$10,000.00	
Total			$90,000.00
TOTAL			$240,000.00
LABOR COST			$150,000.00
UNIT PRODUCTION COST			**$390,000.00**